2007-05-11

Identification and Characterization of Components of the Intraflagellar transport (IFT) Machinery: a Dissertation

Yuqing Hou
University of Massachusetts Medical School

IDENTIFICATION AND CHARACTERIZATION OF COMPONENTS OF THE INTRAFLAGELLAR TRANSPORT (IFT) MACHINERY

A Dissertation Presented

By

Yuqing Hou

Submitted to the Faculty of the University of Massachusetts Graduate School of Biomedical Sciences, Worcester

In partial fulfillment of the requirements for the degree of

DOCTOR OF PHILOSOPHY

February 16, 2007

Department of Cell Biology

COPYRIGHTS

Portions of this thesis have appeared in the following publications:

Hou, Y., H. Qin, J.A. Follit, G.J. Pazour, J.L. Rosenbaum, and G.B. Witman. 2007. Functional analysis of an individual IFT protein: IFT46 is required for transport of outer dynein arms into flagella. *J. Cell Biol*. In press.

Hou, Y., G.J. Pazour, and G.B. Witman. 2004. A dynein light intermediate chain, D1bLIC, is required for retrograde intraflagellar transport. *Mol. Biol. Cell*. 15:4382-4394.

IDENTIFICATION AND CHARACTERIZATION OF COMPONENTS OF THE INTRAFLAGELLAR TRANSPORT (IFT) MACHINERY

A Dissertation Presented
By

Yuqing Hou

The signatures of the Dissertation Defense Committee signifies

completion and approval as to style and content of the Dissertation

_____
George B. Witman, Ph.D., Thesis Advisor

_____
Dannel McCollum, Ph.D., Member of Committee

_____
Julie Jonassen, Ph.D., Member of Committee

_____
William Theurkauf, Ph.D., Member of Committee

_____
Stephen King, Ph.D., Member of Committee

The signature of the Chair of the Committee signifies that the written dissertation meets

the requirements of the Dissertation Committee

_____
Gregory Pazour, Ph.D., Chairman of Committee

The signature of the Dean of the Graduate School of Biomedical Sciences signifies

that the student has met all graduation requirements of the school

_____
Anthony Carruthers, Ph.D.,
Dean of the Graduate School of Biomedical Sciences

Department of Cell Biology
February 16, 2007

Acknowledgments

I would like to thank my graduate advisor Dr. George Witman for his guidance, encouragement, and support. He provided me with endless opportunities to develop my scientific thinking and to communicate my work in writing and at the platform. I was fortunate to have him as my mentor and role model. I am also grateful to Dr. Gregory Pazour for teaching me experimental designs and techniques and for helping me initiate the projects in my early days in the lab. Without them, the evolution of this work and the development of my scientific career would have been impossible. Many thanks to my lab mates, Dr. Maureen Wirschell, Dr. Dianne Casey, Dr. Jovenal SanAgustin, Bethany Walker, John Follet, Dr. Michael Chapman, Dr. Karl Lechtreck, Deborah Cochran for their constant support and helpful discussion in and out of the lab. I would like to express my gratitude to my colleagues in the EM facility. They were invaluable in helping me with the electron microscope. I would also like to thank members from my thesis research advisory committee and thesis defense committee, Drs. Dannel McCollum, Stephen Lambert, William Theurkauf, Gregory Pazour, Julie Jonassen, Stephen King, for their insightful comments and suggestions.

To my friends, I would like to share this achievement with them. I owe a lot of thanks to them for being supportive and I know that they are just there whenever I have difficulties.

I would like to thank my father Hongsheng Hou, my mother Yufen Yang and my grandmother Guimei Yang for their selfless and endless love, support and sacrifices

over the years. I am truly blessed with such a wonderful family, which shows me the virtues of being generous, frank, optimistic, and persistent. I would also like to thank my parents-in-law Yanlin Zhang and Xinyuan Zhang for their understanding and for giving tremendous support in life, both emotionally and financially.

Last, but not the least, I thank my husband, Jeffrey Zhang, for the continuous support and encouragement in my graduate study. I am grateful that we can share this achievement with our lovely daughter Amy.

ABSTRACT

Intraflagellar transport (IFT), the bi-directional movement of particles along the length of flagella, is required for flagellar assembly. The IFT particles are moved by kinesin II from the base to the tip of the flagellum, where flagellar assembly occurs. The IFT particles are then moved in the retrograde direction by cytoplasmic dynein 1b/2 to the base of the flagellum. The IFT particles of *Chlamydomonas* are composed of ~16 proteins, organized into complexes A and B. Alhough IFT is believed to transport cargoes into flagella, few cargoes have been identified and little is known about how the cargos are transported. To study the mechanism of IFT and how IFT is involved in flagellar assembly, this thesis focuses on two questions. 1) In addition to a heavy chain, DHC1b, and a light chain, LC8, what other proteins are responsible for the retrograde movement of IFT particles? 2) What is the specific function of an individual IFT-particle protein? To address these two questions, I screened for *Chlamydomonas* mutants either defective in retrograde IFT by immunofluorescence microscopy, or defective in IFT-particle proteins and D1bLIC, a dynein light intermediate chain possibly involved in retrograde IFT, by Southern blotting. I identified several mutants defective in retrograde IFT and one of them is defective in the *D1bLIC* gene. I also identified several mutants defective in several IFT-particle protein genes. I then focused on the mutant defective in D1bLIC and the one defective in IFT46, which was briefly reported as an IFT complex B protein. My results show that as a subunit of the retrograde IFT motor, D1bLIC is required for the stability of DHC1b and is involved in

the attachment of IFT particles to the retrograde motor. The P-loop in D1bLIC is not necessary for the function of D1bLIC in retrograde IFT. My results also show that as a complex B protein, IFT46 is necessary for complex B stability and is required for the transport of outer dynein arms into flagella. IFT46 is phosphorylated *in vivo* and the phosphorylation is not critical for IFT46's function in flagellar assembly.

TABLE OF CONTENTS

LIST OF TABLES

LIST OF FIGURES

CHAPTER I

INTRODUCTION

Eukaryotic cilia and flagella are organelles usually extending from the cell surface into the environment.[1] Almost every mammalian cell contains one or more cilia (Figure 1.1) (http://www.bowserlab.org/primarycilia/cilialist.html). They can exist as motile cilia, such as the sperm tail and those on the surface of the lower and upper respiratory tracts, the oviduct, the brain ventricle epithelium, and the embryonic node. They also can exist as non-motile cilia, such as the connecting cilium in rod and cone cells, the sensory cilia on olfactory neurons, and primary cilia on many cell types.

While motile cilia are obviously involved in the movement of cells and extracellular material, the function of most non-motile cilia has remained unclear and was considered unimportant or insignificant in textbooks for almost 30 years since their first characterization by electron microscopy. However, this view of cilia has changed dramatically in the past several years as more and more evidence shows that, in addition to their function in motility, cilia play a role as cell antennae and also are involved in cell cycle regulation (Pazour and Witman, 2003; Davenport and Yoder,

---

[1] Most eukaryotic organisms have cilia/flagella, with a few exceptions, such as yeast and higher plants. Historically, the term cilia was used when these organelles are short or exist in large quantity on the cell surface, while flagellum was used when the organelle is long and exists singly on the cell surface. Nevertheless, these words can be used interchangeably since cilia and flagella have the same structure and the structures are usually conserved among organisms.

2005; Singla and Reiter, 2006; Satir and Christensen, 2006).

A critical step in understanding the function of cilia was made with the identification and characterization of a cellular process called intraflagellar transport (IFT) (Rosenbaum and Witman, 2002). The function of IFT is to build and maintain cilia and flagella structurally and to transport signals from cilia to the cell body. Mutant analysis of the Tg737 orpk mouse (which is defective in one of the IFT proteins) first linked primary cilia defects with polycystic kidney disease (Pazour et al., 2000). Ever since then, the list of diseases caused by ciliary defects has been expanding greatly (Table 1.1). There is no doubt that a further understanding of IFT will shed more light on the function of cilia and the mechanism underlying these cilia-related diseases.

Chlamydomonas as a model organism for studies on cilia/flagella

The unicellular green algae *Chlamydomonas* is an excellent model organism for research on cilia/flagella (Harris, 2001). *Chlamydomonas* uses its flagella to swim in water and to glide on solid surfaces. Its flagella also serve as sensory organelles during mating. Most *Chlamydomonas* flagellar proteins are conserved among mammals and much of our knowledge on flagella/cilia structure originally came from studies on *Chlamydomonas*. As a model organism, *Chlamydomonas* has the following advantages: 1) It is biochemically amenable. The two flagella of *Chlamydomonas* can be easily isolated in large amount at high purity. The flagella can then be further fractionated into different subfractions, which correlate to different compartments of the flagellum. 2) *Chlamydomonas* is genetically amenable. It is a single cell organism with a sexual life

cycle of haploid and diploid states. Usually *Chlamydomonas* cells are haploid, but under special conditions they can be kept as diploids. Importantly, flagella are not essential for the survival of *Chlamydomonas*, so mutations affecting the flagella can be easily identified in haploid cells and characterized genetically and biochemically. 3) Many laboratory techniques work well in *Chlamydomonas*, including RNAi, HA or GFP tagging, insertional mutagenesis and protein electroporation. 4) There are excellent databases and libraries available for *Chlamydomonas* (http://www.chlamy.org/), including the completed genomic database, EST database, flagellar proteomic database, centriole proteomic database, a database of genes induced by deflagellation, cDNAs on microarray chips, and genomic libraries in the form of bacterial artificial chromosomes (BAC) and phagemid clones. 5) *Chlamydomonas* is cheap to grow and easy to maintain. 6) *Chlamydomonas* is not a pathogen to humans.

Cilia/flagella structure

The defining structure of cilia/flagella includes a microtubular axoneme, which is assembled from the centriole or basal body, and its surrounding membrane, which is continuous with the cell plasma membrane (Figure 1.2). For motile cilia, the axoneme is usually composed of 9 outer doublet microtubules and a pair of central microtubules. Attached to these microtubules are several complex structures, including outer dynein arms, inner dynein arms, radial spokes, and projections from the central pair microtubules. For non-motile cilia, the axoneme is usually composed of 9 outer doublet microtubules only.

There is one row of outer dynein arms and one row of inner dynein arms attached to the A tubule of the outer doublet microtubules (DiBella and King, 2001). In *Chlamydomonas*, the outer dynein arm pre-assembles in the cell body. Its subunits include 3 dynein heavy chains (DHCs), 2 intermediate chains (ICs), and several light chains (LCs). The outer dynein arm attaches to the doublet microtubule via a docking complex, which is composed of three subunits (DC1, DC2, and DC3). The outer dynein arms are responsible for generating about 4/5 of the power for flagellar movement (Kamiya, 2002). When the docking complex or the outer dynein arm is defective, *Chlamydomonas* cells swim in a slow and jerky manner. The inner dynein arms are more complicated than the outer dynein arms in that there are several different species. The most well characterized subspecies is I1 (also known as subspecies f), which is composed of two DHCs, two ICs and several other subunits. *Chlamydomonas* inner dynein arm mutants swim slowly, and detailed analyses at the movement of these flagella indicate that the inner dynein arms are important for control of the flagellar waveform (Kamiya, 2002)

The regulation of the activity of the dynein arms involves the radial spokes and the central pair apparatus. These structures are believed to serve as mechano-chemical sensors to control motility in 9+2 cilia and flagella (Smith and Yang, 2004). The *Chlamydomonas* radial spoke is composed of a thin stalk and a bulbous head. The spokes are attached to the A tubule of the outer doublet microtubule at the base of the stalk. Their heads contact the central pair apparatus. There are at least 23 proteins in the radial spoke (Yang et al., 2006). 18 of them have been characterized at the molecular

level. Among the 18 spoke proteins, at least 12 have apparent homologues in humans. The central pair apparatus is composed of two single microtubules and their associated structures including the central pair projections, the central pair bridges linking the two tubules, and the central pair caps which are attached to the distal or plus ends of the microtubules. The central microtubule with longer projections is termed the C1 microtubule and the other is called the C2 microtubule. At lease 23 polypeptides in addition to tubulin comprise the central pair apparatus. Eight of them have been characterized at the molecular level.

Though most attention has been paid to the axoneme, the flagellar membrane also is very important. The flagellar membrane is a different compartment from the rest of the plasma membrane, because the transport of molecules into the flagellar membrane is tightly controlled at the base of the flagella. Its physical location makes it better positioned to sense the environment than the rest of the plasma membrane. Several proteins have been shown to be specifically localized on the flagella membrane, including Smo (Corbit et al., 2005) and polycystin-2 (Pazour et al., 2002).

Intraflagellar transport

There are at least 360 proteins in the *Chlamydomonas* flagellum (Pazour et al., 2005). All these proteins need to be transported from the site of synthesis, which is in the cell body, to the flagella. Once in the flagella, they need to be assembled. How these processes occur had been an enigma until the discovery of IFT.

IFT was first observed by differential interference contrast (DIC) microscopy in *Chlamydomonas* (Kozminski et al., 1993) as the bidirectional movement of granule-like particles (IFT particles) along the length of the flagellum (Figure 1.3). The movement from the base to the tip of the flagella is called anterograde IFT and the movement from the tip to the base of the flagella is called retrograde IFT. The proteins composing the IFT particles are called IFT-particle proteins. IFT has been shown to be a conserved process required for flagellar assembly, maintenance and normal function in virtually all ciliated organisms. Much progress has been made in identifying components of the IFT machinery and the functions of IFT as a whole (Rosenbaum and Witman, 2002; Cole, 2003; Scholey, 2003).

Table 1.2 is a list of currently known IFT components in *Chlamydomonas*, *C. elegans*, and mammals. They are sub-grouped into the anterograde IFT motor, the retrograde IFT motor, IFT-particle proteins, and other IFT proteins. Anterograde IFT is powered by kinesin 2 in *Chlamydomonas*, kinesin 2 and OSM-3 in *C. elegans*, kinesin 2 in mammals, and possibly KLP-6 in *C. elegans* and KIF17 in mammals. The retrograde IFT motor is cytoplasmic dynein 1b (also called cytoplasmic dynein 2) in all three organisms. The IFT-particle proteins include ~16 subunits, which were initially isolated in *Chlamydomonas* (Cole et al., 1998). These IFT-particle proteins have been sequenced, but the sequences provide few hints as to the proteins' functions. Recognizable domains consist mainly of WD repeats, TPR domains, and coiled-coil domains, all of which are thought to be involved in protein-protein interactions (Cole, 2003; Figure 1.4). These IFT-particle proteins separate into two complexes during

purification, complex A and complex B. Biochemical analysis has revealed that complex B contains a ~500-kD core composed of IFT88, IFT81, IFT74/72, IFT52, IFT46 and IFT27 (Lucker et al., 2005). More recently, several additional proteins were reported to be associated with IFT in *C. elegans*, and *C. elegans* mutants defective in these proteins have defects in cilia assembly. Since no biochemical data are available to indicate whether they are complex A or complex B proteins, they are grouped as other IFT proteins. As shown in the table, most of the IFT components are conserved among organisms. The conservation of this process among different organisms implies that IFT is an ancient and important cellular process. The small variations among organisms imply that IFT might be modified during evolution to carry out unique functions in specific organisms.

As for the function of IFT, there is no doubt that IFT is required for the assembly of flagella. Mutant analysis of *Chlamydomonas* null mutants defective in IFT motor genes or IFT-particle protein genes shows that they can not assemble flagella at all or can only form short stumpy flagella, which are filled with IFT-particle proteins in the case of retrograde IFT motor defects (Table 1.2). Similar results were obtained from *C. elegans* and mouse mutants defective in IFT components (Table 1.2). IFT is also required for the maintenance of flagella, as *Chlamydomonas* temperature sensitive mutants defective in the anterograde IFT motor or IFT172 gradually resorb their flagella when shifted to the restrictive temperature (Huang et al., 1977; Adams et al., 1982; Pedersen et al., 2005). In addition to its role in flagella assembly and maintenance, IFT has been shown to be involved in signal transduction during mating

in *Chlamydomonas* (Wang et al., 2006) and in the Hedgehog pathway and Wnt pathway in mouse (Singla and Reiter, 2006).

As the significance of IFT is becoming more and more appreciated, researchers are also trying to dissect the mechanism of IFT, including how IFT-particle proteins assemble into large particles, how the IFT motors are regulated, what cargos are carried by IFT, how the cargos are loaded, and how IFT is integrated into the other pathways in cell differentiation and cell cycle regulation. Some progress has been made, although much more is needed. For example, biochemical analysis in *Chlamydomonas* revealed that within the IFT complex B core, IFT81 interacts with IFT72 directly (Lucker et al., 2005). In *C. elegans*, two kinesin motors, heterotrimeric kinesin 2 and homodimeric OSM-3, coordinate to move IFT particles along the middle segment of cilia in the sensory neuron, and then OSM-3 alone moves IFT particles along the distal segment of the cilia (Snow et al., 2004). DYF-1 is probably involved in the activation of OSM-3 by attaching IFT particles to OSM-3, while BBS7 and BBS8 are involved in maintaining the integrity of the whole IFT complex so that both kinesins can move IFT particles together (Ou et al., 2005). IFT172 is involved in the regulation of flagellar assembly/dissembly at the flagellar tip (Pedersen et al., 2005). In mammals, IFT20 has been proposed to be the link between kinsein 2 and the IFT particles (Baker et al., 2003); IFT20 also is associated with the Golgi complex and has been proposed to be involved in trafficking of ciliary membrane components (Follit et al., 2006). IFT particles are associated with pericentrin in the basal body region at the base of the cilia (Jurczyk et al., 2004). Inner dynein arms (Piperno and Mead, 1997; Piperno et al.,

1996), radial spokes (Qin et al., 2004) and some membrane proteins, such as the transient receptor potential vanilloid (TRPV) channels OSM-9 and OCR-2 (Qin et al., 2005), have been shown to be the cargos of IFT.

To elucidate more about the mechanism of IFT, I used *Chlamydomonas* as a model organism and began by screening for mutants defective in IFT components. I identified the first mutants for four IFT particle proteins (IFT140, IFT172, IFT46, and IFT20) and D1bLIC, a dynein light intermediate chain. Then I focused on the analysis of two individual proteins, D1bLIC and IFT46. My work identified D1bLIC as a subunit of the retrograde IFT motor necessary for attaching IFT particles to the motor. I confirmed that IFT46 is a complex B protein and showed that it is specifically involved in outer dynein arm transport into the flagellum.

Table 1.1 **Defects in cililary functions cause several human diseases**

Ciliary function	**Disease phenotype**	**References**
Photoreception	Retinal degeneration	Pazour et al., 2002
Odorant reception	Anosmia	Kulaga et al., 2004
Mechanosensation	Cystic kidney disease	Pazour et al., 2000 Praetorius and Spring, 2001
Gli repressor formation	Polydactyly, neural patterning defects	Liu et al., 2005
Gli activator formation	Neural patterning defects	Huangfu et al., 2003
Convergent extension	Neural tube closure defects	Ross et al., 2005
Unknown	Symptoms of Bardet-Biedl syndrome including obesity, male hypogonadism, diabetes mellitus, hepatic fibrosis, ataxia, dental crowding, et al.	Blacque and Leroux, 2006
Ciliary motility	Situs inversus	Nonaka et al., 1998
	Hydrocephalus	Ibanez-Tallon et al., 2004
	Symptoms from Primary Ciliary Dyskinesia (PCD, also known as Immotile Cilia Syndrome) including sinusitus, bronchiectasis, infertility	Carlen et al., 2005

Modified from Singla and Reiter, 2006.

Table 1.2. **Known IFT components**

Complex type		***Chlamydomonas* protein name**	***Chlamydomonas* mutant phenotype**	***Caenorhabditis elegans* homologue**	**Mammalian homologue**	**References**
IFT motors	Anterograde motor	FLA10[1]	Bald	CeKRP85 (KLP-20)	KIF3A*[2]	[1] Cole et al., 1998 [2] Takeda et al., 1999
		FLA8[1]	Bald	CeKRP95 (KLP-11)	KIF3B*[2]	[1] Miller et al., 2005 [2] Nonaka et al., 1998
		KAP[1]	Bald	CeKAP (KAP-1)	KAP3[2]	[1] Mueller et al., 2005 [2] Yamazaki et al., 1996
		NA		Osm-3[1]	KIF17[2]	[1] Snow et al., 2004 [2] Jenkins et al., 2006
		NA		KLP-6[1]		[1] Peden and Barr, 2005
	Retrograde motor	DHC1b[1,2]	Short, stumpy flagella	CHE-3[3,4]	DHC2	[1] Pazour et al., 1999 [2] Porter et al., 1999 [3] Signor et al., 1999 [4] Wicks et al., 2000
		LC8[1]	Short flagella	XBX-2	DLC-1	[1] Pazour et al., 1998
		D1bLIC[1,3]	Short, stumpy flagella	XBX-1[2]	D2LIC	[1] Perrone et al., 2003 [2] Schafer et al., 2003 [3] Hou et al., 2004
IFT-particle protein	Complex A	IFT144		DYF-2[1]	WDR19	[1] Efimenko et al., 2006
		IFT140	Short, stumpy flagella[1]	CHE-11[2]		[1] Bethany Walker, personal communication [2] Qin et al., 2001
		IFT139		ZK328.7		
		IFT122A		DAF-10[1]		[1] Qin et al., 2001
		IFT122B		IFTA-1[1]		[1] Blacque et al., 2006
		IFT43				

Complex type		***Chlamydomonas* protein name**	***Chlamydomonas* mutant phenotype**	***Caenorhabditis elegans* homologue**	**Mammalian homologue**	**References**
IFT-particle protein	Complex B periphery	IFT172	Bald[1]	OSM-1[2]	SLB*[3,4]	[1] Pederson et al., 2005 [2] Cole et al., 1998 [3] Huangfu et al., 2003 [4] Howard and Maurer, 2000
		IFT80[1]		CHE-2[1,2]		[1] Qin et al., 2001 [2] Fujiwara et al., 1999
		IFT57/55	Short flagella[1]	CHE-13[2]	Hippi*[3,4]	[1] Pazour, unpublished results [2] Haycraft et al, 2003 [3] Gervais et al., 2002 [4] Houde et al., 2006
		IFT20	Short, stumpy or bald flagella[1]	Y110A7A.20	IFT20[2,3]	[1] Witman, unpublished [2] Baker et al., 2003 [3] Follit et al., 2006
	Complex B core	IFT88	Bald[1]	OSM-5[2]	Tg737 (polaris)*[1]	[1] Pazour et al., 2000 [2] Qin et al., 2001
		IFT74/72[1]		C18H9.8		[1] Qin et al., 2004
		IFT81		F32A6.2		
		IFT52	Bald[1,2]	OSM-6[3,]	NGD5*[4,5]	[1] Deane et al., 2001 [2] Brazelton et al., 2001 [3] Collet et al., 1998 [4] Wick et al., 1995 [5] Liu et al., 2005
		IFT46	Short, stumpy flagella[1]	DYF-6[2]		[1] Hou et al., 2007 [2] Bell et al., 2006
		IFT27		NA	NA	
		IFT25		NA	NA	

Complex type		***Chlamydomonas* protein name**	***Chlamydomonas* mutant phenotype**	***Caenorhabditis elegans* homologue**	**Mammalian homologue**	**References**
Other IFT proteins		estExt_GenewiseW_1.C_410007		DYF-13[1]		[1] Blacque et al., 2005
		C_10017		DYF-3 (qilin)[1,2]		[1] Murayama et al., 2005 [2] Ou et al., 2005
		C_420025		DYF-1[1]		[1] Ou et al., 2005
		C_1330001		OSM-12[1,2]	BBS7	[1] Blacque et al., 2004 [2] Ou et al., 2005
		C_970071		BBS8[1,2]	BBS8	[1] Blacque et al., 2004 [2] Ou et al., 2005
		NA	NA	IFTA-2[1]	RabL-5	[1] Schafer et al., 2006

* indicates that mutant mouse is available.

Figure 1.1. **Motile or immotile cilia are on nearly every cell within the mammalian body.** (A) Transmission electron microscopy (TEM) image of a mouse rod cell showing the connecting cilia. (B) Scanning electron microscopy (SEM) image of a mouse olfactory cilium (Kessel and Kardon, 1979). (C) SEM image of a mouse outer hair cell that has three rows of individual stereocilia and a true cilium, the kinocilium (white arrow) (Frolenkov et al., 2004). (D) SEM image of mouse tracheal cilia (Y. Vucica). (E) SEM image of motile cilia present on mouse ependymal cells located in the lateral ventricles (Davenport and Yoder, 2005). (F) SEM image of a mouse sperm, which is bound to an egg. (G) SEM image of oviduct cilia. The central cell has a primary cilum. Surrounding cells are multiciliated with motile cilia (Satir and Christensen, 2006). (H) SEM image of primary cilia of the mouse node (Singla and Reiter, 2006). (I) SEM image of a solitary primary cilium projecting from the surface of an ectodermal cell in the developing limb bud of an embryonic day 10.5 mouse embryo. (Davenport and Yoder, 2005) (J) IF image of a cultured mouse cell with a primary cilia in green (G. Pazour).

Figure 1.1

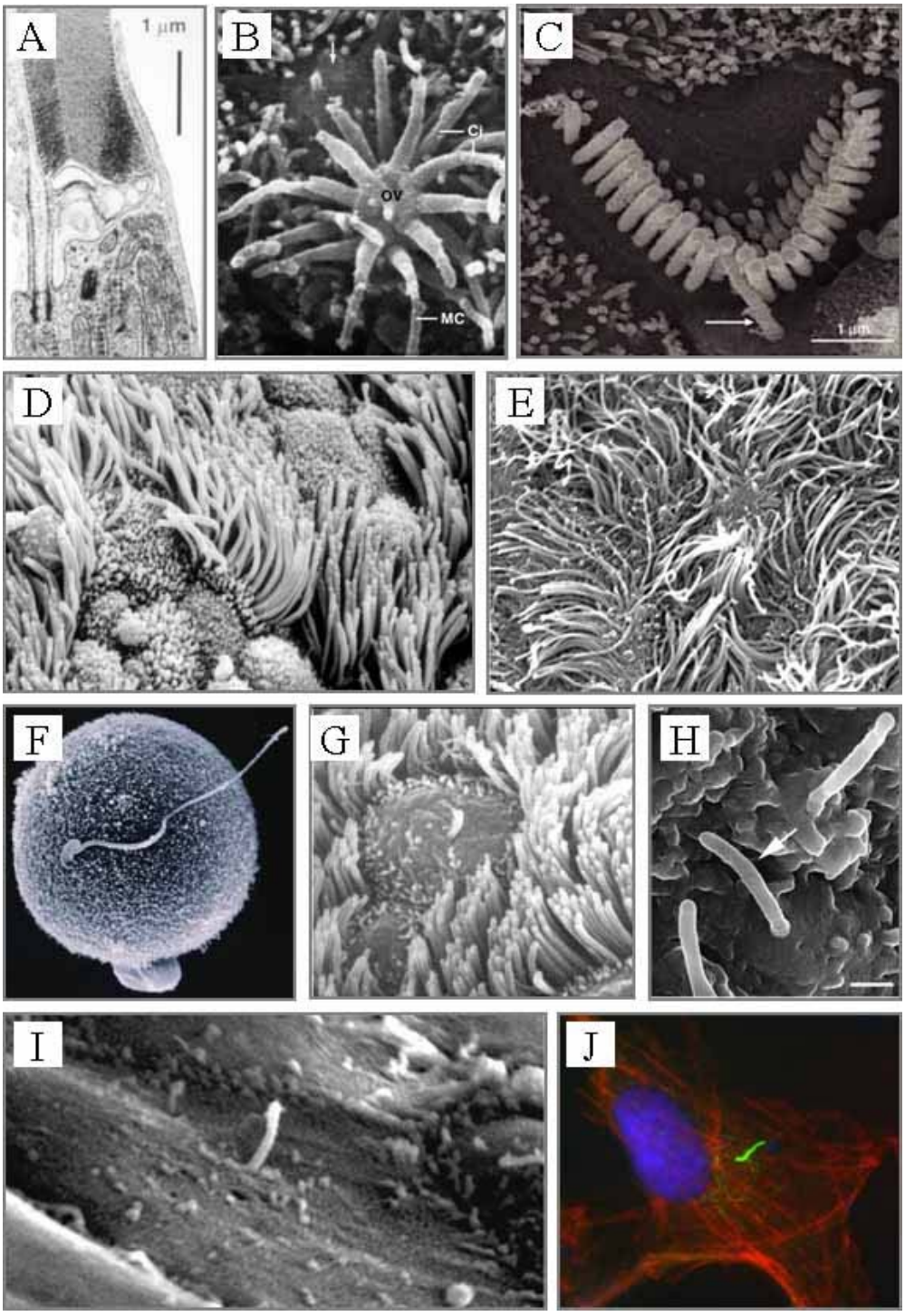

Figure 1.2. **Cilia/flagella structure is conserved among organisms.** (A) TEM image of a cross-section of human motile 9+2 cilum (Satir and Christensen, 2006). (B) TEM image of a cross-section of a *Chlamydomonas* flagellum (Rosenbaum and Witman, 2002). (C) Schematic image of the cross-section of a motile cilium/flagellum (Rosenbaum and Witman, 2002). A and B: A- and B-tubules of outer doublet microtubules; CPP: projections from the central pair of microtubules; FM: flagellar membrane; IA: inner dynein arms; OA: outer dynein arms; RS: radial spokes. Non-motile cilia lack the central pair apparatus, radial spokes, and the dynein arms.

Figure 1.2

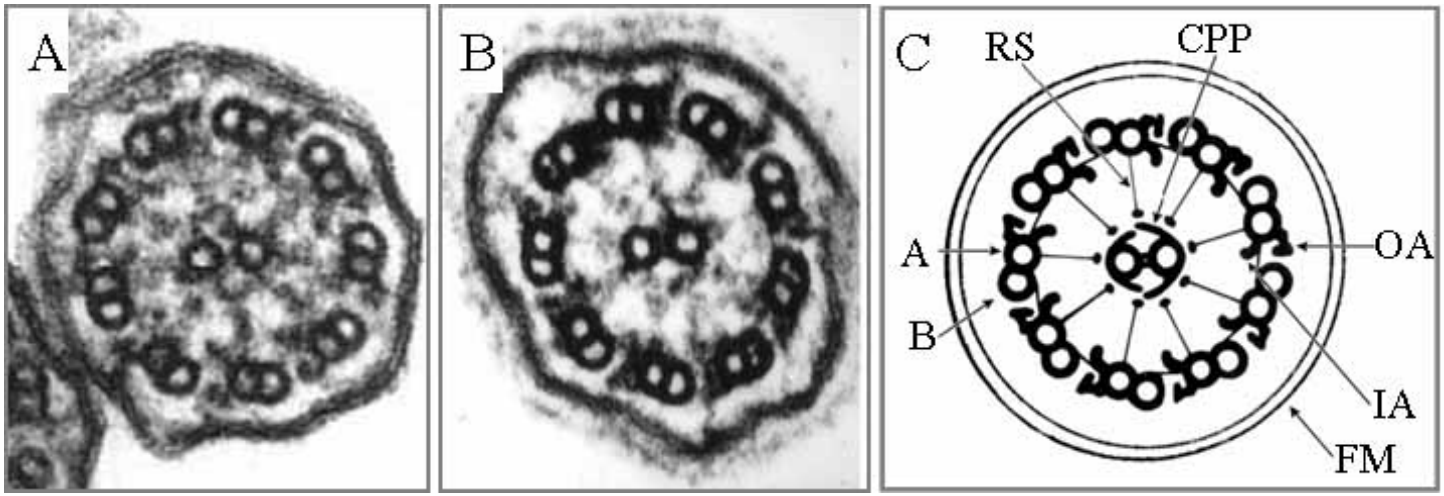

Figure 1.3. **Intraflagellar transport is the bi-directional movement of particles along the length of flagella.** (A) TEM image of a longitudinal section through a *Chlamydomonas* flagellum showing linear arrays of IFT particles between the outer doublet microtubules and the flagellar membrane (Rosenbaum and Witman, 2002). Note the links between the rows of IFT particles and the outer doublet microtubules, as well as the close association between the IFT particles and the flagellar membrane. (B) A schematic picture showing the IFT machinery (Rosenbaum and Witman, 2002). During IFT, linear arrays of IFT particles (yellow) are transported towards the 'plus' (distal) ends of the flagellar outer doublet microtubules (blue) by kinesin-II (pink), and towards the 'minus' (proximal) ends of the microtubules by cytoplasmic dynein 1b (green). The IFT particles, which are composed of at least 16 different proteins, are believed to be carrying precursors that are necessary for the assembly of the flagellar axoneme. The IFT particles are linked to the flagellar membrane (grey lines), which indicates that their cargo might also include membrane proteins.

Figure 1.3

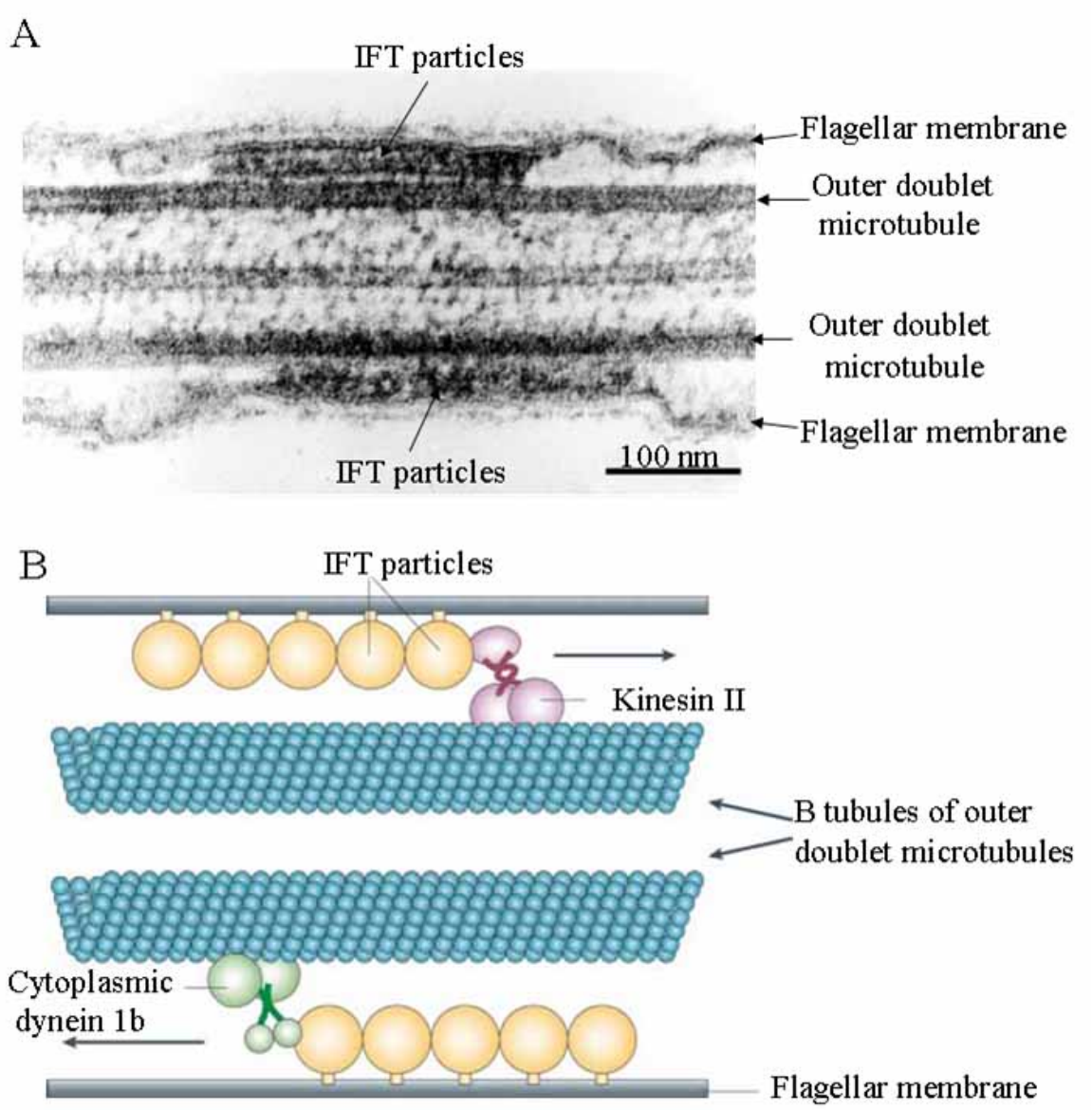
A
IFT particles
Flagellar membrane
Outer doublet microtubule
Outer doublet microtubule
Flagellar membrane
IFT particles
100 nm
B
IFT particles
Kinesin II
B tubules of outer doublet microtubules
Cytoplasmic dynein 1b
Flagellar membrane

Figure 1.4. **Known *Chlamydomonas* IFT-particle proteins.** These IFT-particle proteins fall into two complexes, complex A and complex B, during purification. They were named according to their apparent molecular weight. They have been characterized at the molecular level. Putative protein–protein binding motifs have been identified through sequence analysis. WD: WD40 repeats; DR: degenerate repeats; TPR: tetratricopeptide repeats; COIL: coiled coil. Figure from Cole, 2003.

Figure 1.4

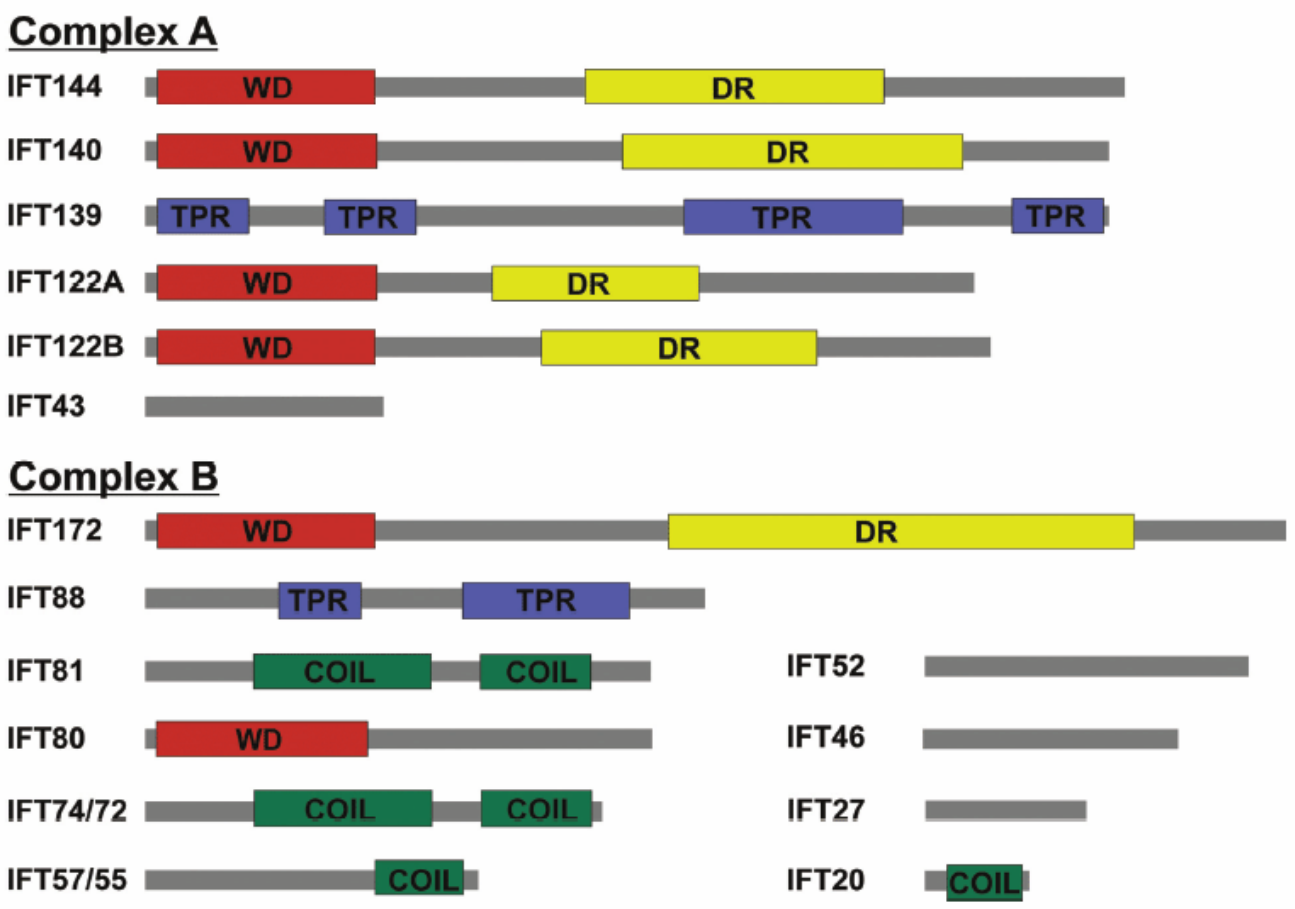
Complex A
IFT144
WD
DR
IFT140
WD
DR
IFT139
TPR
TPR
TPR
TPR
IFT122A
WD
DR
IFT122B
WD
DR
IFT43
Complex B
IFT172
WD
DR
IFT88
TPR
TPR
IFT81
COIL
COIL
IFT52
IFT80
WD
IFT46
IFT74/72
COIL
COIL
IFT27
IFT57/55
COIL
IFT20
COIL

CHAPTER II

MATERIALS AND METHODS

Strains and culture media

Chlamydomonas reinhardtii strains used in the work include: g1 (*nit1*, *NIT2*, *mt+*), 137c (*nit1*, *nit2*, *mt+*), CC124 (*nit1*, *nit2*, *mt–*) (*Chlamydomonas* Genetics Center, Duke University, Durham, NC), A54-e18 (*nit1–1*, *ac17*, *sr1*, *mt+*; Schnell and Lefebvre, 1993; Nelson et al., 1994), and 3088.4 (*dhc1b-1::NIT1*, *nit1*, *mt+*; Pazour et al., 1999). TBD9–1 (*d1blic::NIT1*, *nit1*, *mt+*) was generated by transforming A54-e18 with the plasmid pMN56 linearized with EcoRI (Nelson et al., 1994) and was generously provided by T. Bui and C. Silflow (University of Minnesota at St. Paul) via W. Dentler (University of Kansas, Lawrence). YH43 (*d1blic::NIT1*, *mt-*) is a progeny of a cross between TBD9–1 and CC124. T8a4-11 *(ift46::NIT1*, *nit1*, *pf1*, *mt+*) was generated by K. Kozminski and J. Rosenbaum (Yale University, CT) by transforming KK30A3 (*nit1*, *NIT2*, *pf1*, *mt+*) with the plasmid pMN24 linearized with EcoRI. YH6 (*ift46::NIT1*, *PF1*, *mt+*) is a progeny of a cross between T8a4-11 and CC124. $Sup_{ift46}1$ is a spontaneous partial suppressor for YH6.

Cells were grown in M (Sager and Granick [1953] medium I altered to have 0.0022 M KH_2PO_4 and 0.00171 M K_2HPO_4), M-N (M medium without nitrogen), SGII-NO_3 (Sager-Granick medium lacking ammonium) (Kindle, 1990), or TAP (Tris-acetate-phosphate) (Gorman and Levine, 1965) media.

Antibodies

The antibodies used are listed in Table 2.1.

The rabbit polyclonal antibody to D1bLIC was generated against a maltose binding protein-tagged D1bLIC fusion protein, which contains amino acids 55-427 of D1bLIC. To make the fusion protein, a 1.3-kb fragment of the *Chlamydomonas* D1bLIC cDNA was amplified by PCR from the cloned D1bLIC cDNA using primer pairs D1bLIC-11 (all the primers are shown in Table 2.2) and D1bLIC-12. The PCR product was digested with EcoRI and inserted in the EcoRI site of pMAL-cR1 (New England Biolabs, Beverly, MA). Expression of this construct in *Escherichia coli* produced a protein in which the C-terminal 373 amino acids (starting at the sequence TLLNRFL) of D1bLIC were fused to the maltose-binding protein. John Follit (UMASS) expressed this fusion protein and purified it by amylose affinity chromatography. The antibodies were produced in rabbits (Research Genetics, Huntsville, AL). The same 1.3-kb PCR product was inserted into the EcoRI site of the pGEX-6P vector (Amersham Pharmacia Biotech, Piscataway, NJ). The expression product of this construct was used to affinity purify anti-D1bLIC antibodies as described in Pazour et al. (1999).

The rabbit antibody to IFT46 was generated by Dr. H. Qin (Yale University, New Haven CT) against a synthetic peptide corresponding to the protein's N-terminal 19 amino acids (Pocono Rabbit Farm, Canadensis, PA), and affinity purified using the same 19 amino-acid peptide.

Transformation and genetic analysis

Transformation was performed using the glass bead method of Kindle (1990) as described in Pazour et al. (1995). For insertional mutagenesis, cells of strain g1 were treated with freshly made autolysin for 20 minutes to remove the cell wall. They were then transformed with XbaI linearized pGP505 plasmid which contains the *NIT1* gene (Pazour et al., 1995). The transformants were picked from SGII-NO_3 plates to 125 ml M medium aerated with 95% air + 5% CO_2 and were subjected to light microscopy analysis at middle log phase. Cells with motility defects were named as Y series and subjected to further characterization.

To rescue *d1blic* mutant cells, cloned D1bLIC genomic DNA and linearized plasmid pSP124S (from Dr. S. Purton, University College London; Lumbreras et al., 1998) were cotransformed into cells. The zeocin-resistant cells were recovered as described in Lumbreras et al. (1998) except that zeocin (CAYLA, F-31405 Toulouse cedex 4, France) was used at 4 μg/ml in our experiments. *ift46* mutant cells were co-transformed with linearized plasmid pSP124S and the cloned 4.8-kb fragment, which contains only the wild-type *IFT46* gene.

TBD9–1 and CC124 gametes or T8a4-11 and CC124 gametes were induced to mate by dibutyryl-cAMP and papaverine treatment and then were allowed to form mature zygotes on solid medium as described in Pazour et al. (1999). The plates were then kept at -20°C for 2 days to kill the vegetative cells. Plates were returned to light and 23°C for the tetrads to develop. The colonies that developed from each tetrad were streaked out and single colonies originating from each tetrad were transferred to 125 ml of M medium. Cells were allowed to grow to middle log phase and then were scored for motility by microscopic observation of cells illuminated with dim red light. DNAs from the progenies were prepared for Southern analysis.

Mutant identification by immunofluorescence microscopy and Southern blotting

Strains of the mutant collection were screened by immunofluorescence microscopy using an antibody to IFT172 or IFT139. Strains that accumulate these IFT-particle proteins in the flagella were picked as mutants defective in retrograde IFT.

To check if the DHC1b gene was mutated in the retrograde mutants, three cDNA probes were used in Southern blotting. They were amplified from a cDNA library using primer pair DHC1bcDNA11/DHC1bcDNA12 for probe 1, primer pair DHC1bcDNA07/DHC1bcDNA08 for probe 2, and primer pair DHC1bcDNA09/DHC1bcDNA10 for probe 3.

Strains of the mutant collection were screened by Southern blotting using cDNA probes specific for genes encoding IFT20, IFT27, IFT46, IFT57, IFT72, IFT81, IFT88, IFT122, IFT139, IFT140, and D1bLIC. The genomic DNAs were cut by PstI. cDNA

probes for IFT20, IFT27, IFT57, IFT72, IFT81, IFT88, IFT122, IFT139, and IFT140 were gifts from Dr. J. Rosenbaum's lab. The full-length D1bLIC cDNA probe was amplified by PCR with primers D1bLIC-5 and D1bLIC-6. The 864-bp partical IFT46 cDNA probe was amplified by PCR with primers IFT46-Q1 and IFT46-Q2 by Dr. H. Qin.

Chlamydomonas D1bLIC gene and IFT46 gene cloning

Dr. G. Pazour (UMASS) obtained a pair of the expressed sequence tag (EST) sequences (894070A09) by searching the *Chlamydomonas* EST database (http://www.biology.duke.edu/chlamy_genome/blast/blast_form.html) using the mammalian D2LIC sequence. Starting with the EST sequences, the intervening region of the *Chlamydomonas D1bLIC* cDNA was cloned from a *Chlamydomonas* cDNA library by PCR amplification using primer pairs D1bLIC-5 and D1bLIC-6. The cDNA was used to screen a *Chlamydomonas* genomic library filter (http://www.genome.clemson.edu/orders/) and six positive BAC clones (01O10, 18L01, 22E07, 31J16, 37P12, and 38N05) were obtained. When the BACs were digested with different restriction enzymes and the digests were analyzed by Southern blotting with the *D1bLIC* cDNA as a probe, each was confirmed to contain the same *D1bLIC* gene. The 01O10 BAC clone was subcloned into a 10-kb SmaI-HindIII cassette and then further subcloned into a 7.3-kb SmaI-SacI cassette that contained only the *D1bLIC* gene. 5692 base pairs of genomic DNA, from 819 base pairs upstream of the D1bLIC start codon to 1354 base pairs downstream of the D1bLIC stop codon, were sequenced from

the 7.3-kb SmaI-SacI cassette. The start of the 5' untranslated region and the site of polyadenylation were determined by searching the *Chlamydomonas* EST database. The coding regions were determined by sequencing PCR products (containing sequences from nucleotides 58–1773) from a cDNA library. GenBank accession number for the *Chlamydomonas* D1bLIC is AY616759.

We initially obtained the IFT46 cDNA sequence from Dr. H. Qin. She purified 16S IFT particles from *Chlamydomonas* flagella (Cole et al., 1998) and separated the IFT-particle proteins by PAGE. A band corresponding to IFT46 was excised and microsequenced. Two peptides, VPRPDTKPDYLGLK and IKPFIPDYIPAVGGIDEFIK, were obtained; these identified the protein C_2130007 predicted by the *Chlamydomonas* genome (v. 2; http://genome.jgi-psf.org/cgi-bin/searchGM?db=chlre2). Several EST clones in Genbank that contain these two peptides in their ORF were used to clone the IFT46 cDNA.

A 4.8-kb fragment that contains only the full-length *IFT46* gene was cloned from *Chlamydomonas* genomic DNA following its amplification by PCR with primers IFT46-5 and IFT46-6 using eLONGase Enzyme Mix (Invitrogen, Carlsbad, CA). The sequences of the 5’- and 3’-untranslated regions of the IFT46 cDNA (GenBank accession number: DQ787426) were verified by sequencing the cloned *IFT46* gene; the sequence of the coding region was verified by sequencing a PCR product from a cDNA library.

Sequence analysis

The ProtParam tool at http://us.expasy.org/tools/protparam.html was used to calculate the predicted molecular weight and theoretical pI of D1bLIC and IFT46. D1bLIC and IFT46 homologues were identified by searching the translated nr database at http://www.ncbi.nlm.nih.gov/BLAST/. The predicted *Chlamydomonas* D1bLIC protein or IFT46 protein sequence was compared with the mammalian homologue using the Pairwise BLAST program at http://www.ncbi.nlm.nih.gov/BLAST/. The ScanProsite program at http://us.expasy.org/prosite/ was used to search protein families and domains. Protein motif fingerprints were searched using the PRINTS BLAST database at http://www.bioinf.man.ac.uk/dbbrowser/PRINTS/. The coils program (version 2.2) available at http://www.ch.embnet.org/software/COILS_form.html (Lupas et al., 1991; Lupas, 1996) was used for coiled-coil predictions. Multiple sequences were aligned using ClustalW (1.83) at http://www.ebi.ac.uk/clustalw/. The TreeTop program with the cluster algorithm at http://www.genebee.msu.su/services/phtree_reduced.html was used to compute the phylogenetic tree for DLICs from different species.

RNA and DNA isolation and analysis

DNA was isolated from *Chlamydomonas* by digesting the cells with proteinase K as described in Pazour et al. (1998). For determination of the patterns of gene expression, total RNA was obtained from cells before deflagellation and 30 min after deflagellation by pH shock as described in Witman et al. (1972) and Lefebvre and Rosenbaum (1986). Total RNA was obtained either by digesting the cells with lysis buffer (20 mM Tris pH 8.0, 20 mM EDTA, 5% SDS, and 1 mg/ml proteinase K) followed by

phenol/chloroform (50/50) purification, isopropanol precipitation and then LiCl precipitation or by using TRIzol® LS Reagent (Invitrogen Life Technologies, Carlsbad, CA). Messenger RNAs were purified from total RNA using the Oligotex® kit from Qiagen (Valencia, CA). Messenger RNAs were reverse-transcribed to cDNAs using PowerScript Reverse Transcriptase™ from Clonetech (Mountain View, CA).

Gel electrophoresis, Southern blotting, and northern blotting were performed using standard procedures (Sambrook et al., 1987). Southern blotting with non-radioactive probe was performed using the DIG High Prime DNA Labeling and Detection Starter Kit II (Roche Applied Science, Penzberg, Germany); instead of using the kit's hybridization buffer, I used Church buffer (7% SDS, 1 mM EDTA, 0.25 M Na_2HPO_4, pH 7.2) (Church and Gilbert, 1984) and hybridized at 65ºC.

The mutated region in the *IFT46* gene in the mutant was located by PCR using primer pairs 1 (IFT46-1/IFT46-2), 2 (IFT46-9/IFT46-10), and 3 (IFT46-3/IFT46-4).

IFT46 gene induction upon deflagellation was analyzed by real-time PCR as described in Pazour et al. (2005) using primers IFT46-3 and IFT46-4. The ratio of the amount of IFT46 message after deflagellation to that before deflagellation was calculated for each trial. Three independent sets of mRNA were isolated and analyzed three times each.

To measure mRNA levels of IFT140, IFT139, IFT81, and IFT72, cDNAs were prepared from wild-type and *ift46* cells at the mid-log phase of growth, and quantitated by real-time PCR as described in Pazour et al. (2005) using the primer pairs

IFT140F/IFT140R, IFT139F2/IFT139R2, IFT81F/IFT81R, or IFT72F2/IFT72R2. Two independent sets of mRNA were isolated and analyzed three times each.

To check transcription of the *IFT46* gene, cDNAs were prepared from wild-type cells and from *ift46* and $Sup_{ift46}1$ cells with or without aeration. Real-time PCR was carried out using primer pairs to the 5' end of the gene (IFT46-11/IFT46-2), middle part of the gene (IFT46-9/IFT46-28), and the 3' end of the gene (IFT46-3/IFT46-4). Samples were normalized using G protein β subunit (Pazour et al., 2005; Schloss, 1990). The end products were examined by electrophoresis in a 1.5% agarose gel. Three independent sets of mRNA were isolated and analyzed three times each.

Protein biochemistry

Preparation of *Chlamydomonas* whole cell extracts, isolated flagella and the flagellar membrane-plus-matrix fraction, as well as PAGE and western blotting, were performed as described in Pazour et al. (1999). To obtain the flagellar matrix fraction, fresh flagella in HMDEK buffer (10 mM HEPES, pH 7.2, 5 mM $MgSO_4$, 1 mM DTT, 0.5 M EDTA, and 25 mM KCl) were flash frozen in liquid nitrogen and thawed to effect disruption of the flagellar membrane as described by Zhang and Snell (1995). The sample was centrifuged at 16,000 rpm for 20 min at 4°C using an SS-34 rotor (Sorvall Products, Newtown, CT), and the supernatant was collected. For ultracentrifugation analysis, the samples were fractionated through 12-ml 5–20% sucrose density gradients in a SWTi41 rotor at 36,000 rpm with the ultracentrifuge preset at 64,000 $RAD^2/SEC \times 10^7$. Gradients were fractionated into 0.5-ml aliquots and subsequently analyzed by

SDS-PAGE and western blotting. Thyroglobulin (19.4 S), catalase (11.3 S), and BSA (4.4 S) were used as sedimentation standards.

To determine if IFT46 was phosphorylated, wild-type flagella were treated with calf intestinal phosphatase (New England Biolabs, Ipswich, MA) at 37℃ for 30 minutes. The control sample was treated identically without calf intestinal phosphatase.

For mass spectrometry (MS) analysis of IFT46 phosphorylation, proteins in sucrose gradient fractions containing the IFT46 peak from a wild-type membrane-plus-matrix preparation were concentrated by methanol/chloroform precipitation (Wessel and Flugge, 1984) and then were separated on a 10% acrylamide gel. The gel was stained by coomassie blue and the band that corresponded to IFT46 was excised. The band was analyzed by MS by Dr. John Leszyk at the University of Massachusetts Medical School Proteomic Mass Spectrometry Laboratory.

For immunoprecipitation, protein A-Sepharose beads (Amersham Pharmacia Biotech, Piscataway, NJ) were washed with HMDEK buffer + 3% BSA three times and then incubated with the anti-D1bLIC antibody in the same buffer for 1 h at 4°C. The beads were then washed twice with HMDEK buffer and incubated with freshly made flagellar matrix fraction for 1 h at 4°C. Beads with the immune complex were collected by centrifugation and were washed three times with HMDEK buffer. The supernatant and the final pellet were analyzed for D1bLIC and DHC1b protein levels using SDS-PAGE and western blotting. In the control experiment, affinity-purified pre-immune serum was used instead of affinity-purified anti-D1bLIC antibody.

Electron and immunofluorescence microscopy

Cells were fixed in glutaraldehyde for TEM (Hoops and Witman, 1983) and processed as described in Wilkerson et al. (1995). *Chlamydomonas* cells were fixed and stained for immunofluorescence microscopy by the alternate protocol of Cole et al. (1998) using Alexa Fluor® 488- or 568-conjugated secondary antibodies (Molecular Probes, Eugene, Oregon); images were acquired with an AxioCam camera, AxioVision 3.1 software, and an Axioskop 2 plus microscope (Zeiss, Thornwood, NY). Images were prepared for final publication using Adobe Photoshop 6.0 (Adobe Systems, San Jose, CA).

HA-tagging of *D1bLIC* genes and site-directed mutagenesis

A 2.3-kb SmaI-SacI fragment containing the 3′ end of the *D1bLIC* gene was removed from the 7.3-kb SmaI-SacI cassette containing the *D1bLIC* gene. It was cut by KasI and was blunted by T4 DNA polymerase. A 120-base pair fragment encoding three copies of the influenza hemagglutinin epitope (3HA) from the p3xHA plasmid (from Dr. C. Silflow, University of Minnesota; Silflow et al., 2001) was inserted into the blunted KasI site. The 3HA-tagged cassette was rejoined to the rest of the *D1bLIC* gene to yield a construct with the 3HA tag 63 nucleotides upstream from the stop codon.

A 2.8-kb SmaI-KpnI fragment containing the 5′ end of the *D1bLIC* gene was removed from the 7.3-kb SmaI-SacI *D1bLIC* gene cassette and was used for site-directed P-loop mutagenesis. Two sets of oppositely directed mutagenic primers were designed to amplify the whole plasmid containing the 2.8-kb SmaI-KpnI cassette. The

ends of the PCR products were polished by T4 polymerase and T4 kinase. The modified PCR products were self-ligated to yield mutated circular plasmids. One set of primers M4K and M5K changed the wild-type P-loop from GSRAAGKS to GSRAAGAS and introduced a new SalI site at the DNA level. The second set of primers M3KS and M4KS changed the wild-type P-loop from GSRAAGKS to GSRAAGIA and disrupted an existing NaeI site at the DNA level. Products were sequenced to verify that no additional mutation had been introduced by the PCR. The modified 2.8-kb fragments were inserted back into the 3HA-tagged *D1bLIC* gene to yield a K construct that has a K to A mutation in the P-loop and a KS construct that has a KS to IA mutation in the P-loop.

Detection of the exogenous D1bLIC gene by PCR amplification

Amplification by the PCR was used to check if a desired mutant *D1bLIC* gene was incorporated into the cells rescued with the K construct or the KS construct. The primer pair D1bLIC-3 and D1bLIC-4 were designed to amplify a 700-base pair fragment around the P-loop region from wild-type and rescued cells. No product should be amplified from YH43 (*d1blic*) cells. Products were then cut by SalI or NaeI, and analyzed by electrophoresis in a 1.5% agarose gel.

Site-directed mutagenesis for *IFT46* gene

A 1.4-kb NcoI fragment containing the three phosphorylation sites of the *IFT46* gene was removed from the 4.8-kb fragment containing the *IFT46* gene and was used for

site-directed mutagenesis. Two rounds of site-directed mutagenesis were applied to modify the three sites. In each round, two sets of adjacent but oppositely directed mutagenic primers were designed to amplify the whole plasmid containing the 1.4-kb NcoI cassette. The ends of the PCR products were polished by T4 polymerase and T4 kinase (Biolab, Ipswich, MA). The modified PCR products were self-ligated to yield mutated circular plasmids. In the first round, one set of primers, IFT46MA3 and IFT46MA4, changed S^{77} to A^{77} and introduced a new NheI site at the DNA level. The other set of primers, IFT46MD3 and IFT46MD4, changed S^{77} to D^{77} and introduced a new BstI site at the DNA level. In the second round, one set of primers, IFT46MA1 and IFT46MA2, changed $S^{39}S^{41}$ to $A^{39}A^{41}$ and introduced a new HindIII site at the DNA level. The other set of primers, IFT46MD1 and IFT46MD2, changed $S^{39}S^{41}$ to $D^{39}D^{41}$ and also introduced a new HindIII site at the DNA level. Products were sequenced to verify that no additional mutation at the protein level had been introduced by the PCR. The modified 1.4-kb fragments were inserted back into the remaining *IFT46* gene to yield an A construct in which all three sites were mutated to alanine and a D construct in which all three sites were mutated to aspartic acid.

Table 2.1 **Antibodies used in this work**

Protein	**Antibody**	**Type**[a]	**Reference/Source**
IFT particle protein			
Complex A			
Chlamydomonas IFT140	α-IFT140	P	Gift of B. Walker
Chlamydomonas IFT139	139.1	M	Cole et al., 1998
Complex B			
Chlamydomonas IFT172	172.1	M	Cole et al., 1998
Chlamydomonas IFT81	81.1	M	Cole et al., 1998
Chlamydomonas IFT72	α-IFT72$_2$	P	Qin et al., 2004
Chlamydomonas IFT57	57.1	M	Cole et al., 1998
Chlamydomonas IFT46	α-IFT46	P	Hou et al., 2007
Chlamydomonas IFT20	α-IFT20	P	Gift of M. Chapman
IFT retrograde motor			
Chlamydomonas Dynein heavy chain DHC1b	α-DHC1b	P	Pazour et al., 1999
Chlamydomonas Dynein light intermediate chian D1bLIC	α-D1bLIC	P	Hou et al., 2004
Outer arm dynein			
Intermediate chain			
Chlamydomonas IC1	α-IC1	M	King et al., 1985, 1986
Chlamydomonas IC2	α-IC2	M	King et al., 1985
Outer arm dynein docking complex			
Chlamydomonas DC2	α-DC2	P	Wakabayashi et al., 2001
Inner arm dynein			
Intermediate chain			
Chlamydomonas IC138	α-IC138	P	Hendrickson et al., 2004
Tubulin			
Chlamydomonas α-tubulin	B5-1-1	M	Sigma-Aldrich, Inc. (St Louis, MO)
Chlamydomonas α-tubulin	α-α-tubulin	P	Silflow and Rosenbaum 1981
Chlamydomonas β-tubulin	α-β-tubulin	M	Gift of G. Piperno (Mt. Sinai School of Medicine, NY)
Influenza hemagglutinin epitope (HA)	3F10	R	Roche Molecular Biochemicals (Indianapolis, IN)

[a]M, mouse monoclonal; P, rabbit polyclonal; H, human; R, rat monoclonal.

Table 2.2 **Primers used in this work**

Primer name	**Primer sequence***
DHC1bcDNA07	5’ GACACGTTTGCGGAGCTAGT 3’
DHC1bcDNA08	5’ AAGAAGGCGTACGAGTTGGA 3’
DHC1bcDNA09	5’ ACCAATATGCCGCGTACCT 3’
DHC1bcDNA10	5’ AGCTCCGCCCAGAAGTTAAT 3’
DHC1bcDNA11	5’ CGCTGAGCAGCTTGTATCAC 3’
DHC1bcDNA12	5’ CACCCACTACACGCAAGAAG 3’
D1bLIC-3	5’ CGGTTCTGCTAGGCGCAAAG 3’
D1bLIC-4	5’ TCCGAGTTCACGATCTCCTC 3’
D1bLIC-5	5’ ACGTTGCTCAATCGCTTCTT 3’
D1bLIC-6	5’ ACCGTTCCTTCACACGAAAG 3’
D1bLIC-11	5’ GGAATTCACGTTGCTCAATCGCTTCTT 3’
D1bLIC-12	5’ GGAATTCTTCCTTCACACGAAAGCGTA 3’
M4K	5’ GCGCCGGCCGCTCGCGAGCC 3’
M5K	5’ GTCGACGTTGCTCAATCGCTTCTTGTATCCC 3’
M3KS	5’ TATCGCCACGTTGCTCAATCGCTTC 3’
M4KS	5’ CCGGCCGCTCGCGAGCCC 3’
IFT46-Q1	5’ GCAAGACCTGCTGTTGGCCGC 3’
IFT46-Q2	5’ CCACTGCTGGATCTTCTTGGC 3’
IFT46-1	5’ CCAAGGTCCCTCCATTACAA 3’
IFT46-2	5’ GTGCTTTCCAGCCTCATAGC 3’
IFT46-3	5’ GCCCTTCATCCCTGACTACA 3’
IFT46-4	5’ CTTGTGGATGTCGTTGATGG 3’
IFT46-5	5’ TGTGCTCCAATGACCAAAGA 3’
IFT46-6	5’ AAGCAAGACGGGAGCTATGA 3’
IFT46-9	5’ ACTCTCACCAACGGGCTATG 3’
IFT46-10	5’ TACGCCTCTTGCAGACACAC 3’
IFT46-11	5’ ATGGATGACTCTATGGACTACCCTGAC 3’
IFT46-28	5’ GCTTGTACTCCTGTGCGTTG 3’
IFT46MA1	5’ GCGGAAAGCTTCGCGGGAGCGGAT 3’
IFT46MA2	5’ CTCAGCCAGGTTCACCTCCTGCGAGAG 3’
IFT46MD1	5’ GACGAAAGCTTCGCGGGAGCGGAT 3’
IFT46MD2	5’ CTCGTCCAGGTTCACCTCCTGCGAGAG 3’
IFT46MA3	5’ AGCACCAACGGGCTATGAGGCTGG 3’
IFT46MA4	5’ AGCGTCCGCGCTGGAGCAGCT 3’
IFT46MD3	5’ ATCCAACGGGCTATGAGGCTGG 3’
IFT46MD4	5’ CCAGTGTCCGCGCTGGAGCA 3’
IFT140F	5’ ACAAGGTGAAGGCCATGAAG 3’
IFT140R	5’ GTAGTCCCGGTACTCGTCCA 3’
IFT139F2	5’ ACTACGAGAACGCCTGGAAG 3’
IFT139R2	5’ AGGATCTCCTTGCGGATTTT 3’
IFT81F	5’ AGGAGATCAACAACGCCATC 3’
IFT81R	5’ GTGCAGCATGTGGTATTTGG 3’
IFT72F2	5’ CCTCAAGTTCCAGGCCAAG 3’
IFT72R2	5’ CGGTAGTTGGTCTCGCTCTC 3’

* The mismatched nucleotides that introduce mutations and change restriction sites are underlined.

CHAPTER III

IDENTIFICATION OF IFT MUTANTS

Introduction

Intraflagellar transport was first reported in *Chlamydomonas* in 1993. At the time that I started my thesis work, it had been shown that FLA10 is one of the motor subunits for anterograde IFT and that DHC1b is the heavy chain of the retrograde IFT motor. It also had been shown that LC8 was involved in retrograde IFT. Approximately 16 IFT-particle proteins had been identified in *Chlamydomonas* (Cole et al., 1998). Sequence analysis of IFT components and mutant analysis of IFT88, one of the IFT complex B proteins, had shown that IFT is a conserved process required for flagella assembly and maintenance, and that ciliary defects are linked to polycystic kidney disease. As an emerging research area with potential implications for human diseases, there were many questions waiting to be answered about IFT. Two of them were: 1) Since dyneins are large complexes composed of multiple subunits, what are the other components of the retrograde IFT dynein motor? 2) What are the specific functions for these IFT-particle proteins?

To help answer the above questions, I took the approach of mutant analysis. Since *Chlamydomonas* does not need flagella to survive, and flagella are necessary for its mobility, mutants with flagella defects can be easily identified by checking the mobility under the light microscope. With a collection of mutants pre-selected for flagella defects, one can perform studies using a forward genetic approach or a reverse

genetic approach (Pazour and Witman, 2000). In a forward genetic approach, one can identify a mutant with an interesting phenotype and then identify the mutant gene. In the reverse genetic approach, one begins with a gene of interest and by screening the collection of mutants, can identify a mutant defective in that gene. Both approaches are greatly facilitated by insertional mutagenesis. In insertional mutagenesis, DNA vectors with selectable markers are transformed into the cells. The vector is integrated at random throughout the chromosome and usually causes a deletion or insertion at the site of integration. The mutation is usually tagged with the vector sequence and can be cloned in a forward genetic approach. Alternatively, a mutant defective in a gene of interest can be screened out by Southern blotting or PCR in a reverse genetic approach.

In this part of my thesis research, I created mutants with flagella defects by insertional mutagenesis. Since IFT is important for flagella assembly, maintenance and function, we predicted that defects in the proteins involved in intraflagellar transport probably would make the cells non-motile. Therefore non-motile mutants were selected. Together with some other non-motile mutants from collaborating labs, these mutants were further characterized to identify those defective in retrograde IFT or individual IFT proteins.

To identifiy mutants defective in retrograde IFT, I stained the non-motile mutants with antibodies to IFT-particle proteins. When retrograde IFT is defective, IFT particles can be transported into flagella and the cells can form short axonemes. However, since IFT-particle proteins can not be transported out of the flagella, they accumulate in the flagella and can be detected by immunofluorescent staining. Defects

in retrograde IFT are probably caused by mutations in the retrograde IFT motor subunits. Once these mutants are identified, we can possibly identify the mutant genes by a forward genetic approach.

To identify the mutants defective in individual IFT proteins, I screened the mutant collection by Southern blotting using cDNA probes for individual IFT proteins. Once identified, these mutants can be further characterized in a reverse genetic approach to determine the functions of these IFT proteins.

Results

Creation of a collection of insertional mutants with abnormal motility. 2660 transformants were generated by insertional mutagenesis as described in Materials and Methods. Among them, 4 have extra long flagella and 88 have defects in motility (Table 3.1). Among the 88, 31 are non-motile. We also got 53 non-motile mutants created by insertional mutagenesis from Dr. W. Dentler, who had done some preliminary analysis on these mutants (Table 3.2).

Identification of mutants defective in retrograde IFT. To identify mutants defective in retrograde IFT, the collection of non-motile mutants was screened by immunofluorescence microscopy. The cells were stained with an antibody to IFT172, one of the IFT complex B proteins. In wild-type cells, the majority of IFT172 localizes at the basal body region while a smaller amount is distributed along the length of the flagella as puncta (Figure 3.1A). Among mutants stained, 5 (V91.1, Y77, TB4H3, 3f12

and TBD9-1) (Figure 3.1C-H) showed a staining of IFT172 distinct from that of wild-type cells, but similar to that of the *dhc1b* mutant (Figure 3.1B) (Pazour, et al., 1999). DHC1b is the heavy chain of the retrograde IFT dynein motor. All these mutants showed an increased level of IFT172 in the flagella as well as a decreased level of IFT172 in the basal body region, indicating that the retrograde IFT is defective. Four of them have short, stumpy flagella; TBD9-1 has variable length flagella.

Western blotting showed that all of the above mutants are missing DHC1b (Figure 3.2). Two of them (V91.1 and Y77) showed RFLPs for DHC1b cDNA probes on Southern blots (Figure 3.3). These two are probably *dhc1b* mutants. Since *DHC1b* is a very large gene, it is still possible that the other three are DHC1b mutants. Another possibility is that they are defective in other proteins which are required for DHC1b stability or expression. Thus these three are potentially interesting mutants for further study of retrograde IFT.

Identification of mutants defective in IFT genes. The mutant collection was screened by Southern blotting using 10 cDNA probes specific for genes encoding IFT-particle proteins IFT20, IFT27, IFT46, IFT57, IFT72, IFT81, IFT88, IFT122, IFT139 and IFT140 (see Material and Methods) and a cDNA probe for D1bLIC, which was a candidate for the retrograde motor subunit (see CHAPTER IV). Three mutants (T10b12-1, T10b12-9 and T3b8-9) have RFLPs for the *IFT20* probe (Figure 3.4A-C). Three mutants (T8a4-11, T88a9-11 and T8a4-10) have RFLPs for the *IFT46* probe (Figure 3.4D-F). Two mutants (Y125 and 4-4h3) have RFLPs for the *IFT172* probes

(Figure 3.4G and H). One mutant (22-5d3) has an RFLP for the *IFT140* probe (Figure 3.4I), and one (TBD9-1) has an RFLP for the *D1bLIC* probe (Figure 3.4J).

Among these mutants, *IFT20* is deleted in T10b12-1 and T10b12-9. Thus they are null mutants for IFT20. Part of the 3' end of *IFT172* is deleted in 4-4h3. Western blotting showed that there is no IFT172 protein in Y125 and 4-4h3 cells (Figure 3.5A). Thus both of them probably are null mutants for IFT172. TEM revealed that Y125, with a normal basal body region, can not form flagella at all (Figure 3.5B). In the above screening of the mutant collection by immunofluorescence microscopy, TBD9-1 was identified as a potential interesting mutant for retrograde IFT. Thus D1bLIC is probably involved in retrograde IFT. Further characterization of D1bLIC and TBD9-1 is described in CHAPTER IV. Further characterization of the IFT46 mutant is described in CHAPTER V.

Summary

In this chapter, a collection of insertional mutants with flagella defects was created. In the collection, three mutants were identified by immunofluorescence microscopy as probably defective in novel retrograde IFT components. Several other mutants were identified by Southern blotting as defective in IFT-particle protein genes.

Table 3.1. **Insertional mutants with motility defects created in this work**

	Name	Phenotype in 125 ml aerated M medium*	Phenotype after autolysin treatment
1	Y01	slow	
2	Y02	slow	
3	Y03	slow smooth	
4	Y04	slow	
5	Y10	pal+several swimmer	swim normally
6	Y11	pal+several swimmer	swim slightly slow
7	Y12	pal	still
8	Y13	long fla	
9	Y14	long fla	
10	Y16	pal	swim abnormally
11	Y17	pal+several swimmer	
12	Y19.1	pal+several swimmer	swim abnormally
13	Y19.3	pal+abnormal swimmer	abnormal swimmer
14	Y27	fast jerky	
15	Y28.1	slow	
16	Y29	slow	
17	Y30.1	pal	slow jerky
18	Y30.3	slow	
19	Y32	slow	
20	Y34.1	slow	
22	Y42.2	slow	
23	Y42.3	pal	still
24	Y45.3	slow	
25	Y46	slow	
26	Y47.1	pal	still
27	Y47.2	slow	
28	Y52	pal+several swimmer	
29	Y54	pal+several swimmer	swim normally
30	Y58	pal	still

31	Y59	slow	
32	Y60	abnormal swimmer	
33	Y64	pal	swim normally
34	Y68.1	pal+single; still	
35	Y68.4	single; still	still
36	Y71	pal or single cells or groups of 2 cells	still
37	Y73	pal or single; still	still
38	Y75	pal or single cells or groups of 2 cells	still
39	Y76	large clusters	still
40	Y77	pal or single cells or groups of 2 cells	still
41	Y78	pal	still
42	Y79	pal	still
43	Y80	pal	still
44	Y81	pal	still
45	Y82	pal or single cells or groups of 2 cells	still
46	Y84	slow	
47	Y85	slow jerky	
48	Y86	slow strange	
49	Y92	pal or single; still	
50	Y94	abnormal jerky moving	
51	Y95	slow jerky	
52	Y96	abnormal swimmer	
53	Y100	single still or pal, some move slightly	
54	Y105	slow jerky?	
55	Y107	pal, or some moving?	single still
56	Y109	Pal	single still
57	Y114	Pal	single still
58	Y120	slow jerky?	
59	Y121	single still or pal	single still
60	Y122	long fla	
61	Y125	pal	single still
62	Y126	slow jerky?	

63	Y129	single still or pal	slow jerky
64	Y131	pal	single still
65	Y137	still or twirl, tremble	
66	Y138	slow jerky?	
67	Y139	pal	single still
69	Y156	single still or pal	single still
70	Y161	pal	single still
71	Y167	pal	single still
72	Y168	pal	some moving
73	Y170	slow jerky?	
75	Y172	slow	
76	Y173	slow	
77	Y174	pal	single still
78	Y177	pal	single still
79	Y178	abnormal swimmer, stick to glass easily, normal length fla	
80	Y181	pal	single still
81	Y183	pal	some moving
82	Y191	pal	single still
83	Y193	pal or single still	single still
84	Y208	single still	single still, 20 hrs later some move slightly
85	Y209	pal	single still
86	Y228	pal	slow jerky
87	Y229	pal	single still
88	Y230	abnormal swimmer, slow twirl, two normal length fla	
89	Y232	slow jerky?	
90	Y234	abnormal swimmer, erratic quick swimming, tremble	
91	Y236	abnormal swimmer	
92	Y237	long fla	

* pal, palmelloid; fla, flagella.

Table 3.2. I**nsertional mutants with motility defects from Dr. W. Dentler**

Mutant name	Original name	Phenotype (All lack visible flagella by DIC and phase microscopy)	*dhc1b* poly-morphism (by M. Porter)	Notes	Puc probe	# nit inserts	Tetrads			Random Progeny			
18-1	4-4h3	Bald or short stumpy	No			1							
18-2	5-3d7	Bald - BB & transition region fine but no flagellum proper.	No		pvu 2: 1 <10 kb	pvu 2: 3 NR							
18-3	5-4b9	Bald - normal BB and transition region, no flagella	No										
18-4	6-6a3	bald											
18-5	6-8a10	Bald, normal transition region, no flagella	No										
18-6	7f7c1 or T7F7c1	Bald - normal bb & trans region, no flagella		Linkage possible	pvu-2: 1 ~3kb	pvu-2: 1 NR		0	0	4	0	0	0
18-7	7f13f3	Bald - normal trans region but no flagella											
18-8	15-2e5	Bald. Nice BB & transition region but no flagellum	No										
18-9	19-3h5	bald w/ good BB & normal trans region. Flagellar collar not well formed.				pvu-2: 6 NR							

18-10	20-1b10a7	Normal transition region. Most bald but some w/ short mts that extend beyond the transition region.	No		pvu 2: 2 puc	pvu 2: 2 NR							
18-11	22-2b4	bald											
18-12	22-3b5	Bald											
18-13	22-3b8	Bald - good BB & trans region Flagella do not grow longer than transition region.			pvu 2: 1 ~3kb	pvu 2: 1 NR	0	0	0	2	0	0	4
18-14	22-5d3	Bald - pairs of basal bodies but no mts beyond cup lip	No										
18-15	25-1e9	Bald - mts near tips of basal cup lip but no longer. Memb balloons over tip											
18-16	*T7d8-6*	Bald mutant, normal bb pairs, no flagellar mts				pvu 2 - 1 NR	0	0	0	5	0	0	5
18-17	T7e4-11	Bald											
18-18	T8a4-11	bald											
18-19	T88a9-11	bald											
18-20	TB4F10												
18-21	T9f6-10	bald											
18-22	T11f9-5	Bald - mts extend past basal cup. Beaded bar at the tip of flagellar memb.	No	No plasmid rescue	pvu 2 - 1 <10kb	pvu 2 - 2 NR	0	0	0	29	0	0	14

18-23	T11f9-6	Bald or short stumpy. Something extends beyond the basal cup. BB paired in normal position.	No			pvu 2 - 5 NR							
18-24	22-3d7	Normal BB & very short flagella. Shifts in the collar tunnel. If tunnel is not there flagellum still fails to grow.			pvu 2: 6 puc	pvu 2: 2 NR							
18-25	B1241-1												
18-26	4-4f7	Normal flagellar MTs, bb, transition region. Caps may be present on central MT - t a plate appears in a 0.6µm long flagellum. Transition region to tip = 0.7± .2µm		linkage unlikely mating - 5 tetrads analyzed, but no co-segregation of stumpy mutant w/ the nit gene	pvu 2: 4 puc	pvu 2: 3 NR							
18-27	4-e2	Normal BB, transition zone, short Mts - no caps; Loose outer cell wall; Transition region to tip = 0.5 ± .2 µm	No	LINKAGE POSSIBLE	1 puc	2 nit	0	0	0	5	0	0	4
18-28	5-5c7	Short flagellar stubs about 0.5-1µm long.	No										
18-29	7-f3e3	7/20 labeled A-F3E3 Two stumpy flagella - very short, normal trans regions.	No		pvu 2: 1 ~ 3kb	pvu 2: 1 NR							

18-30	10-f4c-12: on photos as XX/4 c12	Stumpy - Normal bb/transition region ; flagellum does not grow past end of flagellar cell wall collar.			sal 1: 2 puc	sal 1: 1 NR							
18-31	TBD9-1												
18-32	19-3c4	Stumpy											
18-33	T3a1-2	Stumpy. Mts intact to end of memb; Flagella reach end of the cell wall tunnel.	No		pvu 2: 2 puc	pvu 2: 2 NR							
18-34	T8a7-10	Stumpy. Mts pass normal trans zone & some ~ 1µM. No caps but mts extend intact to the membrane tip	No		pvu 2: 4 s	pvu 2: 1 NR							
18-35	T8c11-1	Stumpy w/ good trans region, mts to tip, flagellum barely reaches end of cell wall. CP may have cap			pvu 2: 4	pvu 2: 2 NR							
18-36	T9d8-5	stumpy											
18-37	T9d9-10	Bald/ short stumpy. Mts good to the membrane. Length varies from just past the normal looking transition region to mts growing to the outer edge of the cell wall.		not linked	pvu-2: 1 ~3kb	pvu-2: 1 NR	0	0	0	15	8	9	14
18-38	T9f9-10	Stumpy w/ flagella ~1 µm long. Mts intact to the flagellar tip. No cap	No		pvu 2: no puc,	pvu 2: 1 NR							

18-39	T9f9-9	Stumpy, Mts to the memb but occasional 3-4µm flagella seen.	No		pvu-2: 1 ~3kb	pvu-2: 1 NR							
18-40	T10a9-2	Stumpy. Mts to the memb, no cap, stubs just past the end of the cell wall. Normal BB and MT rootlet arrays	No		pvu 2:	pvu 2: 1 NR							
18-41	T10b10-6	stumpy											
18-42	T10b12-1	stumpy											
18-43	T10b12-9	stumpy											
18-44	T10e4-9	stumpy											
18-45	T10d10-6	stumpy											
18-46	T11f8-9	Stumpy w/ mts intact to the memb. BB& paired flagella and transition region. Flagellar mts extend to the membrane, about level of cell wall		LINKAGE LIKELY – SOURCE OF 2C4 PROBE	pvu-2: 1 2.8 kb	pvu-2: 2 NR	3	0	0	1 6 7			1 2 0
18-47	3b12 now: *stf-1a*	Normal BB & transition zone. Mts end in filamentous structures - as if not well assembled. Flagellar tip filled w/ fuzzy material, Transition region to tip = 0.6 µm	Maps w/ cytoplasmic dynein Dhc 1B RFLPs	not linked (mated - most do not cosegregate w/ stumpy. 9 tetrads 1 of 9 produced 2:2 segregation and rest of them were mixed.)	pvu-2: 1 ~2 kb	pvu-2: 1 NR	Matings unsuccessful but mutation is due to cDHC 1B: Porter et al., 1999						

18-48	3f12 or 3f12a	Normal BB & transition regions. Mts seem to fall apart at tips, although this may be due to fuzzy material at Mt ends. no trace of caps. Transition region to tip = 0.56 ± .09µm			pvu 2 - no puc	pvu 2 - 1 NR							
18-49	25-1d9	Stumpy - normal cytoplasmic and BBmts and normal transition region. Flagellar mts start and then fray toward short tip, that reaches a bit bast the flagellar collar	No		pvu 2: 5 puc,	pvu 2: 2 NR							
18-50	T3b8-9 *stf1b* T3b8-11 *stf1b*	stumpy flagella TEM: Stumpy - flagellar mts start to grow but fray at ends, no caps seen, some transition regions seem like they may be defective Like T3B8-9 -	Maps w/ cytoplasmic dynein Dhc 1B RFLPs		pvu 2: 2 puc	pvu 2: 1 NR	Matings unsuccessful but mutation is due to cDHC 1B: Porter et al., 1999						
18-51	T9a10-9	Mts grow past basal cup but the memb filled w/ filamentous material (not linearly like fraying mts. Nothing longer than 1.5µm.	No		pvu 2: 1 <10 kb	pvu 2: 1 NR							

18-52	TB4H3	Plasmid rescue used to isolate clones from HindIII digested mutant DNA. A 0.9kb probe was isolated by digesting the plasmid and the probe was used to recognize polymorphic fragments in A54 and TB4 DNA digested with HindIII, Spt-I, Sal-I, Xba-I, and XhoI. Probed the Chlamy l library and found 3 different clones. Transformed the mutant with the clones but have not recovered motility.	Anh Plasmid rescued with HindIII, Xho1, SphI, Xba1, Pst1, Sal1h3 Polymorph with HindIII	pvu-II – 1 nit, 1 puc*									
18-53	*T8a4-10*	Stumpy-bald. Mts barely make it past transition region. Some transition regions may be malformed and one has a double transition region. This is not uniform among all cells.	not linked	pvu-2: 1 2.8kb	pvu-2: 2	0	0	0	1 2	0	8	4

Mutants numbered 1-X were made by insertion of linearized pmn24 into A54 e^{18} mt^{+} nit1D ac17Sr^{1} (B 22)from Pete Lefebvre, Dept. of Genetics and Cell Biology, University of Minnesota, St. Paul, MN. This mutant is mating type "+" and has the e^{18} deletion in the 5' end of the nitrate reductase (NR) gene.

Insertional mutants labeled w/ the prefix "T" were made in nit1-305 w/ EcoR1 digested pMN 24 by Keith Kozminski in J. Rosenbaum's lab at Yale. The nit-1 305 mutation is a point mutation in NR that renders it nonfunctional but it does not have the e^{18} deletion. Keith described all as stumpy or bald. Their positions in this chart are based on a rescreening of these mutants by Heather Johnson in June/July 1994. Cells were grown in liquid SGII-NO_3 on a light/dark cycle, examined by microscopy before and after putting them in distilled water, which disrupts the cell wall and makes stumpy flagella much more visible.

Mutants w/ TB and JR– obtained from C. Silflow. Generated in A54 w/ pMN 56

Figure 3.1. **Five mutants were identified as defective in retrograde IFT.** Wild-type (A), *dhc1b* (B), V91.1 (C), Y77 (D), TB4H3 (E), 3f12 (F), and TBD9-1 (G and H) cells were stained with an anti-IFT172 antibody (in green). The cell bodies are in red due to autofluorescence. In wild-type cells, the majority of IFT172 localizes in the basal body region while a lesser amount is distributed as dots along the flagella. In the *dhc1b* mutant, due to the defect in retrograde IFT, almost all the IFT172 localizes in the short, stumpy flagella. In the other mutants, IFT172 accumulates in the flagella, indicating that retrograde IFT is defective. Scale bar: 5 μm.

Figure 3.1

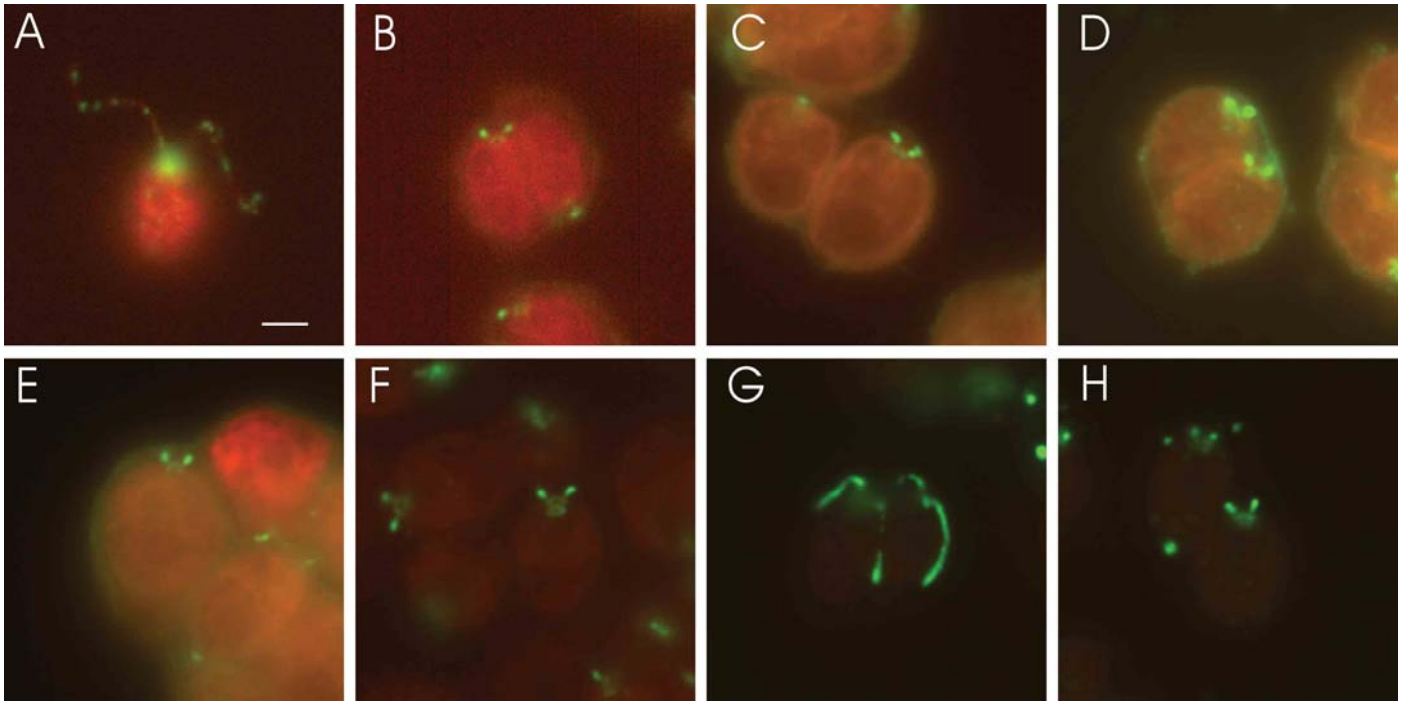

Figure 3.2. **Western blots of the retrograde IFT mutants with an anti-DHC1b antibody.** Whole cell lysates from wild-type (WT) and V91.1 (A), Y77 (B), TB4H3 (C), 3f12 (C), and TBD9-1 (C) were probed with an anti-DHC1b antibody on different blots. The outer dynein arm heavy chain γ-DHC (A), tubulin (B), and a non-specific band (C) served as loading controls. No DHC1b was detected in these mutants on these blots (TBD9-1 actually has a greatly reduced level of DHC1b -- see CHAPTER VI).

Figure 3.2

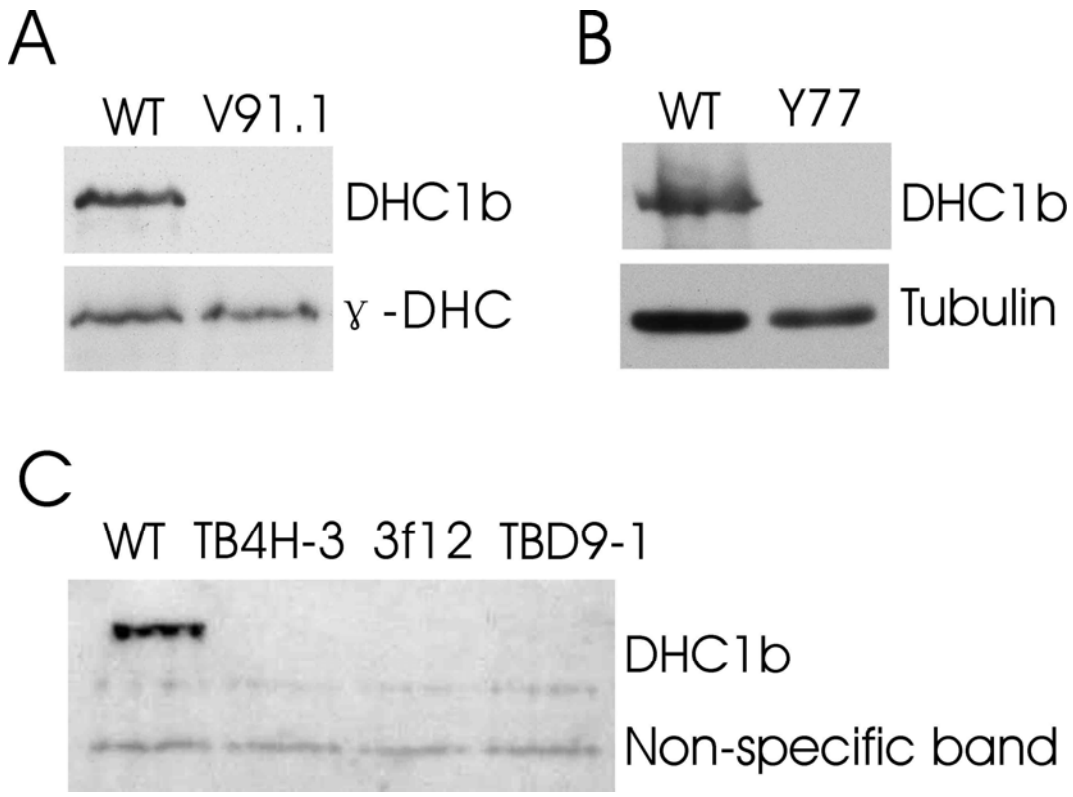
A
WT V91.1
DHC1b
γ -DHC
B
WT Y77
DHC1b
Tubulin
C
WT TB4H-3 3f12 TBD9-1
DHC1b
Non-specific band

Figure 3.3. **Two retrograde IFT mutants have defects in the *DHC1b* gene.** (A) Schematic diagram of *DHC1b* gene structure. Boxes show the exons. Arrows indicate the locations of the primers used to amplify the three cDNA probes used in the screen. (B) Genomic DNAs from control cells of different mating types with normal DHC1b gene (WT) and V91.1 were cut by PstI and probed with DHC1b cDNA probe 1. This probe is mating-type specific (c.f. lanes 1 and 2). The arrow indicates the shifted band in V91.1. (C) Genomic DNAs from control cells with normal DHC1b gene (WT) and Y77 were cut by PstI and probed with DHC1b cDNA probes 2 and 3. One of the bands specific to cDNA probe 3 is shifted in Y77 and is indicated by an arrow. The other band specific to cDNA probe 3 is normal in Y77 and is indicated by *. The band specific to cDNA probe 2 is normal in Y77 and is indicated by an arrow head. Fragment sizes were calculated using the gene sequences from the *Chlamydomonas* genome (http://genome.jgi-psf.org/Chlre3/Chlre3.home.html).

Figure 3.3

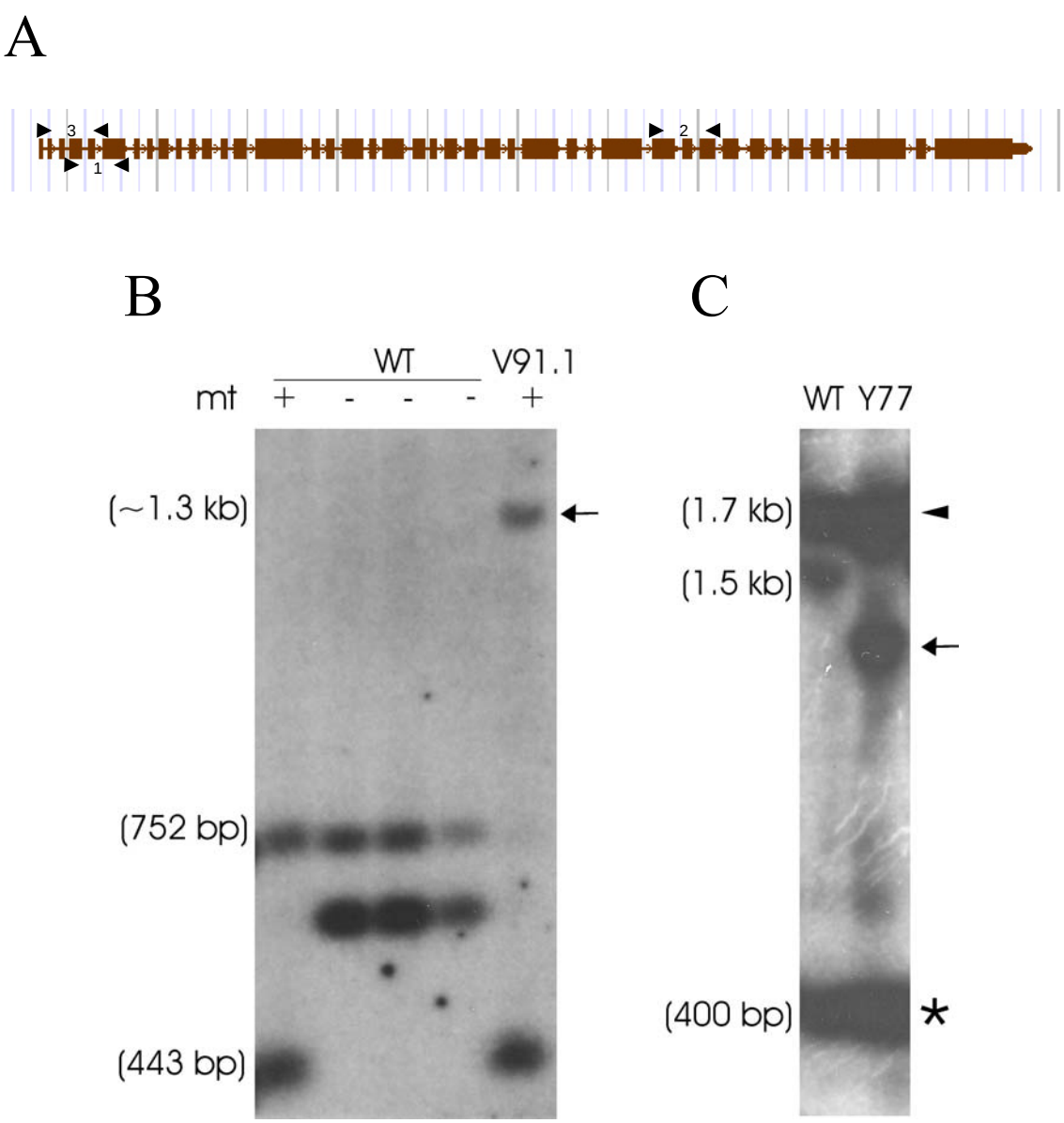

Figure 3.4. **Several mutants were identified as defective in IFT-particle protein genes or D1bLIC, a potential retrograde IFT motor subunit.** Southern blots of T10b12-1 (A), T10b12-9 (B), and T3b8-9 (C) with cDNA probes to *IFT27* and *IFT20* showed that T10b12-1 and T10b12-9 are null mutants for *IFT20*. Southern blots of T8a4-11 (D), T88a9-11 (E), and T8a4-10 (F) with a cDNA probe to *IFT46* showed that these mutants have RFLPs for the *IFT46* gene. Southern blots with cDNA probes to the 5' end of the *IFT172* gene (Y125, G) or to the 3' end of *IFT172* (4-4h3, H) showed that these mutants have RFLPs for the *IFT172* gene. A Southern blot of 22-5d3 (I) with a cDNA probe to *IFT140* showed that this mutant has an RFLP for the *IFT140* gene. A Southern blot of TBD9-1 (J) with a cDNA probe to *D1bLIC* showed that this mutant has an RFLP for the *D1bLIC* gene. * indicates the missing or shifted bands in the mutants. Fragment sizes were calculated using the gene sequences from the *Chlamydomonas* genome (http://genome.jgi-psf.org/Chlre3/Chlre3.home.html).

Figure 3.4

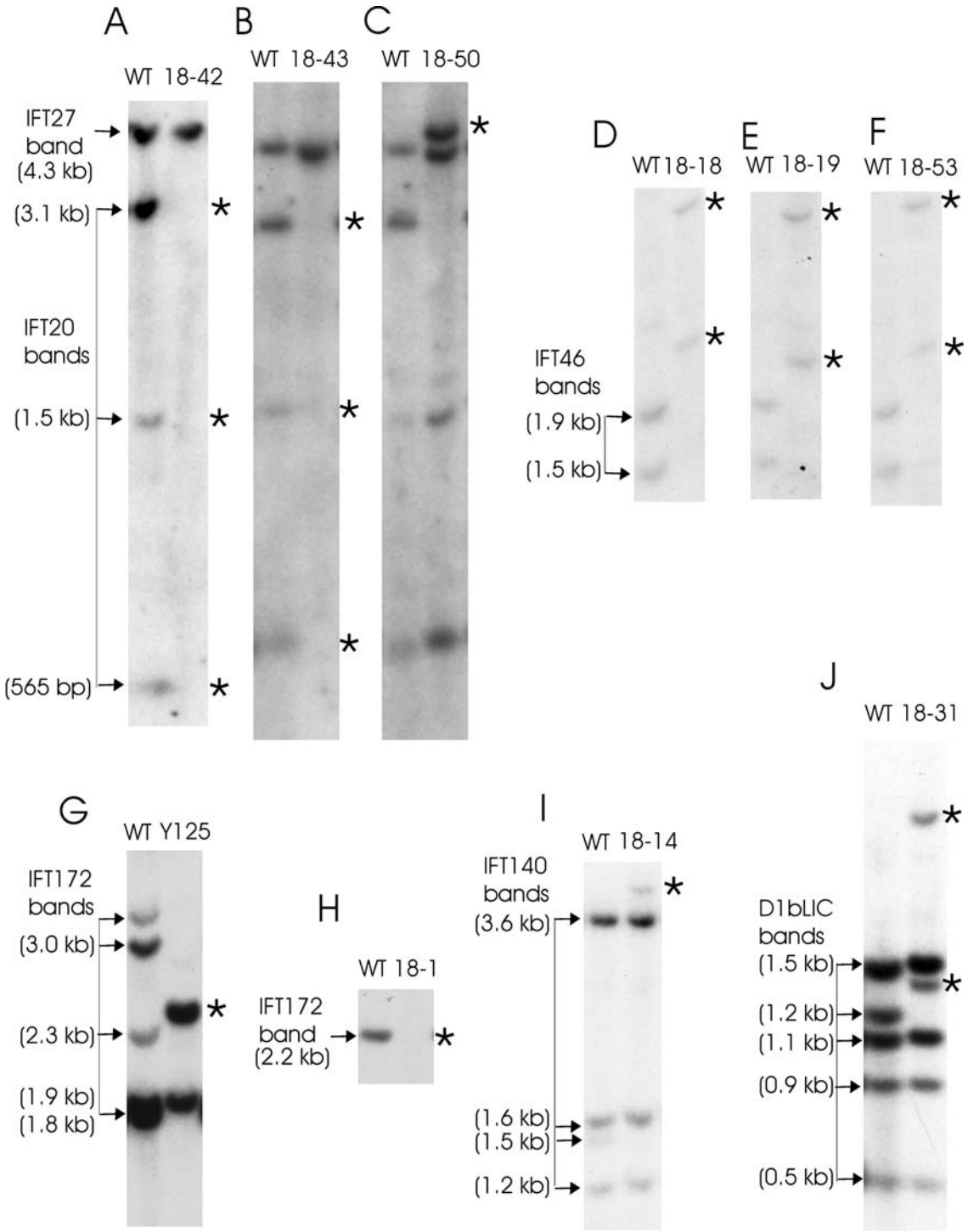
A
WT 18-42
IFT27
band
(4.3 kb)
(3.1 kb)
IFT20
bands
(1.5 kb)
(565 bp)
B
WT 18-43
C
WT 18-50
D
WT18-18
IFT46
bands
(1.9 kb)
(1.5 kb)
E
WT 18-19
F
WT 18-53
G
WT Y125
IFT172
bands
(3.0 kb)
(2.3 kb)
(1.9 kb)
(1.8 kb)
H
WT 18-1
IFT172
band
(2.2 kb)
I
WT 18-14
IFT140
bands
(3.6 kb)
(1.6 kb)
(1.5 kb)
(1.2 kb)
J
WT 18-31
D1bLIC
bands
(1.5 kb)
(1.2 kb)
(1.1 kb)
(0.9 kb)
(0.5 kb)

Figure 3.5. **Two mutants are null for IFT172 and can not form flagella beyond the transition region.** (A) Western blots showed that Y125 and 4-4h3 do not have IFT172 protein. Tubulin was probed as a loading control. (B) A TEM image of Y125 showed that it has normal basal bodies, yet can not form flagella beyond the transition region. Scale bar: 100 nm.

Figure 3.5

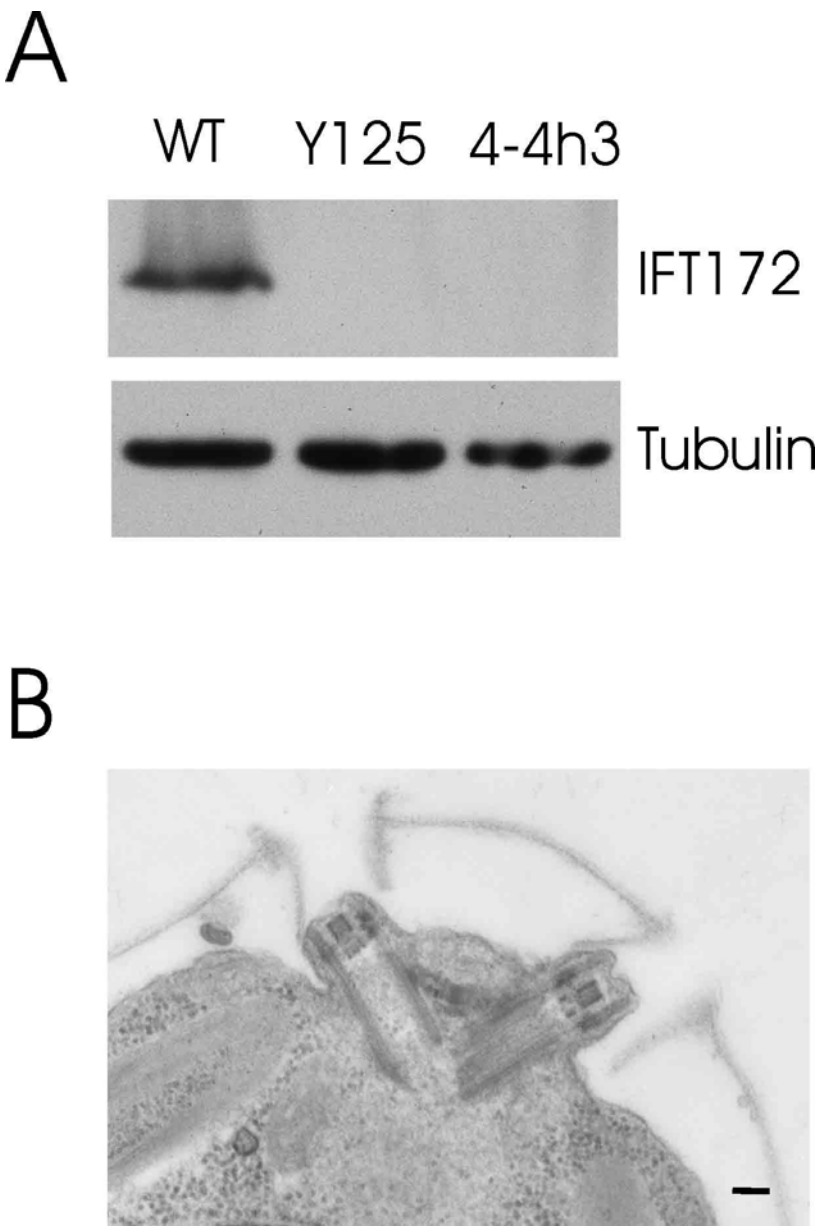

CHAPTER IV

A DYNEIN LIGHT INTERMEDIATE CHAIN, D1bLIC, IS REQUIRED FOR RETROGRADE IFT

Introduction

As previously stated in CHAPTER I, intraflagellar transport (IFT) is the rapid, bidirectional movement of granule-like particles along the length of eukaryotic cilia and flagella (Rosenbaum and Witman, 2002). Although conserved among organisms and important in numerous cell types, the mechanism of IFT is not well understood. Studies from *Chlamydomonas* and *C. elegans* show that two dynein subunit genes are necessary for retrograde IFT. One encodes LC8, which is a light chain of several dynein isoforms and thus is presumably a subunit of the retrograde IFT motor (King et al., 1996; Pazour et al., 1998). The other encodes DHC1b, which is a cytoplasmic dynein heavy chain (DHC) isoform (Pazour et al., 1999; Porter et al., 1999; Signor et al., 1999). Its mammalian ortholog, DHC2, is associated with mammalian cilia (Mikami et al., 2002) and also was reported to play a role in the organization and/or function of the Golgi apparatus (Vaisberg et al., 1996).

Dyneins are typically large multisubunit complexes. For example, conventional cytoplasmic dynein 1 (a.k.a. dynein 1a in invertebrates) is composed of two heavy chains (DHC1/1a), 2 or 3 ICs, several LICs, and numerous LCs (King, 2000; Reilein et al., 2001). It is likely that the retrograde IFT motor also contains subunits in addition to LC8 and DHC1b. A novel dynein LIC, D2LIC, was identified as a bona fide component

of cytoplasmic dynein 2 in mammalian cells (Grissom et al., 2002) and was inferred to play a role in maintaining Golgi organization by binding cytoplasmic dynein 2 to its Golgi-associated cargo. Like dynein 1 LICs, mammalian D2LIC contains a phosphate-binding domain (P-loop) at its N-terminus; although P-loop domains are involved in binding the β, γ - phosphate group of ATP or GTP in many nucleotide-binding and -hydrolyzing proteins (Via et al., 2000), it is not known if this domain has any physiological role in dynein LICs.

Independently of this study, the *Chlamydomonas* homologue of D2LIC was cloned around the same time as the work reported here, and shown to be associated with DHC1b (Perrone et al., 2003), although its function was not examined. In *C. elegans*, the D2LIC homologue is XBX-1; deletion of XBX-1 resulted in stunted sensory cilia that accumulated IFT-particle proteins, suggesting that XBX-1 functions in retrograde IFT (Shafer et al., 2003). Surprisingly, however, XBX-1 accumulated, along with IFT-particle proteins, in the short sensory cilia of the *C. elegans che-3* mutant (Shafer et al., 2003), which is defective in DHC1b/DHC2, but did not accumulate with the IFT-particle proteins in the short flagella of a *Chlamydomonas* DHC1b mutant (Perrone et al., 2003). Moreover, the P-loop that is conserved in mammalian and *Chlamydomonas* D2LIC homologues is absent in *C. elegans* XBX-1. These observations raised the possibility that the D2LIC homologues function differently in *C. elegans, Chlamydomonas*, and humans.

This part of my thesis research, using *Chlamydomonas reinhardtii* as a model system, was undertaken to learn more about the role of this LIC in IFT and the possible function of its P-loop.

Results

Cloning and sequence analysis of D1bLIC. The *D1bLIC* gene, the *Chlamydomonas* ortholog of human *D2LIC*, was cloned as described in Materials and Methods, and 5692 base pairs of the *D1bLIC* gene region were sequenced. When the 5692 base pairs were blasted against the then newly released *C. reinhardtti* genome v.1.0, an exact match on scaffold 319 was identified, which corresponded to the gene model genie.319.8 predicted by Green Genie.

The predicted D1bLIC protein is composed of 427 amino acids (Figure 4.1A), with a molecular weight of 46.6 kD and a theoretical pI of 9.37. It is 28% identical to human D2LIC in the region of amino acids 28–372. Like all mammalian dynein LICs so far identified, D1bLIC has a P-loop near its N-terminus. Similar to D2LIC, it has a predicted coiled-coil domain near its C-terminus from amino acids 376–398. A BLAST search using D1bLIC as query yielded human D2LIC and the mouse homologue for D2LIC as the best matches as well as homologous proteins or ESTs from other species, such as rat, fly, nematode, chicken, *Trypanosome*, etc., but not from nonciliated organisms such as *Arabidopsis thaliana.* A BLAST search of the *Chlamydomonas* genome (JGI v.1.0 and v.2.0) with human D2LIC did not reveal any genes that were more closely related to the query than D1bLIC. A phylogenetic analysis of D1bLIC,

some of its probable homologues, and dynein 1 LICs shows that D1bLIC and human D2LIC group together, distinct from the dynein 1 LICs. (Figure 4.1B). These results indicate that the D1bLIC we cloned is the *Chlamydomonas* ortholog of human D2LIC.

Identification of a *d1blic* mutant. To investigate the function of D1bLIC, I screened the collection of insertional mutants by Southern blotting with a full-length *D1bLIC* cDNA probe (Figure 4.2A). As described in CHAPTER III, one line (TBD9-1) showed a restriction fragment length polymorphism with this probe. PstI cuts the wild-type *D1bLIC* gene into six fragments, of which two are about the same size and thus are not separated on the Southern blot (Figure 4.2A). For the wild-type cells, the full-length cDNA probe identified five bands on Southern blots digested with PstI (Figure 4.2B). In TBD9-1 cell line, the 1.2-kb band, which corresponds to the 5' end of the coding region, is missing, and two new bands of ~1.4 and 3.5 kb are present (Figure 4.2B). Integration at this point is likely to produce a null allele. To test this, cells were analyzed by northern and western blot analysis. As reported (Perrone et al., 2003), the wild-type cells express a ~2.2-kb D1bLIC message that is up-regulated by deflagellation, which is characteristic for messages encoding flagellar proteins. However, this message is not detectable in the mutant cells using either 5' or 3' cDNA probes (Figure 4.2C). Consistent with the idea that this is a null allele, an affinity-purified polyclonal antibody to D1bLIC (see Materials and Methods) detected with high specificity a single band of ~ 48.5 kD in the wild-type whole-cell lysate, but detected no proteins in the mutant whole-cell lysate (Figure 4.2D).

To make sure that the mutant was defective only in D1bLIC, I crossed the original mutant with wild-type cells (CC124), and selected one progeny (called YH43) that is defective in D1bLIC as determined by Southern and western blots (Figure 4.3, A and B). When aerated in 125 ml M medium, most of the mutant cells were nonmotile with short, stumpy flagella, whereas a few had longer flagella of variable length, which sometimes were even near normal length, and swam abnormally. The mutant cells were cotransformed with plasmid pSP124S that contains the *ble* gene and with either a 10-kb SmaI-HindIII genomic fragment or a 7.3-kb SmaI-SacI genomic fragment, both of which contain the *D1bLIC* gene (Figure 4.2A). Both genomic fragments rescued the phenotype to wild-type swimming behavior (7 of 43 *ble* transformants for the 10-kb fragment and 10 of 216 *ble* transformants for the 7.3-kb fragment). Figure 4.3, A and B, show Southern and western blot analyses of some of the cells rescued by the 10-kb fragment, confirming that the exogenous *D1bLIC* gene was incorporated into the genome to express D1bLIC protein. The 10-kb fragment contains the *D1bLIC* gene, most of a predicted gene downstream of the *D1bLIC* gene, and the 3' end of a predicted gene upstream of *D1bLIC*. The 7.3-kb fragment contains only the *D1bLIC* gene and the 3' end of the upstream gene, which is of unknown function (JGI v.2.0). Thus, the rescue of the phenotype via these fragments is strong evidence that the flagellar defect observed in this cell line is caused by the defect in the *D1bLIC* gene.

Retrograde IFT is defective in the *d1blic* mutant. To investigate if D1bLIC is involved in retrograde IFT, I examined the localization of IFT particles in *d1blic* mutant cells by

immunofluorescence and electron microscopy. In wild-type cells, the majority of IFT-particle proteins localize in the peri-basal body region, while a few are distributed along the length of the flagella (Cole et al., 1998; Pazour et al., 1999; Deane et al., 2001) as illustrated in Figure 4.4 with an antibody to IFT172. In the *d1blic* mutant, IFT172 accumulates at the tip of the short stumpy flagella or in large inclusions randomly located along the flagella of cells with longer flagella. Accumulation of IFT-particle proteins in short flagella is characteristic of mutants with defects in retrograde IFT (Pazour et al., 1998, 1999; Porter et al., 1999). In contrast, cells rescued for the motility phenotype by transformation with the cloned gene showed a normal distribution of IFT172.

EM analysis showed that flagella from *d1blic* mutants are filled with an electron-dense substance not observed in flagella from wild-type cells or in rescued cells (Figure 4.5). This material is identical in appearance to the IFT particles that accumulate in *fla14* mutant flagella (Pazour et al., 1998) and *dhc1b* mutant flagella (Pazour et al., 1999). These results confirm that IFT particles accumulate in the short flagella of the *d1blic* mutant. Therefore, the primary defect in the *d1blic* mutant flagella is a loss of retrograde IFT. The IFT particles are moved into the flagellum by anterograde IFT, but become trapped there because some aspect of retrograde IFT is abnormal.

In contrast to what was observed in *fla14* cells, which are defective in LC8, the *d1blic* mutation does not appear to affect components of the axoneme, as inner and outer dynein arms and radial spokes are present along with a normal appearing central

pair of microtubules that are properly positioned in the axoneme. The flagellar defects in *d1blic* mutant cells are less severe than those in *dhc1b* mutant cells, whose flagella are always short and stumpy and may lack a normal axoneme.

The *d1blic* mutant is not defective in growth rate or in Golgi localization or morphology. Cytoplasmic dynein is involved in many cell activities. To see if D1bLIC is involved in cell division or cell cycle control, I checked the growth rate of the *d1blic* mutant (Figure 4.6A). There was no significant difference in growth rate between wild-type cells and *d1blic* mutant cells, indicating that D1bLIC is not involved in any essential cell process in *Chlamydomonas*.

It has been suggested that human D2LIC is involved in maintenance of the Golgi apparatus (Grissom et al., 2002). To investigate a possible role for D1bLIC in Golgi maintenance in *Chlamydomonas*, I examined Golgi localization and morphology in the *d1blic* mutant by EM. As seen in Figure 4.6B, the Golgi had normal morphology in the *d1blic* mutant cells. Golgi apparatuses in both wild-type and mutant cells are always observed on the opposite side of the nucleus from the flagella and are adjacent to a large membrane-bound vacuole on the side toward the cell surface.

DHC1b is reduced in *d1blic* mutant cells and vice versa. Previous studies showed that DHC1b is the heavy chain of the retrograde IFT motor. To investigate the relationship between DHC1b and D1bLIC, I looked at the level of each protein in a mutant defective in the other protein and found that in the absence of one protein, the level of the other protein in the whole cell lysate is greatly decreased (Figure 4.7). This result implies that

DHC1b and D1bLIC exist in the same complex. Because the majority of DHC1b (Pazour et al., 1999) and D1bLIC (see below and Figure 4.8) are in the peri-basal body region in wild-type cells, this result also implies that DHC1b and D1bLIC are associated with one another in the cell body before they move into the flagella. Lack of either one of the proteins probably affects stability of the complex and causes the other protein to be degraded.

D1bLIC is in the same complex as DHC1b. To further investigate if DHC1b and D1bLIC exist in the same complex, I first looked at the cellular localization of both DHC1b and D1bLIC by immunofluorescence microscopy (Figure 4.8). As reported (Perrone et al., 2003), DHC1b and D1bLIC have a similar cellular localization: they both localize in the peri-basal body region and along the flagella in the wild-type cell. To investigate if they distribute together in various flagellar fractions, we fractionated flagella into the membrane plus matrix fraction, different ATP-wash fractions, a high-salt extract fraction and an extracted axoneme fraction. Western blotting by antibodies to D1bLIC, DHC1b, IFT172, IFT139, and outer dynein arm IC IC1 showed that DHC1b and D1bLIC had a similar distribution in the different flagella fractions, which was different from that of IFT-particle proteins or the outer dynein arm (Figure 4.9A). These results indicate that DHC1b and D1bLIC are in the same subcompartment in the flagella. When the flagellar matrix fraction was further fractionated by sucrose density gradient centrifugation, DHC1b and D1bLIC comigrated at ~12S (Figure 4.9B). To further confirm that D1bLIC is in the same complex as DHC1b, I immunoprecipitated

D1bLIC from the flagella matrix fraction using the anti-D1bLIC antibody and found that DHC1b, but not outer dynein arm component IC1, was coimmunoprecipitated (Figure 4.9C). These results confirm that D1bLIC and DHC1b are subunits of the same dynein complex.

Localization of DHC1b in the *d1blic* mutant flagella is normal. As noted above, the phenotype of the *d1blic* mutant is less severe than that of the *dhc1b* mutant. This suggests that the DHC1b remaining in the *d1blic* mutant retains some function even in the absence of the LIC subunit. To investigate the specific role of D1bLIC in cytoplasmic dynein 1b function and IFT, I examined the distribution of DHC1b in *d1blic* mutant cells with near full-length flagella, because these cells are likely to have the highest levels of DHC1b protein. I envisioned three main possibilities: 1) DHC1b is abnormally concentrated in the peri-basal body region with very little in the flagella, suggesting that D1bLIC has a role in attaching cytoplasmic dynein 1b as cargo to IFT particles moving in an anterograde direction; 2) DHC1b accumulates along with the IFT particles in the mutant flagella, suggesting that DHC1b motor function is defective in the absence of D1bLIC; or 3) DHC1b is normally distributed in the flagella, suggesting that motor activity is unimpaired in the absence of the LIC. When *d1blic* mutant cells were stained with the antibody to DHC1b, the distribution of DHC1b was not noticeably different than that observed in wild-type cells (Figure 4.10). Significantly, DHC1b did not accumulate in patches throughout the flagella, as was observed for the IFT particles. These observations suggest that DHC1b retains motor activity and can

move out of flagella normally in the absence of D1bLIC. The fact that the mutant flagella accumulate IFT particles but not DHC1b protein further suggests that D1bLIC has a role in binding the IFT particle to the cytoplasmic dynein 1b motor for retrograde transport.

D1bLIC's P-loop is not required for the protein's function in retrograde IFT. Sequence analyses show that both D1bLIC and D2LIC have a P-loop at their N-termini. The conservation of the P-loop throughout evolution suggests that it is involved in D1bLIC function. To investigate this, I first fused the 3' end of the wild-type *D1bLIC* gene to DNA encoding a 3HA tag. The 3HA-tagged gene rescued the mutant cells to wild-type swimmers, which expressed 3HA-tagged D1bLIC (43R, Figure 4.11B). Site-directed mutagenesis was then applied to the 3HA-tagged *D1bLIC* gene to create two constructs with a mutated P-loop. The K construct has a K to A mutation. The KS construct has a KS to IA mutation. These mutations have been shown to disrupt the P-loop function in other proteins (Saraste et al., 1990; Silvanovich et al., 2003). PCR amplification showed that the constructs were incorporated into the genomes (Figure 4.11A) and western blots with anti-HA antibody and anti-D1bLIC antibody showed that these transformed cells express HA-tagged D1bLIC protein (Figure 4.11B). These transformants have normal length flagella (Figure 4.11C) and swim like wild-type cells. Immunostaining of these cells with anti-IFT172 antibody shows that IFT172 protein is normally distributed in these cells (Figure 4.11D). This result implies that the P-loop is not required for the normal function of D1bLIC in retrograde IFT. Because IFT is required for the mating

process (Pan and Snell, 2002), we checked the mating ability of these cells by mixing the gametes of the rescued cells with wild-type gametes and observed that they can form normal mating clusters and subsequently quadriflagellate cells. This result shows that the P-loop also is not important for the mating process.

Summary

D1bLIC, the *Chlamydomonas* ortholog of mammalian D2LIC, was cloned. Using D1bLIC cDNA as a probe, a *Chlamydomonas d1blic* insertional mutant was identified. Phenotype characterization indicated that D1bLIC is involved in retrograde IFT. Immunostaining, flagellar fractionation, and coimmunoprecipitation data showed that D1bLIC and DHC1b are in the same complex. Mutant analysis further revealed that in the absence of D1bLIC, DHC1b is unstable and vice versa. Site-directed mutagenesis was applied to investigate the function of the D1bLIC P-loop in IFT *in vivo*. Taken together, these results show that D1bLIC is a subunit of the retrograde IFT motor. D1bLIC is required for the stability of DHC1b and for attachment of IFT particles to DHC1b in retrograde IFT. The P-loop in D1bLIC is not required for its function in retrograde IFT or mating.

Figure 4.1. **D1bLIC is the *Chlamydomonas* ortholog of mammalian D2LIC.** (A) D1bLIC cDNA sequence and its predicted amino acid sequence. The P-loop from amino acids 47–54 is indicated by a box, and the predicted coiled-coil domain from amino acids 376–398 (predicted by COILS using the MTIDK matrix and a window of 21) is underlined. (B) Phylogenetic tree for dynein 1 and dynein 2 LICs from different species. The predicted D1bLIC sequence (in bold) was aligned with a subset of cytoplasmic dynein 1 and 1b/2 LIC sequences in GenBank using CLUSTAL W, and a phylogenetic tree was drawn by cluster algorithm. CrIC1: *Chlamydomonas* outer arm dynein IC IC1. Branch lengths represent evolutionary relatedness. Numbers at branch points are bootstrap values. The *Chlamydomonas* D1bLIC groups closely with the mammalian and other presumptive D2LICs, but much less closely with cytoplasmic dynein 1 LICs. Cr, *C. reinhardtii*; Ce, *C. elegans*; Dm, *D. melanogaster*; Hs, *Homo sapiens*; Rn, *Rattus novegicus*; Mn, *Mus musculus*; Xl, *Xenopus laevis*; Gg, *Gallus gallus*. Sequences used for phylogenetic analysis are as follows: MnD2LIC (AAH39070); HsD2LIC (NP_057092); CeD2LIC (T20505); DmD2LIC (NP_609289); CrD1bLIC (AY616759); MnDLIC2 (XP_134573); HsDLIC2 (NP_006132); RnDLIC2 (I55514); RnDLIC1 (NP_665715); MmDLIC1 (NP_666341); HsDLIC1 (NP_057225); GgDLIC1 (I50637); XlDLIC1 (AAG42486); CrIC1 (Q39578).

Figure 4.1

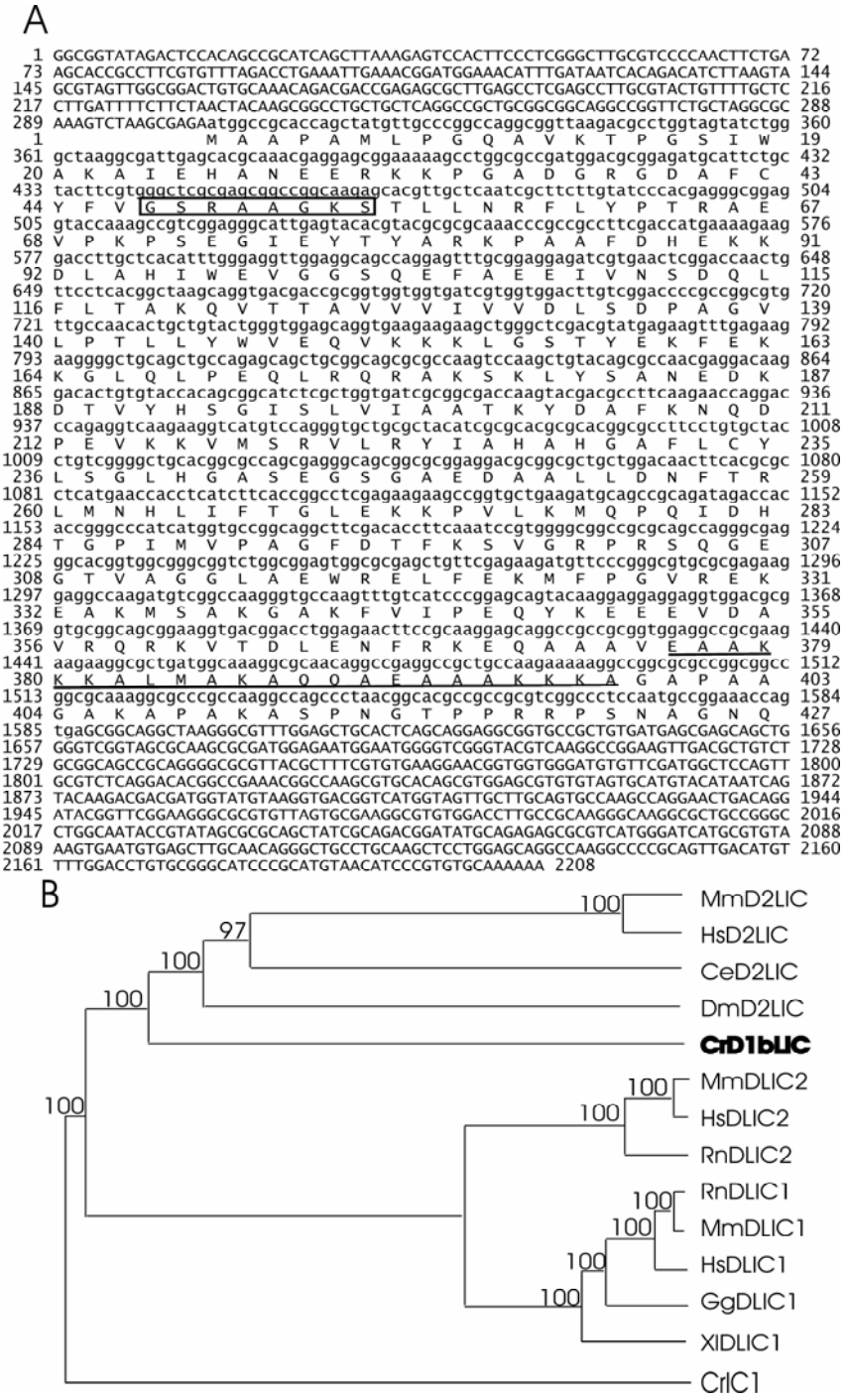
A
1 GGCGGTATAGACTCCACAGCCGCATCAGCTTAAAGAGTCCACTTCCCTCGGGCTTGCGTCCCCAACTTCTGA 72
73 AGCACCGCCTTCGTGTTTAGACCTGAAATTGAAACGGATGGAAACATTTGATAATCACAGACATCTTAAGTA 144
145 GCGTAGTTGGCGGACTGTGCAAACAGACGACCGAGAGCGCTTGAGCCTCGAGCCTTGCGTACTGTTTTGCTC 216
217 CTTGATTTTCTTCTAACTACAAGCGGCCTGCTGCTCAGGCCGCTGCGGCGGCAGGCCGGTTCTGCTAGGCGC 288
289 AAAGTCTAAGCGAGAatggccgcaccagctatgttgcccggccaggcggttaagacgcctggtagtatctgg 360
1 M A A P A M L P G Q A V K T P G S I W 19
361 gctaaggcgattgagcacgcaaacgaggagcggaaaaagcctggcgccgatggacgcggagatgcattctgc 432
20 A K A I E H A N E E R K K P G A D G R G D A F C 43
433 tacttcgtgggctcgcgaagcggccggcaaaagcacgttgctcaatcgcttcttgtatcccacgagggcggag 504
44 Y F V G S R A A G K S T L L N R F L Y P T R A E 67
505 gtaccaaagccgtcggagggcattgagtacacgtacgcgcgcaaacccgccgccttcgaccatgaaaagaag 576
68 V P K P S E G I E Y T Y A R K P A A F D H E K K 91
577 gaccttgctcacatttgggaggttggaggcagccaggagtttgcggaggagatcgtgaactcggaccaactg 648
92 D L A H I W E V G G S Q E F A E E I V N S D Q L 115
649 ttcctcacggctaagcaggtgacgaccgcggtggtggtgatcgtggtggacttgtcggaccccgccggcgtg 720
116 F L T A K Q V T T A V V V I V V D L S D P A G V 139
721 ttgccaacactgctgtactgggtggagcaggtgaagaagaagctgggctcgacgtatgagaagtttgagaag 792
140 L P T L L Y W V E Q V K K K L G S T Y E K F E K 163
793 aaggggctgcagctgccagagcagctgcggcagcgcgccaagtccaagctgtacagcgccaacgaggacaag 864
164 K G L Q L P E Q L R Q R A K S K L Y S A N E D K 187
865 gacactgtgtaccacagcggcatctcgctggtgatcgcggcgaccaagtacgacgccttcaagaaccaggac 936
188 D T V Y H S G I S L V I A A T K Y D A F K N Q D 211
937 ccagaggtcaagaaggtcatgtccagggtgctgcgctacatcgcgcacgcgcacggcgccttcctgtgctac 1008
212 P E V K K V M S R V L R Y I A H A H G A F L C Y 235
1009 ctgtcggggctgcacggcgccagcgagggcagcggcgcggaggacgcggcgctgctggacaacttcacgcgc 1080
236 L S G L H G A S E G S G A E D A A L L D N F T R 259
1081 ctcatgaaccacctcatcttcaccggcctcgagaagaagccggtgctgaagatgcagccgcagatagaccac 1152
260 L M N H L I F T G L E K K P V L K M Q P Q I D H 283
1153 accgggcccatcatggtgccggcaggcttcgacaccttcaaatccgtggggcggccgcgcagccagggcgag 1224
284 T G P I M V P A G F D T F K S V G R P R S Q G E 307
1225 ggcacggtggcgggcggtctggcggagtggcgcgagctgttcgagaagatgttcccgggcgtgcgcgagaag 1296
308 G T V A G G L A E W R E L F E K M F P G V R E K 331
1297 gaggccaagatgtcggccaagggtgccaagtttgtcatcccggagcagtacaaggaggaggaggtggacgcg 1368
332 E A K M S A K G A K F V I P E Q Y K E E E V D A 355
1369 gtgcggcagcggaaggtgacggacctggagaacttccgcaaggagcaggccgccgcggtggaggccgcgaag 1440
356 V R Q R K V T D L E N F R K E Q A A A V E A A K 379
1441 aagaaggcgctgatggcaaaggcgcaacaggccgaggccgctgccaagaaaaaggccggcgcgccggcggcc 1512
380 K K A L M A K A Q Q A E A A A K K K A G A P A A 403
1513 ggcgcaaaggcgcccgccaaggccagccctaacggcacgccgccgcgtcggccctccaatgccggaaaccag 1584
404 G A K A P A K A S P N G T P P R R P S N A G N Q 427
1585 tgaGCGGCAGGCTAAGGGCGTTTGGAGCTGCACTCAGCAGGAGGCGGTGCCGCTGTGATGAGCGAGCAGCTG 1656
1657 GGGTCGGTAGCGCAAGCGCGATGGAGAATGGAATGGGGTCGGGTACGTCAAGGCCGGAAGTTGACGCTGTCT 1728
1729 GCGGCAGCCGCAGGGGCGCGTTACGCTTTCGTGTGAAGGAACGGTGGTGGGATGTGTTCGATGGCTCCAGTT 1800
1801 GCGTCTCAGGACACGGCCGAAACGGCCAAGCGTGCACAGCGTGGAGCGTGTGTAGTGCATGTACATAATCAG 1872
1873 TACAAGACGACGATGGTATGTAAGGTGACGGTCATGGTAGTTGCTTGCAGTGCCAAGCCAGGAACTGACAGG 1944
1945 ATACGGTTCGGAAGGGCGCGTGTTAGTGCGAAGGCGTGTGGACCTTGCCGCAAGGGCAAGGCGCTGCCGGGC 2016
2017 CTGGCAATACCGTATAGCGCGCAGCTATCGCAGACGGATATGCAGAGAGCGCGTCATGGGATCATGCGTGTA 2088
2089 AAGTGAATGTGAGCTTGCAACAGGGCTGCCTGCAAGCTCCTGGAGCAGGCCAAGGCCCCGCAGTTGACATGT 2160
2161 TTTGGACCTGTGCGGGCATCCCGCATGTAACATCCCGTGTGCAAAAAA 2208
B
MmD2LIC
HsD2LIC
CeD2LIC
DmD2LIC
CrD1bLIC
MmDLIC2
HsDLIC2
RnDLIC2
RnDLIC1
MmDLIC1
HsDLIC1
GgDLIC1
XlDLIC1
CrlC1
100
97
100
100
100
100
100
100
100
100
100

Figure 4.2. **An insertional mutant, TBD9–1, is defective in D1bLIC.** (A) Schematic diagram of *D1bLIC* gene structure. The 10.0-kb fragment from SmaI to HindIII and the 7.3-kb fragment from SmaI to SacI were used for later rescue experiments. The regions corresponding to the 5' cDNA probe, 3' cDNA probe used in the northern blotting, the full-length cDNA probe used in the Southern blotting, and the antigen region for antibody preparation are indicated by lines underneath. Black boxes, exons; black dot, polyA signal addition site; Sm, SmaI; K, KpnI; P, PstI; H, HindIII; Sa, SacI. (B) Southern blotting indicates the *D1bLIC* gene is disrupted in TBD9–1. Genomic DNA from wild-type cells and TBD9–1 cells was cut by *Pst*I and probed with the full-length *D1bLIC* cDNA probe. The TBD9–1 DNA is lacking one 1.2-kb PstI band present in wild-type DNA and has two additional bands of ~1.4 and 3.5 kb as indicated by arrowheads. This implies that there is an insertion in the 1.2-kb PstI region of the *D1bLIC* gene in TBD9–1 cells, whereas the rest of the gene is intact. (C) Northern blotting indicates *D1bLIC* mRNA is disrupted in TBD9-1. Total RNA from TBD9-1 cells and wild-type cells before (N) and 30 min after deflagellation (D) were probed with 5' or 3' *D1bLIC* cDNA probes. The *D1bLIC* mRNA is ~2.2 kb and is up-regulated by deflagellation in wild-type cells. No signal was detected by the 3' cDNA probe in RNA from TBD9-1. Two faint bands of ~5 and 1.8 kb were detected by the 5' cDNA probe in RNA from TBD9-1 cells; they are slightly down-regulated by deflagellation. The bottom panel was probed with fructose-bisphosphate aldolase (FBA) cDNA as a loading control. (D) D1bLIC protein is missing in TBD9-1. A western blot of whole cell lysates from TBD9-1 cells and wild-type cells probed with the anti-D1bLIC

antibody shows that D1bLIC migrates at ~48.5 kD in wild-type cells and that no protein is present in TBD9-1 cells. The bottom panel was probed with an anti– β -tubulin antibody as a loading control.

Figure 4.2

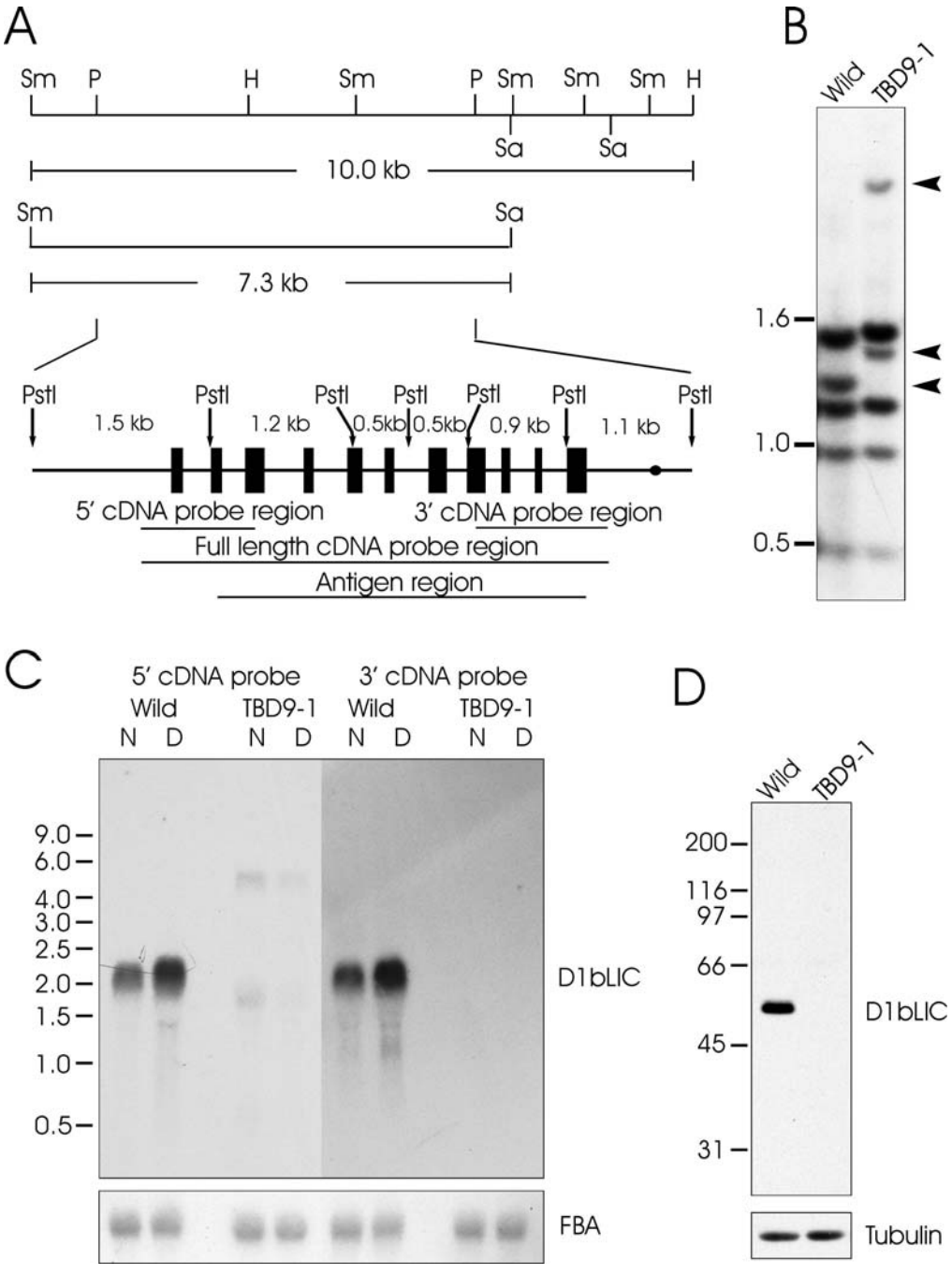
A
Sm P H Sm P Sm Sm Sm H
Sa Sa
10.0 kb
Sm Sa
7.3 kb
PstI PstI PstI PstI PstI PstI PstI
1.5 kb 1.2 kb 0.5kb 0.5kb 0.9 kb 1.1 kb
5′ cDNA probe region
3′ cDNA probe region
Full length cDNA probe region
Antigen region
B
Wild TBD9-1
1.6
1.0
0.5
C
5′ cDNA probe
3′ cDNA probe
Wild TBD9-1 Wild TBD9-1
N D N D N D N D
9.0
6.0
4.0
3.0
2.5
2.0
1.5
1.0
0.5
D1bLIC
FBA
D
Wild TBD9-1
200
116
97
66
45
31
D1bLIC
Tubulin

Figure 4.3. **The phenotype of YH43 can be rescued by the cloned *D1bLIC* gene.** (A) *D1bLIC* DNA is restored in cells rescued for the motility defect by transformation with the *D1bLIC* gene. Genomic DNA from wild-type cells (137c), YH43, and some of the cells rescued by the 10-kb *D1bLIC* genomic fragment (43R1, 43R5, 43R15, 43R17, 43R19, and 43R22) was cut by SmaI and analyzed on Southern blots probed with the full-length *D1bLIC* cDNA. In addition to the mutated *D1bLIC* gene, different bands were detected in the rescued cells, indicating the incorporation of the wild-type *D1bLIC* transgene at different sites. (B) D1bLIC protein is detected in rescued cells. Western blots of wild-type cells (137c), YH43, and some of the rescued cells (43R1, 43R5, 43R15, 43R17, 43R19, and 43R22) probed with the anti-D1bLIC antibody showed that the rescued cells express D1bLIC protein. β-tubulin was probed in the bottom panel as a loading control.

Figure 4.3

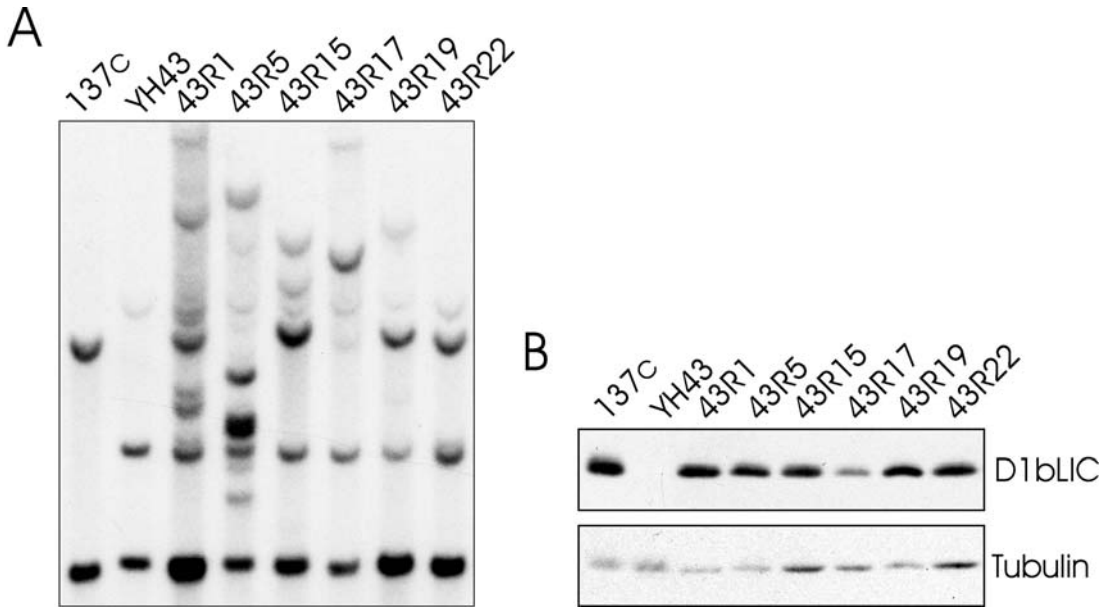
A
137C
YH43
43R1
43R5
43R15
43R17
43R19
43R22
B
137C
YH43
43R1
43R5
43R15
43R17
43R19
43R22
D1bLIC
Tubulin

Figure 4.4. **Immunofluorescence microscopy shows that the YH43 cell accumulates IFT-particle proteins in its short flagella.** Wild-type cells, YH43 cells (*d1blic*), and rescued cells were stained with an anti-IFT172 antibody (green). Cell bodies are red due to autofluorescence. Most of the IFT172 protein is in the peri-basal body region with a lesser amount spread along the flagella in the wild-type cells. In the *d1blic* mutant cells, IFT172 is redistributed from the peri-basal body region to the flagella, which are usually short and stumpy but sometimes longer. In mutant cells rescued with the wild-type *D1bLIC* gene, IFT172 is distributed as in wild-type cells. Scale bar, 5 μm.

Figure 4.4

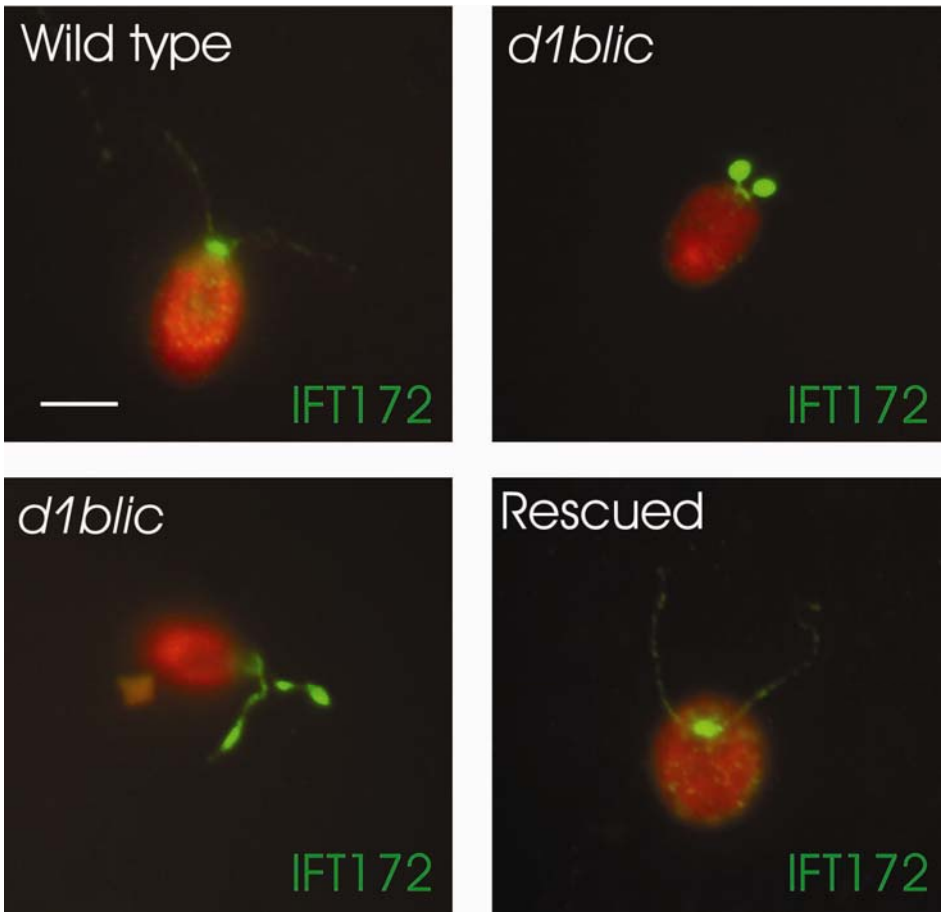
Wild type
IFT172
d1blic
IFT172
d1blic
IFT172
Rescued
IFT172

Figure 4.5. **Electron microscopy shows that *d1blic* flagella accumulate IFT particles.** In wild-type cells (a and b) and the rescued cells (g and h) the space between the flagellar membrane and doublet microtubules is usually devoid of material. In contrast, in the *d1blic* mutant cells (c, d, e, and f) the space between the doublet microtubules and the flagellar membrane is filled with electron-dense material identical in appearance to IFT particles (Kozminski *et al.*, 1993, 1995; Pazour *et al.*, 1998). Note that the *d1blic* mutant cells have an apparently normal axoneme. Scale bars, 100 nm.

Figure 4.5

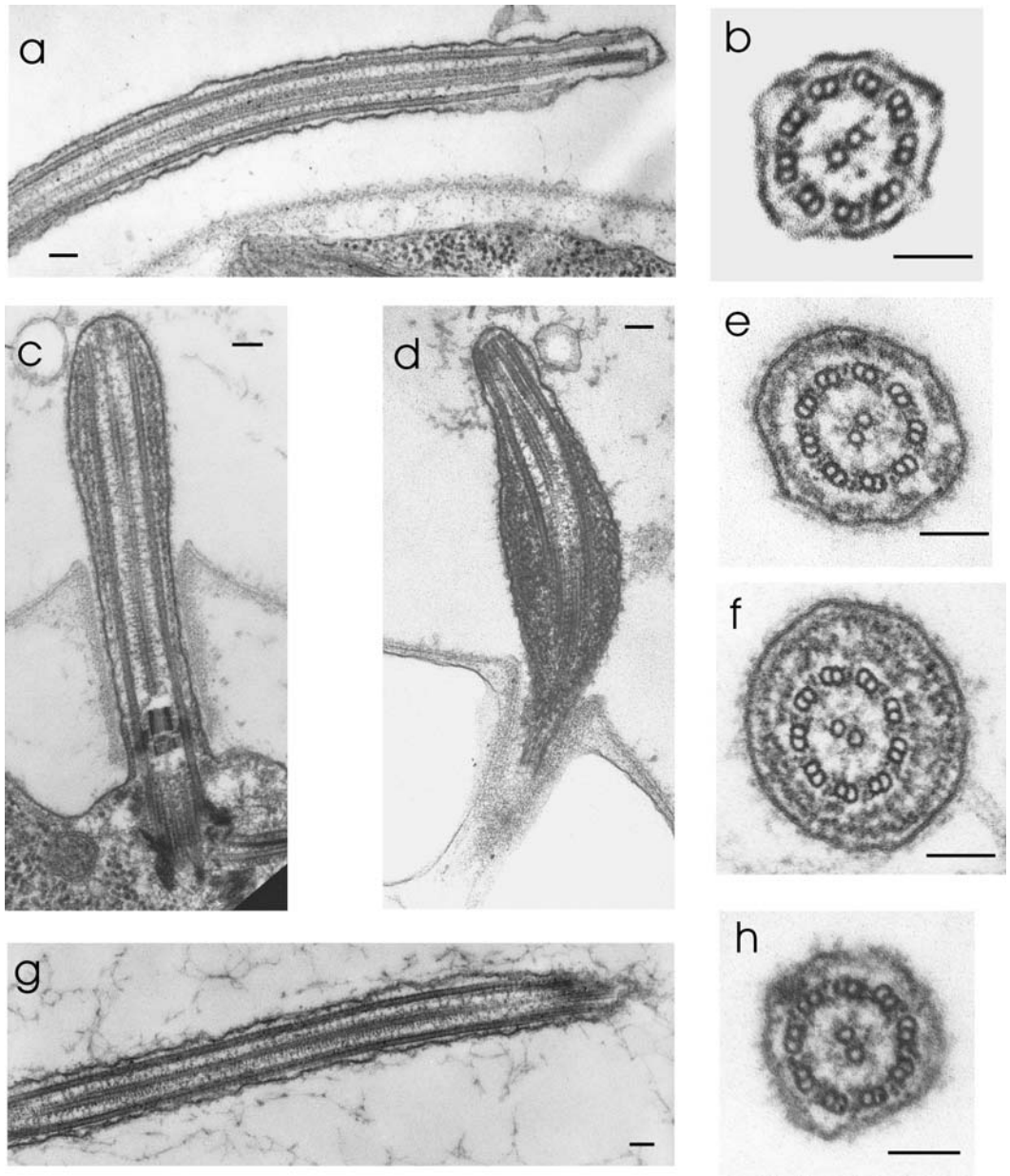

Figure 4.6. **The *d1blic* mutant is normal in cell growth rate and localization and morphology of the Golgi apparatus.** (A) Growth curves for wild-type cells and *d1blic* mutant cells. Wild-type cells and *d1blic* cells were grown in liquid M medium with aeration with 5% CO_2. Every 24 h a sample was removed and the cells counted with a hemocytometer. On day 3, a second set of cultures was inoculated by diluting cells from the first series to 10^5 cells/ml. (B) The Golgi apparatus of *d1blic* mutant cells is morphologically normal. Like the wild-type cells, the *d1blic* cells have a pair of Golgi apparatuses on the opposite side of the nucleus from the basal bodies. The Golgi apparatus is composed of 4–8 cisternae and is adjacent to a large membrane-bound vesicle on the *trans* side.

Figure 4.6

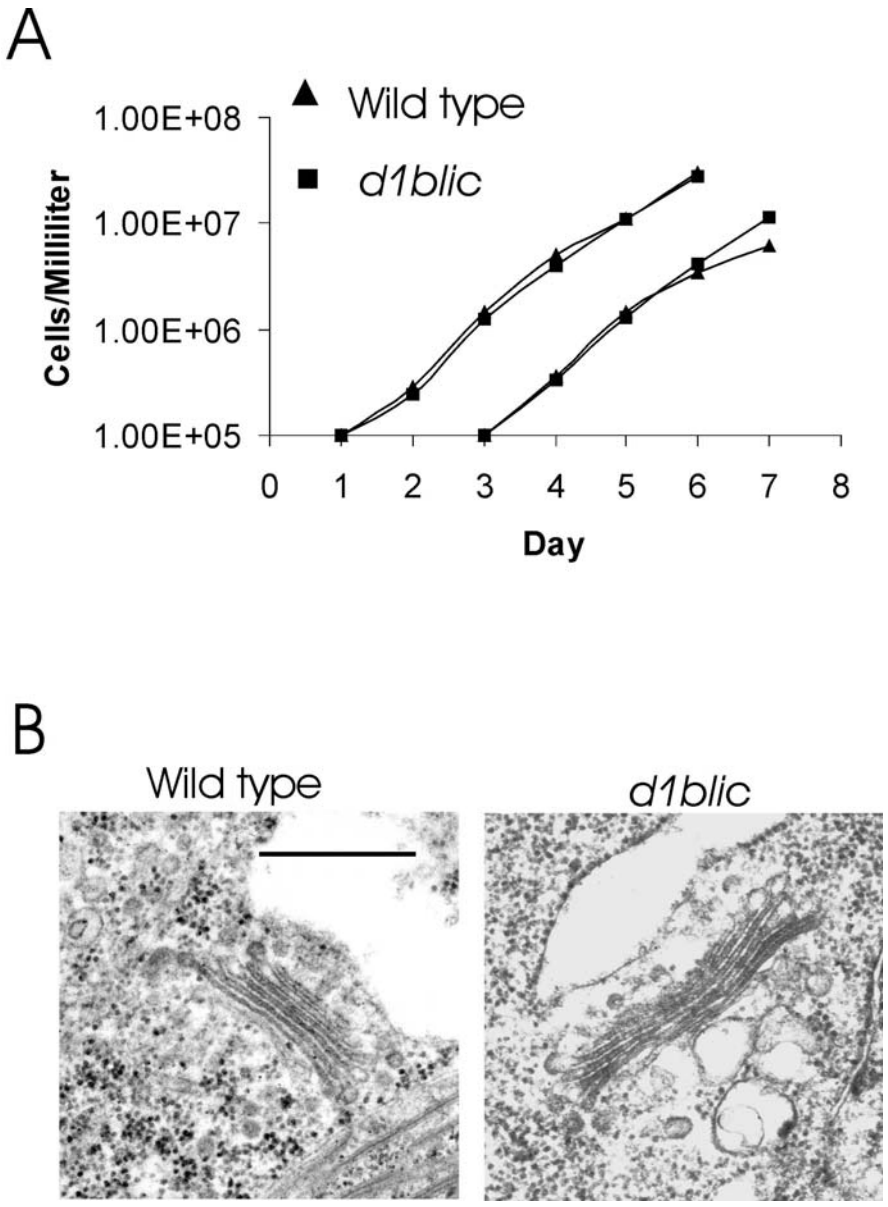
A
Wild type
d1blic
1.00E+08
1.00E+07
1.00E+06
1.00E+05
Cells/Milliliter
0
1
2
3
4
5
6
7
8
Day
B
Wild type
d1blic

Figure 4.7. **The level of DHC1b is reduced in *d1blic* mutant cells and vice versa.** Western blots of whole-cell lysates from wild-type cells, *d1blic* mutant cells, and *dhc1b* mutant cells were probed with anti-DHC1b or anti-D1bLIC antibodies. The DHC1b level is reduced in the *d1blic* mutant; the D1bLIC level is greatly reduced in the *dhc1b* mutant. β -tubulin was probed with an anti– β -tubulin antibody as a loading control.

Figure 4.7

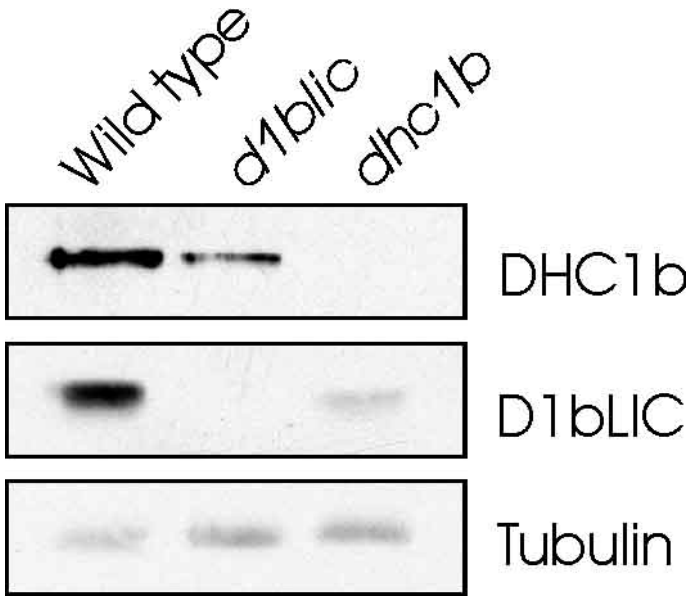

Figure 4.8. **D1bLIC and DHC1b have a similar cellular localization.** Wild-type cells (left panels) were stained with anti-D1bLIC antibody or anti-DHC1b antibody. The null mutants (right panels) served as controls and were stained in the same way. The antigens are in green and the cell bodies are in red. Both DHC1b and D1bLIC are located primarily in the peri-basal body region and sparsely distributed along the flagella.

Figure 4.8

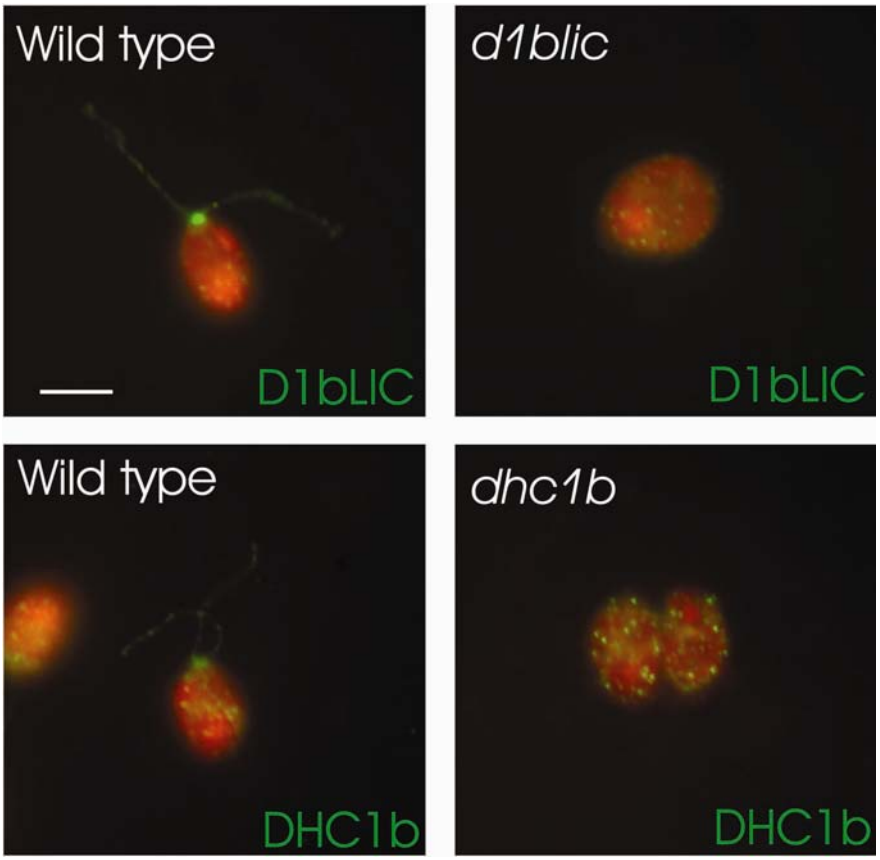

Figure 4.9. **D1bLIC is in the same complex as DHC1b.** (A) D1bLIC and DHC1b have a similar distribution in flagellar fractions. Wild-type flagella were fractionated into detergent-soluble membrane plus matrix (M+M), ATP wash 1 (ATP1), ATP wash 2 (ATP2), ATP wash 3 (ATP3), salt extract (Salt), and salt-extracted axonemes (Axo). Extracts from an equal number of flagella were probed with anti-D1bLIC, anti-DHC1b, anti-IFT172, anti-IFT139, and anti-IC1 antibodies. As reported by Pazour *et al.* (1999), DHC1b is contained primarily in the first ATP wash, with a lesser amount in the membrane plus matrix fraction and very little in the other fractions. In contrast, IFT172 and IFT139 are concentrated primarily in the membrane plus matrix fraction, whereas outer dynein arm intermediate chain IC1 is located primarily in the salt extract. Like DHC1b, D1bLIC also is contained primarily in the first ATP wash. (B) D1bLIC and DHC1b cosediment with each other. The matrix fraction from wild-type flagella was fractionated by centrifugation in a 5–20% sucrose gradient. Fractions were probed with anti-D1bLIC and anti-DHC1b antibodies. D1bLIC and DHC1b comigrate in a sharp peak at ~12 S. (C) DHC1b is coimmunoprecipitated by anti-D1bLIC antibody. Anti-D1bLIC antibody (IP) or preimmune serum (Control) was used for the immunoprecipitation experiments. The resulting supernatants (Sup) and pellets (Pel) were probed with anti-D1bLIC, anti-DHC1b, and anti-IC1 antibodies. Both D1bLIC and DHC1b were immunoprecipitated by the anti-D1bLIC antibody but not by preimmune serum. IC1 remained in the supernatant from both the anti-D1bLIC antibody and preimmune serum immunoprecipitations.

Figure 4.9

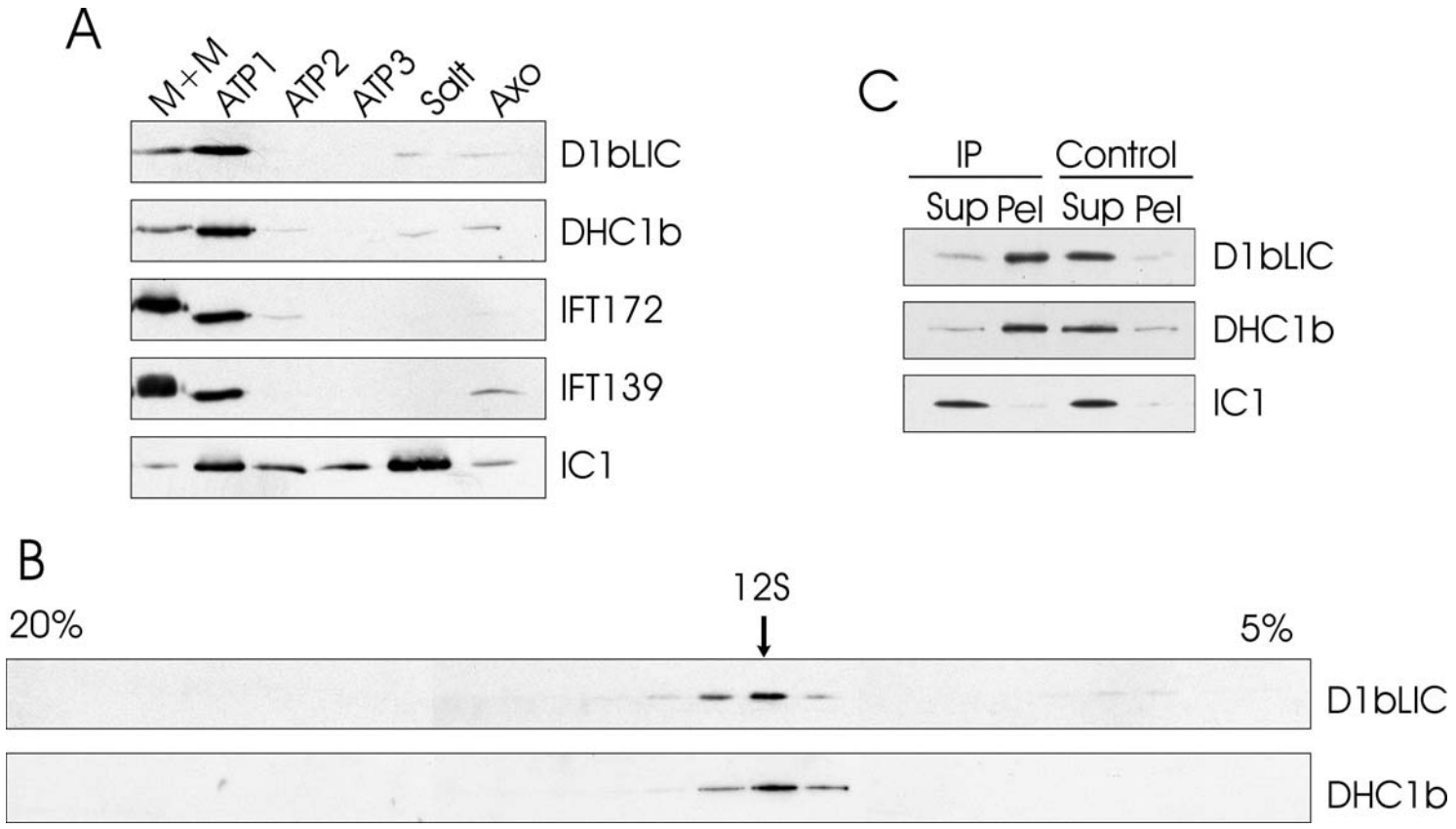
A
M+M
ATP1
ATP2
ATP3
Salt
Axo
D1bLIC
DHC1b
IFT172
IFT139
IC1
C
IP
Control
Sup Pel Sup Pel
D1bLIC
DHC1b
IC1
B
20%
12S
5%
D1bLIC
DHC1b

Figure 4.10. **DHC1b has a normal localization in *d1blic* mutant cells.** Wild-type (a and b) and *d1blic* mutant cells with near full-length flagella (c and d) or shorter flagella (e and f) were stained with the anti-DHC1b antibody and were imaged by fluorescence microscopy (a, c, and e) or DIC microscopy (b, d, and f). Arrowheads indicate the bulges, shown in Figure 4.4 to be filled with IFT particles, in *d1blic* mutant flagella. DHC1b protein is in green and cell bodies in red. The DHC1b protein was present as puncta along the length of both wild-type and *d1blic* mutant flagella. No obvious accumulation of DHC1b protein was observed in the bulges on the *d1blic* flagella. Scale bar, 5 μm.

Figure 4.10

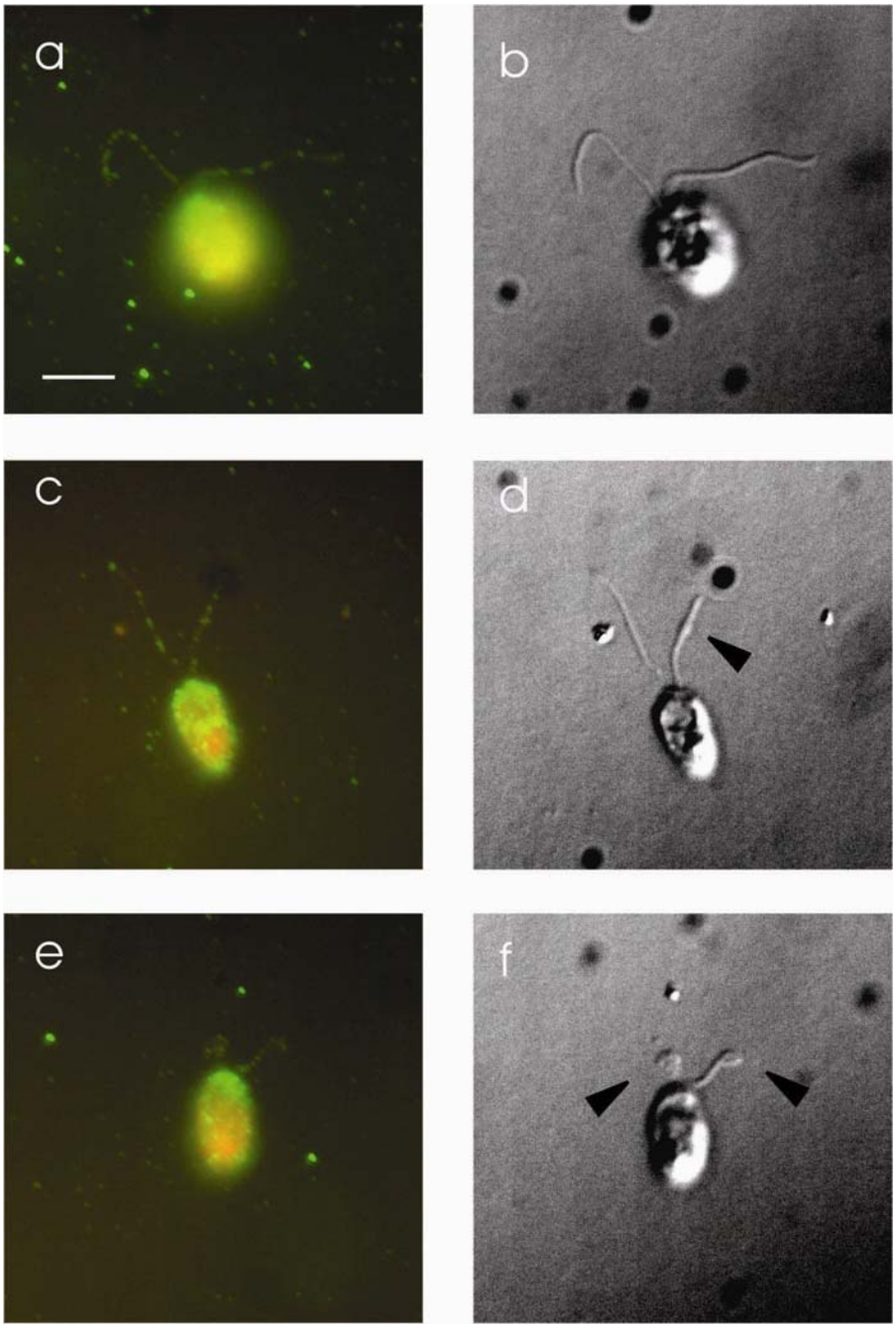

Figure 4.11. **The P-loop is not required for D1bLIC's function in IFT.** (A) PCR amplification shows that the mutated exogenous *D1bLIC* genes were incorporated into the cell lines transformed with mutated P-loop constructs K and KS. The P-loop region was amplified using genomic DNA from wild-type cells (W), *d1blic* mutant cells (M), and cells transformed with mutated P-loop construct K (1, 2, and 3) or construct KS (1, 2, and 3). As expected, a ~700-base pair product obtained from wild-type cells was cut by NaeI into two ~350-base pair products, but was not cut by SalI. No specific product was obtained from mutant cells. The ~700-base pair products obtained from cells transformed with the K construct contained a *Sal*I site and thus could be cut by SalI into two ~350-base pair fragments. The ~700-base pair products obtained from cells transformed with the KS construct lack the NaeI site and thus remained ~700 base pairs in length after NaeI treatment. (B) Western blotting shows that the transformed cells express the 3HA-tagged D1bLIC protein. Whole-cell lysate from wild-type cells (W), cells transformed with the 3HA-tagged wild-type *D1bLIC* gene (43R), cells transformed with the K construct (1, 2, and 3), and cells rescued with the KS construct (1, 2, and 3) were probed with the anti-HA antibody or the anti-D1bLIC antibody. The anti-HA antibody did not recognize any band in the wild-type cell lysate, but recognized a doublet of ~56–57 kD in the transformed cell lysates. Western blotting using the anti-D1bLIC antibody on an equivalent blot confirmed that these doublets represented HA-tagged D1bLIC protein, which migrated at a higher position than the endogenous D1bLIC protein in the wild-type cells. (C) DIC images of wild-type cells, *d1blic* cells, and *d1blic* cells transformed with the K (K) and KS (KS) constructs.

Flagellar length is completely restored in cells transformed with the K or KS constructs. Scale bar, 5 μm. (D) IFT172 is normally distributed in *d1blic* cells transformed with the K and KS constructs. Wild-type cells, *d1blic* cells, and *d1blic* cells transformed with the K (K) and KS (KS) constructs were stained with an anti-IFT172 antibody (green). Cell bodies are red due to autofluorescence. Scale bar, 5 μm.

Figure 4.11

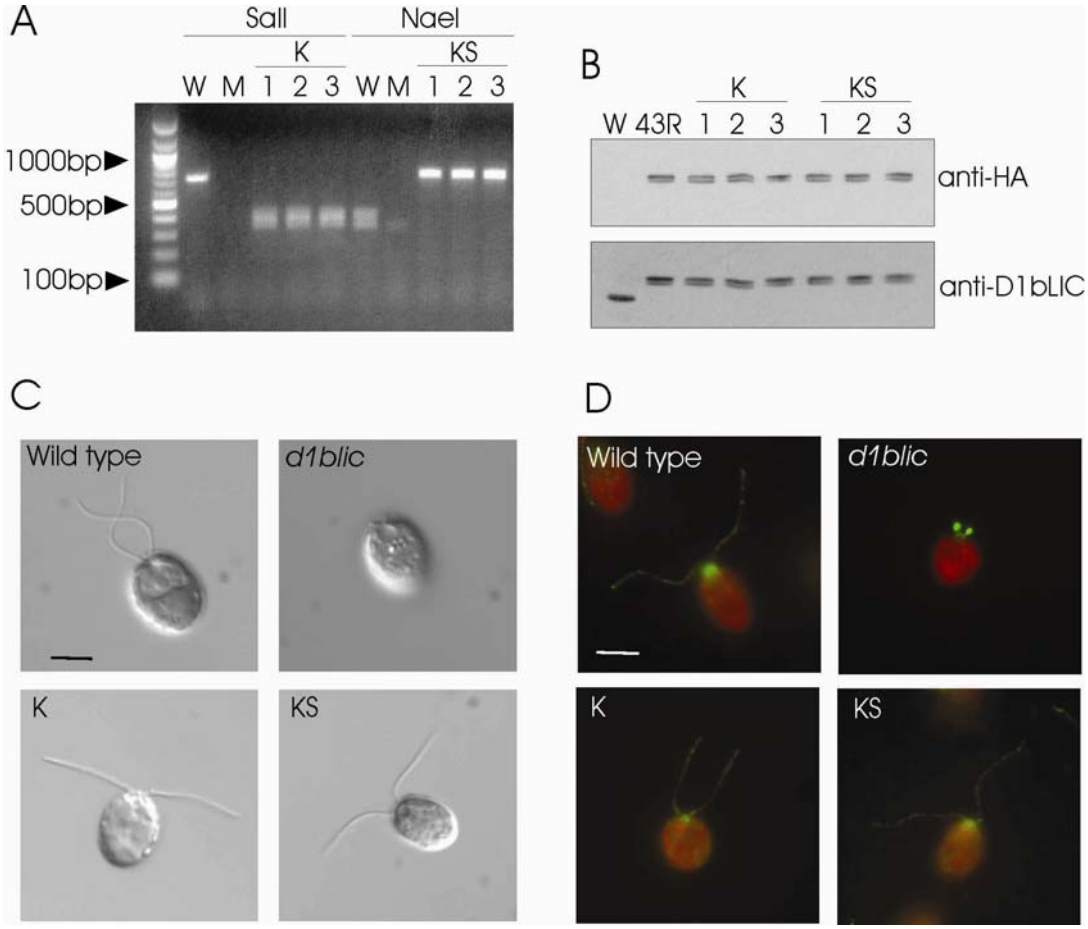
A
SalI
NaeI
K
KS
W M 1 2 3 W M 1 2 3
1000bp
500bp
100bp
B
K
KS
W 43R 1 2 3 1 2 3
anti-HA
anti-D1bLIC
C
Wild type
d1blic
K
KS
D
Wild type
d1blic
K
KS

CHAPTER V

FUNCTIONAL ANALYSIS OF AN INDIVIDUAL IFT PROTEIN: IFT46 IS REQUIRED FOR TRANSPORT OF OUTER DYNEIN ARMS INTO FLAGELLA

Introduction

Before I began my thesis work, *Chlamydomonas* IFT-particle protein null mutants were known only for IFT88 (Pazour et al, 2000) and IFT52 (Brazelton et al., 2001); neither of them form flagella. As shown in CHAPTER III, by screening the collection of flagella mutants, I identified several mutants defective in IFT-particle proteins. Preliminary data on these mutants showed that mutants defective in *IFT20*, *IFT172* and *IFT140* also do not have flagella, while mutants defective in the *IFT46* gene have short stumpy flagella. At that time, little was known about the specific functions of individual IFT-particle proteins. Since the mutants defective in IFT46 can form some flagellar structure, these mutants had the potential to be informative as to the specific function of IFT46 in flagellar assembly. Therefore, I decided to focus on IFT46 for the remainder of my thesis research.

To obtain more information on IFT46, I first confirmed that *Chlamydomonas* IFT46 is an IFT complex B protein. Then I focused on characterizing one of the mutants defective in the *IFT46* gene, and a suppressor of that mutant. My results show that IFT46 is required for the stability of IFT complex B and is specifically involved in

outer dynein arm transport into flagella. IFT46 is phosphorylated *in vivo* and the phosphorylation is not critical for IFT46's function in flagellar assembly.

While I was working on *Chlamydomonas* IFT46, Dr. G. Pazour showed that mammalian IFT46 localizes to cilia and is tightly associated with complex B proteins but not with complex A proteins (Hou et al., 2007). Recently, the *C. elegans* orthologue of IFT46 was identified as DYF-6 (Bell et al., 2006). DYF-6 is required for cilia assembly and GFP tagged DYF-6 undergoes IFT.

Results

IFT46 is conserved among ciliated organisms. The gene and cDNA encoding *Chlamydomonas* IFT46 were cloned as described in Materials and Methods. The cDNA (accession number: DQ787426) contains a 1,035-nucleotide ORF predicted to encode a 37.9-kD protein (Figure 5.1) with a pI of 4.61. The cDNA has a stop codon 18 nucleotides upstream of the predicted start codon, and a polyA consensus sequence at nucleotides 1703-1707. ESTs have a polyA tail 12-14 nucleotides downstream of the polyA consensus sequence. Therefore, the ORF is complete. No structural domains or motifs were identified within the sequence.

Database searches revealed that IFT46 is conserved across organisms that have cilia, including *Danio rerio* (XP_694278; BLAST E= 1e-47), *Apis melifera* (XP_396519; BLAST E=1e-47), *Drosophila melanogaster* (NP_609890; BLAST E=1e-17), *Mus musculus* (NP_076320; BLAST E= 2e-61), and *Homo sapiens* (CAB66868; BLAST E= 8e-62). The protein also is homologous to *C. elegans* DYF-6

(NP_741887; BLAST E= 9e-34), which recently was reported to undergo IFT in dendritic cilia when fused to GFP (Bell et al., 2006). No similar sequence was found in non-ciliated organisms, including *Saccharomyces cerevisiae* and *Arabidopsis thaliana*.

Chlamydomonas IFT46 is an IFT complex B protein. *Chlamydomonas* IFT46 was initially identified as an IFT complex B protein based on its co-sedimentation with other complex B proteins in sucrose gradients (Cole et al., 1998). Characterization of our cloned protein indicates that it behaves exactly as expected for a 46-kD complex B protein. 1) Six unique peptides corresponding to the cloned protein were identified in the membrane-plus-matrix fraction of the flagellar proteome, but no peptides from it were found in any other fraction, a distribution similar to that for known IFT-particle proteins but unusual for non-IFT proteins (see Figure 5.3c in Pazour et al., 2005). 2) Real-time PCR results showed that expression of the protein is up-regulated 10.4 ± 2.03 (S.E.) fold upon deflagellation, which is characteristic of flagellar proteins, including other complex B proteins (Pazour et al., 2005). 3) An antibody to a peptide contained in the cloned protein was generated and shown to react specifically with a single protein of M_r ~46,000 in western blots of whole cell lysates (Figure 5.2A). 4) Immunofluorescence microscopy with the antibody as probe showed that the majority of the cloned protein is located in the basal body region with a lesser amount in puncta along the length of the flagella (Figure 5.2B), a distribution identical to that of other IFT-particle proteins (Cole et al., 1998; Deane et al., 2001; Figure 3.1A); moreover, the protein colocalized with complex B protein IFT172 but not complex A protein IFT139

(see below and Figure 5.6B). 5) When the flagellar membrane-plus-matrix fraction was analyzed by sucrose density gradient centrifugation, the cloned protein co-migrated precisely with IFT81, a complex B protein, but not with IFT139, a complex A protein (Figure 5.2C). These results indicate that the cloned protein is indeed IFT46, and confirm that IFT46 is a complex B protein.

IFT46 is necessary for flagellar assembly. As mentioned in CHAPTER III, three strains (T8a44-11, T88a9-11 and T8a4-10) were identified as defective in *IFT46* gene by Southern blotting in a screen for mutants defective in IFT-particle protein genes. Since they all showed the same RFLPs on Southern blots (Figure 3.4D-F) and are likely to be sister strains (originating from the same insertional event), only one of them, T8a44-11, was further characterized. Analysis by PCR showed that the mutant allele, which I term *ift46-1*, has a deletion or disruption somewhere between the fourth exon and the seventh exon of the *IFT46* gene (Figure 5.3A and 5.3B) and is a null allele (see below). This mutant has short, stumpy flagella.

Strain T8a44-11 was backcrossed to wild-type cells, and a progeny, YH6, which lacked the *pf1* mutation carried by the parental strain, was selected for detailed characterization. As in T8a44-11, the *IFT46* gene in YH6 is disrupted, as shown by Southern blotting (Figure 5.3C, lane 2). No IFT46 can be detected in lysates of YH6 cells (Figure 5.3D, lane 2), indicating that full-length IFT46 is not expressed in YH6 cells. Like T8a44-11, YH6 cells have short stumpy flagella that barely extend beyond the flagellar collar (Figure 5.4). They are non-motile.

To confirm that the mutant phenotype of YH6 was caused by the disruption of the *IFT46* gene, YH6 cells were transformed with a 4.8-kb fragment containing only the wild-type *IFT46* gene (Figure 5.3A). Numerous wild-type swimmers with full-length flagella were recovered. Southern blotting revealed that the exogenous *IFT46* gene had integrated into the genome at different sites in several of these rescued strains (Figure 5.3C, lanes 3-9), confirming that the rescued strains were independently derived. Therefore, restoration of motility was due to incorporation of the transgene, and not caused by disruption of some other gene. Western blotting confirmed that expression of IFT46 was restored in the transformants (Figure 5.3D, lanes 3-9). These results demonstrate that the short flagella phenotype of YH6 is caused by the absence of IFT46. Hereafter, this strain will be referred to as the *ift46* mutant.

The *ift46* mutant has unique defects in its axoneme. Although very short, *ift46* flagella are longer than those of mutants with defects in the complex B proteins IFT88 (Pazour et al., 2000) and IFT52 (Brazelton et al., 2001), which do not form flagella beyond the transition region. Because flagella are formed in the *ift46* mutant, I was able to compare them with flagella from wild-type and rescued cells by EM to identify flagellar defects associated with loss of IFT46. Serial sections of wild-type flagella have shown that the outer doublet microtubules are connected by rod-like "peripheral links" in the most proximal part of the flagella (Figure 5.4A, panel a); the rows of dynein arms begin at a level slightly more distal but still within the flagellar collar (Figure 5.4A, panel b) (Hoops and Witman, 1983). The *ift46* flagella have 9 outer

doublet microtubules and frequently extend to the limits of the flagellar collar or beyond (Figure 5.4A, panels f-p), but dynein arms were never observed in longitudinal or cross-sections of these axonemes. In addition, the mutant flagella lack the projections into the lumens of the B-tubule (Hoops and Witman, 1983) and frequently have defects in the central pair of microtubules (Figure 5.4A, panels f-k). In contrast to mutants with defects in the retrograde IFT motor (Pazour et al., 1999; Porter et al., 1999; Hou et al., 2004 and CHAPTER IV), few if any IFT particles accumulate in the *ift46* mutant flagella. It is important to note that the flagella from the rescued cells (Figure 5.4A, panels d and e) have typical wild-type morphology with normal inner and outer dynein arms and central pair microtubules; this confirms that the ultrastructural defects seen in the mutant are due to loss of IFT46.

To determine whether the dynein arm deficiency in the *ift46* mutant is caused by degradation of dyneins within the cell body, by an inability to transport dyneins into the flagella, or by an inability to assemble them onto the axonemes, we analyzed whole cell lysates and flagella from *ift46* and wild-type cells by western blotting (Figure 5.4B). The cell lysates of the mutant contained normal levels of the outer arm dynein IC IC2 and the inner arm dynein IC IC138. Therefore, the dyneins are present in the mutant cells. However, both IC2 and IC138 were completely absent from the *ift46* mutant flagella, indicating that the dyneins are not transported into the flagella. In contrast, DC2, a component of the outer dynein arm docking complex, which is transported into the wild-type flagellum and assembled onto the doublets independently of the outer dynein arm (Wakabayashi et al., 2001), is transported into the *ift46* flagella. The

presence of DC2 in the flagella provides additional evidence that the lack of dynein arms is not simply due to the short length of the mutant flagella or to a general failure to transport proteins into the flagellum. These data confirm the ultrastructural findings that the *ift46* mutant has a defect in transporting dynein arms into the flagella.

IFT complex B is unstable in the absence of IFT46. To investigate the role of IFT46 in IFT complex assembly, I examined the cellular levels of IFT complex B and A proteins in cell lysates of wild-type and *ift46* cells (Figure 5.5, lanes WT and *ift46*). When normalized with tubulin, the levels of complex B proteins IFT20, IFT57, IFT72 and IFT81 were greatly decreased in the mutant cells relative to the wild-type cells. The only complex B protein not reduced in the absence of IFT46 was IFT172, the level of which was the same as or greater than in wild-type cells, depending on the preparation, suggesting that the level of IFT172 is controlled independently from that of the other complex B proteins. In contrast to the decrease in most complex B proteins seen in the *ift46* mutant, the levels of complex A proteins IFT139 and IFT140 were greatly increased in *ift46* cells relative to wild-type cells.

To investigate if these differences in protein levels were due to changes in synthesis or stability, I used real-time PCR to measure transcript levels for several complex A and B proteins in wild-type and *ift46* cells. Transcript levels in the mutant were increased ~2.8 and ~2.0 fold for complex A proteins IFT140 and IFT139, and ~1.8 and ~1.6 fold for complex B proteins IFT81 and IFT72, respectively. Therefore, the mutant responds to its defect by increasing the mRNA levels of at least these

complex A and B proteins. The increase in complex A proteins in the mutant presumably reflects this increase in mRNA abundance. However, because the levels of most complex B proteins are drastically decreased in the mutant, even though complex B mRNA levels in general appear to be increased, it is likely that these proteins are specifically degraded in the absence of IFT46.

Complex A and B proteins are located in distinct compartments in the basal body region. To determine if the absence of IFT46 and the accompanying large decrease in most other complex B proteins affected the transport of IFT172 or complex A into or out of the flagellum, I used immunofluorescence microscopy to examine *ift46* cells that were double labeled with antibodies to tubulin and IFT172 or IFT139 (Figure 5.6A). In both cases, the IFT-particle proteins were concentrated around the basal bodies and in the short flagella. Thus, both proteins are transported into the flagella in the absence of IFT46. Surprisingly, however, the distributions of IFT172 and IFT139 differed from each other in the cell body, with that of IFT172 (Figure 5.6A, panels a-d) appearing to have almost no overlap with that of IFT139 (Figure 5.6A, panels e-h), which was more anterior and often concentrated into two distinct lobes.

To clarify whether this difference in distribution was normal or due to loss of IFT46, wild-type cells were double labeled with antibodies to IFT46 and IFT172 or IFT139. In most cases, IFT46 and IFT172 co-localized precisely with each other in the peri-basal body region (Figure 5.6B, panels a-c), consistent with the other evidence that IFT46 is a complex B protein. In contrast, although IFT139 co-localized with IFT46 at

the extreme apical end of the cell, the labeling of IFT46 almost always extended more posteriorly than did that of IFT139 (Figure 5.6B, panels d-f). This is the first observation that complex A and complex B proteins differ in their distribution, and indicates that the complexes, or at least a subset of them, are not physically associated in the cell body. This together with the above results for the *ift46* mutant also shows that, in the absence of IFT46, the co-localization of IFT172 with complex A proteins at the extreme apical end of the cell is lost.

The observation that IFT172 was transported into the short flagella of the *ift46* mutant (Figure 5.6A) raised the question of whether IFT172 was being transported into the flagella independently of other complex B proteins, or in association with incomplete complex B particles possibly assembled from the small amount of complex B proteins still present in the mutant. To address this question, I used immunofluorescence microscopy to examine the distribution of another complex B protein, IFT57, the levels of which are greatly reduced in the mutant. Like IFT172, the residual IFT57 was transported into the short flagella of the *ift46* mutant (Figure 5.6C). These results support the hypothesis that a small number of incomplete complex B particles assemble from the residual complex B proteins and are capable of being transported into the flagellum in the absence of IFT46. The resulting low level of IFT may account for the ability of the *ift46* cells to assemble their short flagella.

Loss of IFT46 is specifically correlated with loss of the outer dynein arm in a partially suppressed strain. *ift46* cells are completely non-motile. However, on one occasion,

swimming cells were observed in an unaerated, stationary phase culture of *ift46* cells. Cells from this culture were cloned, and a partially suppressed strain, $Sup_{ift46}1$, was isolated. $Sup_{ift46}1$ cells are usually non-motile when grown in M medium with aeration, but are stimulated to form flagella of variable length (Figure 5.7) and swim with a slow jerky movement in the absence of aeration. The suppressed phenotype is the result of a rare spontaneous mutation that allows transcription of the 3' end of the IFT46 gene (see below).

To elucidate the effect of the partial suppressor mutation on IFT46 and other IFT-particle proteins, the levels of the proteins in stimulated $Sup_{ift46}1$, wild-type and *ift46* cells were compared by western blotting. In the $Sup_{ift46}1$ cells, complex B proteins IFT20, IFT57, IFT72 and IFT81 were increased to a level between those of *ift46* and wild-type cells (Figure 5.6), whereas the levels of complex A proteins IFT139 and IFT140 were decreased to a level between those of *ift46* and wild-type. Importantly, IFT46 is still undetected in the suppressed strain. This result indicates that the partial suppression of *ift46* involves an increased stability of IFT complex B in the absence of full-length IFT46. It is possible that a C-terminal fragment of IFT46 is expressed in $Sup_{ift46}1$ cells and incorporated into complex B, stabilizing it (see below). Such a fragment would not be detected by our antibody to the N terminus of IFT46.

The slow, jerky swimming of $Sup_{ift46}1$ is typical of outer dynein arm mutants. Therefore, I used immunofluorescence microscopy to check for the presence of outer and inner dynein arms in $Sup_{ift46}1$ flagella. No outer arm dynein was detected using an

antibody to the α heavy chain of outer arm dynein (Figure 5.7A, panels a-i). In contrast, labeling of $Sup_{ift46}1$ flagella by an antibody to inner arm dynein I1 intermediate chain IC138 was normal (Figure 5.7A, panels j-r). These results show that transport into the flagellum of inner arm dynein I1, but not outer arm dynein, is restored in the suppressed strain.

To determine the extent to which the ultrastructural defects of *ift46* were restored in the partially suppressed strain, $Sup_{ift46}1$ cells and flagella were examined by electron microscopy (Figure 5.7B). The inner arms, radial spokes and central microtubules were present and appeared normal. However, no outer dynein arms were observed. Therefore, the suppressor strain assembles flagella that lack the outer dynein arm but appear normal in every other way. Western blotting showed that the levels of both outer arm dynein and outer dynein arm docking complex proteins, as represented by IC2 and DC2, respectively, were normal in $Sup_{ift46}1$ cells (Figure 5.5). Thus, the inability to transport and assemble outer arms in the flagella is not due simply to an absence of these components from the cell cytoplasm. These results indicate that IFT46 is specifically needed to transport outer dynein arm components into the flagellum. The inner dynein arm and central pair defects observed in the *ift46* mutant are likely due to a more general deficiency in IFT caused by the reduced number of complex B particles.

The phenotype of $Sup_{ift46}1$ cells is stable and dependent on growth conditions. I investigated if suppression of *ift46* cells occurred frequently in the absence of aeration and also

if the suppression in $Sup_{ift46}1$ cells was stable during vegetative growth. Twenty-four single colonies each of *ift46* cells and $Sup_{ift46}1$ cells were inoculated into 1 ml of M medium in wells of 24-well plates. After 2 or 3 days, no swimming cells were observed in the wells inoculated with *ift46* cells. In contrast, each well of $Sup_{ift46}1$ cells contained slow swimmers. The same experiment was repeated using 24 single colonies from one of the 24 wells of $Sup_{ift46}1$ cells, and the same result was obtained. Thus, both the *ift46* phenotype and its suppressed phenotype are stable. The suppressed phenotype appears to be the result of a rare spontaneous event, which was observed only once in 2 years of culturing *ift46* mutant cells.

The suppression was more readily observed in non-aerated cultures, so I also examined the affect of growth conditions on expression of the suppressed phenotype. Cultures of cells were inoculated in M medium at 1.3×10^5 cells/ml and aerated by bubbling with 95% air + 5% CO_2 (Witman, 1986). After two days, the cells had multiplied to a concentration of 1.3×10^6 cells/ml and almost no motile cells were observed. One culture was then continued on aeration while another was removed from aeration but shaken at ~ 60 rpm to keep the cells suspended, as bubbling does. One day later, cell density and the percentage of motile cells were determined for each culture. The cells grown with continuous aeration had reached a density of 5.4×10^6 cells/ml, and no motile cells were observed. The non-aerated culture had reached a density of 4.5×10^6 cells/ml, and 13.2% of the cells were either swimming slowly or otherwise moving. Therefore, reduced aeration of $Sup_{ift46}1$ cells enhances the suppression from a

non-motile state to a motile state. This stimulation of the suppressed phenotype is likely to be due to hypoxia.

The 3'-end of the IFT46 gene is transcribed in $Sup_{ift46}1$ cells. To investigate if the suppressor mutation is intragenic or extragenic, the suppressed strain was crossed to a wild-type strain (S1D2). Only 6 out of 316 randomly selected progeny exhibited the non-parental *ift46* phenotype. The other progenies either have the wild-type or the suppressor phenotype. Therefore, the suppressor mutation is either very tightly linked to the *IFT46* gene, or is intragenic and reverts at a high frequency.

To determine if the suppressor mutation caused a change in the transcription of the *IFT46* gene, wild-type, *ift46*, and $Sup_{ift46}1$ cells were examined by reverse transcription PCR using primer pairs designed to assay for the presence of the 5' end, middle, and 3' end of the *IFT46* mRNA (Figure 5.8). In wild-type cells, all three regions were detected. In the *ift46* mutant, only the 5' end was detected, indicating that the 5' end of the gene is transcribed, but a full-length mRNA is not made. Because our antibody to the N-terminus of IFT46 did not detect a product, it appears that the truncated mRNA is not translated into a stable protein. Therefore, *ift46* is a null allele. In $Sup_{ift46}1$ cells, both the 5' end and the 3' end, but not the middle, were reproducibly detected. Therefore, the suppressor mutation results in transcription and possibly translation of the 3' end of the IFT46 gene. Our antibody would not detect a product containing the C-terminal end of IFT46 but lacking its N-terminal end. However, the possibility that the suppressor mutation results in translation of the N-terminal part of

IFT46 fused with the C-terminal part of IFT46 can be ruled out, because our antibody did not detect any product in $Sup_{ift46}1$ cells. Transcripts encoding the 3' end of the IFT46 gene were detected in $Sup_{ift46}1$ cells in both the presence and absence of aeration, so the suppressor mutation, not stress, causes transcription of the 3' end of the gene.

IFT46 is phosphorylated *in vivo* and the phosphorylation is not essential for flagellar assembly. In western blots of both whole cell lysates and flagella preparations, the anti-IFT46 antibody always detected a doublet band, with the upper band more prominent than the lower band (Figure 5.9A). After treatment of the samples with calf intestinal phosphatase, the upper band disappeared and the lower band became darker (Figure 5.9B), indicating that the upper band is a phosphorylated form of IFT46 and the lower band is the non-phosphorylated form.

To test if phosphorylation of IFT46 has a role in IFT or flagellar assembly, three phosphorylation sites ($S^{39}S^{41}S^{77}$) were identified by MS (see Materials and Methods). Two *ift46* constructs, which mimic either the non-phosphorylated form (A construct) or the phosphorylated form (D construct), were created and were transformed into the *ift46* mutant. Numerous wild-type swimmers were recovered, and Southern blotting (Figure 5.9C) showed that the modified *ift46* genes were incorporated at different sites in the genomes of the transformants. Western blots (Figure 5.9D) showed that those strains transformed with the A construct expressed IFT46 protein that co-migrated with the lower band from wild-type cells, whereas strains transformed with the D construct expressed IFT46 protein that co-migrated with the upper band from wild-type cells. No

phenotypic differences were observed between these strains and wild-type cells, indicating that the phosphorylation of IFT46 is not critical for flagellar assembly or function under our normal growth conditions.

Summary

Chlamydomonas IFT46 was previously reported to co-sediment with other IFT complex B proteins (Cole et al., 1998). Here it is confirmed that *Chlamydomonas* IFT46 is a complex B protein based on co-sedimentation and co-immunolocalization with other complex B but not complex A proteins. The analysis of a *Chlamydomonas ift46* mutant and a suppressed strain of the mutant indicate that IFT46 is necessary for complex B stability and is specifically required to transport outer dynein arm complexes into the flagella. *Chlamydomonas* IFT46 is phosphorylated at at least three sites near the N-terminus and the phosphorylation is not critical for the function of IFT46 in flagellar assembly.

Figure 5.1. **Alignment of IFT46 orthologues.** CrIFT46 is highly conserved with its orthologues from other organisms from amino acid 100 to 315. Amino acid identities are marked with asterisks; similarities are marked with either one or two dots. Sequences used in this alignment are: human (AAH22856), mouse (NP_076320), zebrafish (XP_694278), honey bee (XP_396519), CrIFT46 (DQ787426).

Figure 5.1

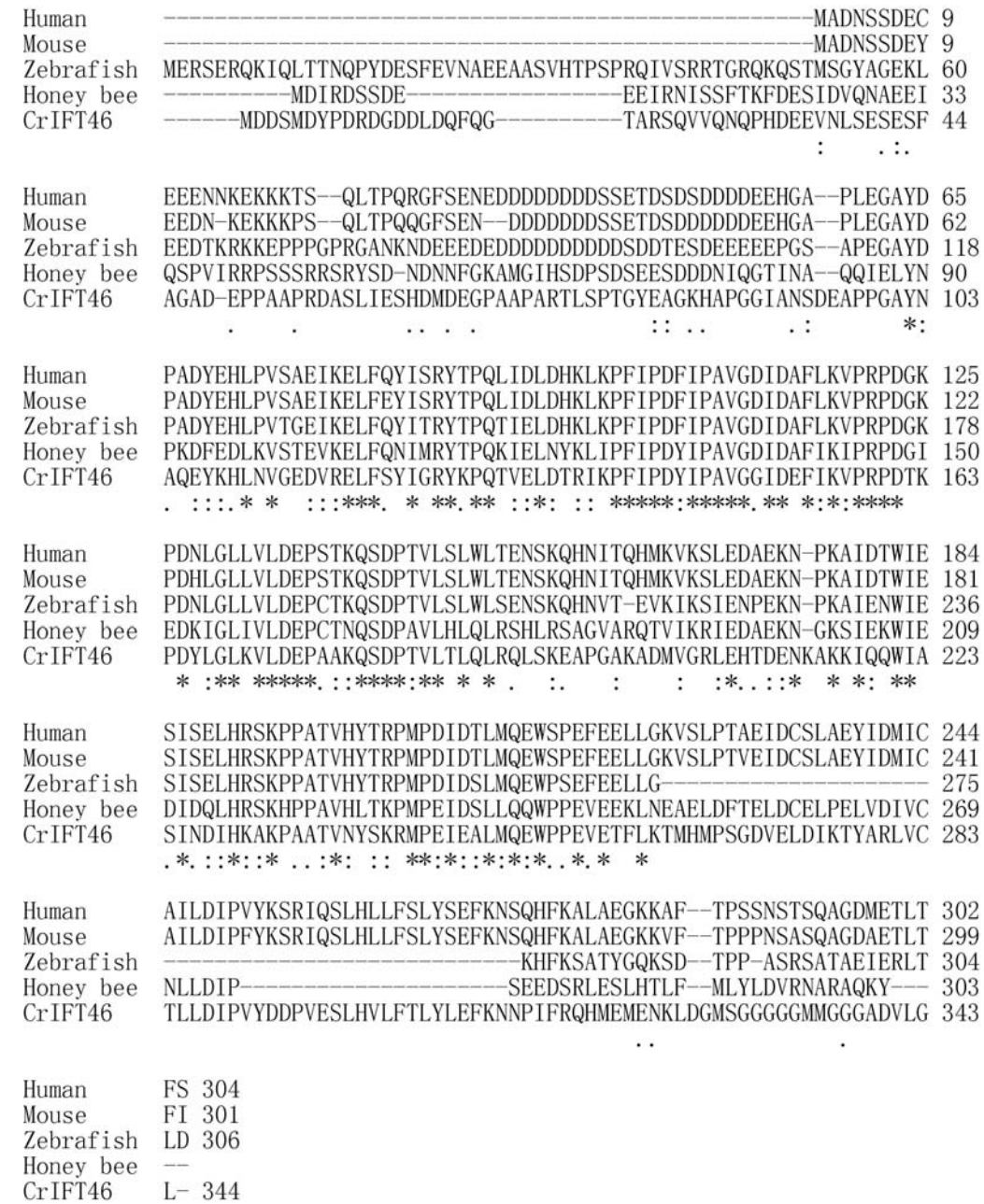
Human ----------MADNSSDEC 9
Mouse ----------MADNSSDEY 9
Zebrafish MERSERQKIQLTTNQPYDESFEVNAEEAASVHTPSPRQIVSRRTGRQKQSTMSGYAGEKL 60
Honey bee ----------MDIRDSSDE----------EEIRNISSFTKFDESIDVQNAEEI 33
CrIFT46 ------MDDSMDYPDRDGDDLDQFQG----------TARSQVVQNQPHDEEVNLSESESF 44
Human EEENNKEKKKTS--QLTPQRGFSENEDDDDDDDDSSETDSDSDDDDEEHGA--PLEGAYD 65
Mouse EEDN-KEKKKPS--QLTPQQGFSEN--DDDDDDDSSETDSDDDDDDEEHGA--PLEGAYD 62
Zebrafish EEDTKRKKEPPPGPRGANKNDEEEDEDDDDDDDDDDDSDDTESDEEEEEPGS--APEGAYD 118
Honey bee QSPVIRRPSSSRRSRYSD-NDNNFGKAMGIHSDPSDSEESDDDNIQGTINA--QQIELYN 90
CrIFT46 AGAD-EPPAAPRDASLIESHDMDEGPAAPARTLSPTGYEAGKHAPGGIANSDEAPPGAYN 103
Human PADYEHLPVSAEIKELFQYISRYTPQLIDLDHKLKPFIPDFIPAVGDIDAFLKVPRPDGK 125
Mouse PADYEHLPVSAEIKELFEYISRYTPQLIDLDHKLKPFIPDFIPAVGDIDAFLKVPRPDGK 122
Zebrafish PADYEHLPVTGEIKELFQYITRYTPQTIELDHKLKPFIPDFIPAVGDIDAFLKVPRPDGK 178
Honey bee PKDFEDLKVSTEVKELFQNIMRYTPQKIELNYKLIPFIPDYIPAVGDIDAFIKIPRPDGI 150
CrIFT46 AQEYKHLNVGEDVRELFSYIGRYKPQTVELDTRIKPFIPDYIPAVGGIDEFIKVPRPDTK 163
Human PDNLGLLVLDEPSTKQSDPTVLSLWLTENSKQHNITQHMKVKSLEDAEKN-PKAIDTWIE 184
Mouse PDHLGLLVLDEPSTKQSDPTVLSLWLTENSKQHNITQHMKVKSLEDAEKN-PKAIDTWIE 181
Zebrafish PDNLGLLVLDEPCTKQSDPTVLSLWLSENSKQHNVT-EVKIKSIENPEKN-PKAIENWIE 236
Honey bee EDKIGLIVLDEPCTNQSDPAVLHLQLRSHLRSAGVARQTVIKRIEDAEKN-GKSIEKWIE 209
CrIFT46 PDYLGLKVLDEPAAKQSDPTVLTLQLRQLSKEAPGAKADMVGRLEHTDENKAKKIQQWIA 223
Human SISELHRSKPPATVHYTRPMPDIDTLMQEWSPEFEELLGKVSLPTAEIDCSLAEYIDMIC 244
Mouse SISELHRSKPPATVHYTRPMPDIDTLMQEWSPEFEELLGKVSLPTVEIDCSLAEYIDMIC 241
Zebrafish SISELHRSKPPATVHYTRPMPDIDSLMQEWPSEFEELLG---------- 275
Honey bee DIDQLHRSKHPPAVHLTKPMPEIDSLLQQWPPEVEEKLNEAELDFTELDCELPELVDIVC 269
CrIFT46 SINDIHKAKPAATVNYSKRMPEIEALMQEWPPEVETFLKTMHMPSGDVELDIKTYARLVC 283
Human AILDIPVYKSRIQSLHLLFSLYSEFKNSQHFKALAEGKKAF--TPSSNSTSQAGDMETLT 302
Mouse AILDIPFYKSRIQSLHLLFSLYSEFKNSQHFKALAEGKKVF--TPPPNSASQAGDAETLT 299
Zebrafish ----------KHFKSATYGQKSD--TPP-ASRSATAEIERLT 304
Honey bee NLLDIP----------SEEDSRLESLHTLF--MLYLDVRNARAQKY--- 303
CrIFT46 TLLDIPVYDDPVESLHVLFTLYLEFKNNPIFRQHMEMENKLDGMSGGGGGMMGGGADVLG 343
Human FS 304
Mouse FI 301
Zebrafish LD 306
Honey bee --
CrIFT46 L- 344

Figure 5.2. **C*hlamydomonas* IFT46 is an IFT complex B protein.** (A) The antibody to IFT46 specifically recognizes a ~46-kD doublet in western blots of whole cell lysates; the doublet is due to phosphorylation (see Figure 5.9A and B). (B) IFT46 has a typical cellular localization for an IFT-particle protein. Cells were labeled with the anti-IFT46 antibody. Images of the same cell were acquired focusing at the flagella (a and c), or at the basal body region (b and d) with much less exposure time. The majority of IFT46 is located at the peri-basal body region with a lesser amount distributed along the flagella as distinct dots. Scale bar: 5 μm. (C) IFT46 co-migrates with IFT81, an IFT complex B protein, in sucrose gradients. The flagellar membrane-plus-matrix was fractionated in a 5% to 20% sucrose gradient. The fractions were analyzed by western blotting using antibodies to complex B proteins IFT172 and IFT81, complex A protein IFT139, and IFT46. Under these experimental conditions, complex B separated from complex A, and IFT172 dissociated from complex B.

Figure 5.2

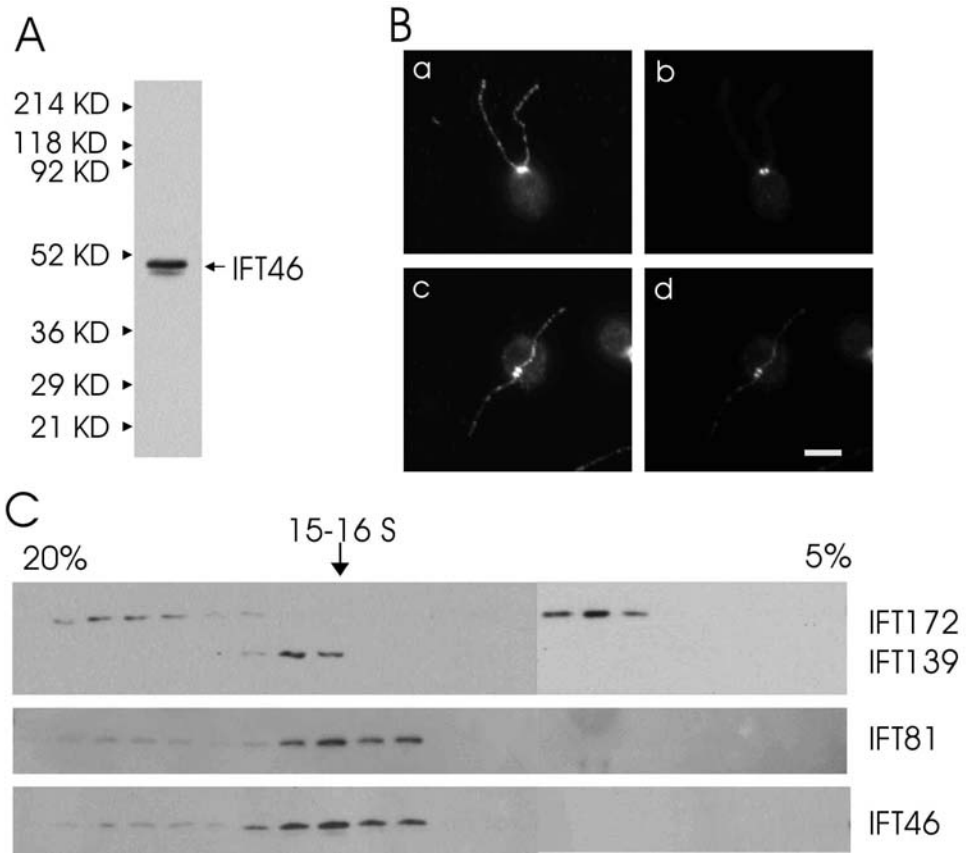
A
214 KD
118 KD
92 KD
52 KD
IFT46
36 KD
29 KD
21 KD
B
a
b
c
d
C
20%
15-16 S
5%
IFT172
IFT139
IFT81
IFT46

Figure 5.3. **The non-motile phenotype of YH6 is caused by a null mutation in the *IFT46* gene.** (A) *IFT46* gene structure. There are two PstI sites (P) within the *IFT46* gene. Three primer sets used for PCR to map the mutation region in the mutant are indicated by arrowheads. Regions corresponding to the ~4.8-kb genomic fragment used for rescue experiments, the cDNA probe used for screening the mutant collection, and the genomic DNA probe used for Southern blotting also are shown. (B) PCR amplification using primers to different regions of the *IFT46* gene showed that strain T8a4-11 is defective in the middle portion of the gene. (C and D) The non-motile phenotype of YH6, a progeny of T8a4-11 and wild-type cells, was rescued by transforming the mutant cells with the wild-type *IFT46* gene. Genomic DNAs from wild-type cells, YH6, and rescued cells were cut by PstI and analyzed by Southern blotting using a *IFT46* genomic DNA probe (C). The rescued cells (6R29 through 6R38) have the 1.5-kb fragment originating from the transgene (the 1.9-kb fragment is missing because it was not present in its entirely in the transgene) and two hybridizing bands (*) originating from the mutated *ift46* gene. They also have other hybridizing bands, indicating that the *IFT46* transgenes were incorporated at different sites. Western blots of whole cell lysates (D) show that YH6 cells lack the IFT46 protein and that the rescued cells express IFT46 protein. The same blot was stripped and probed with an anti-tubulin antibody as control (lower panel).

Figure 5.3

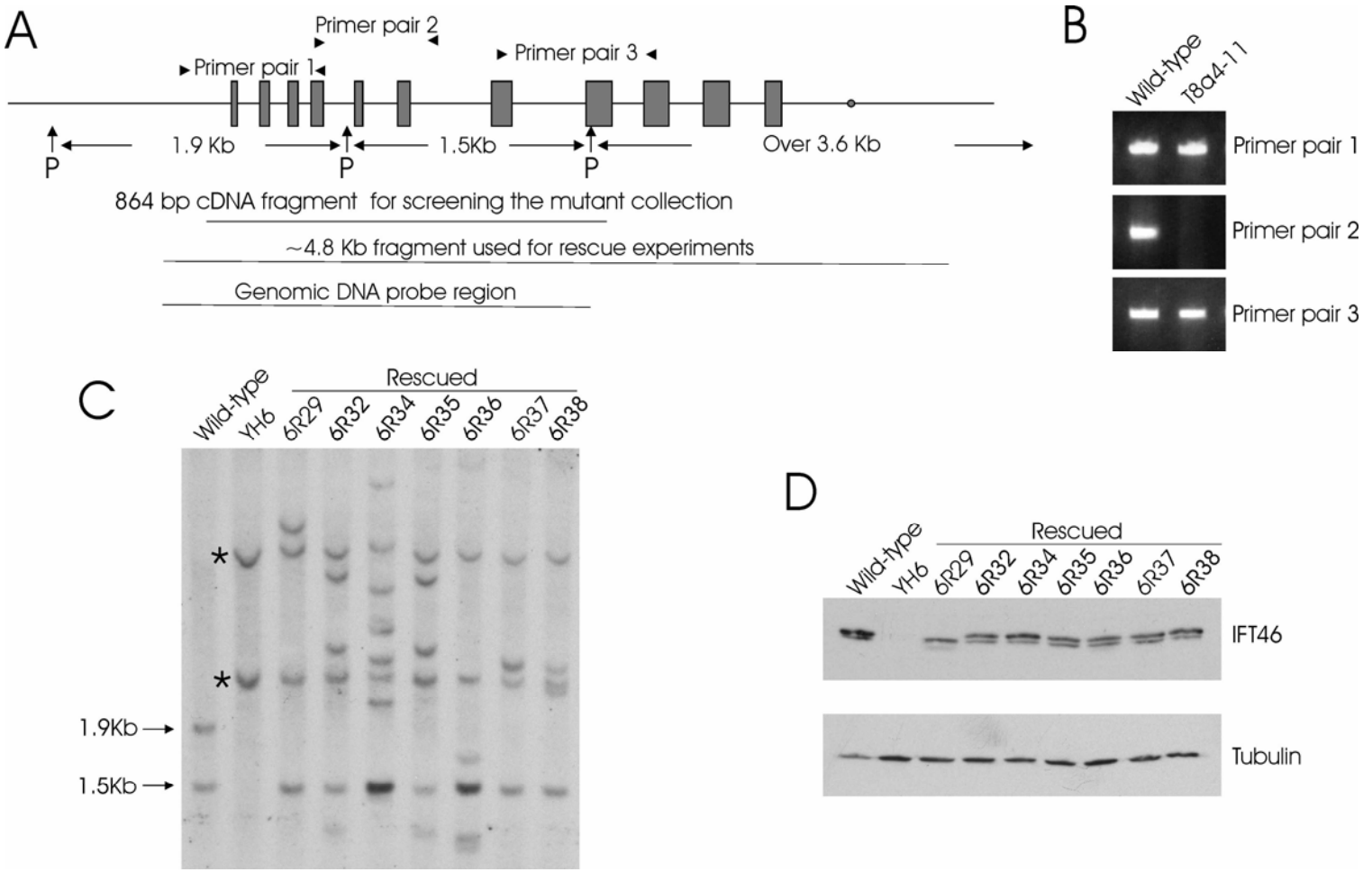
A
Primer pair 2
Primer pair 1
Primer pair 3
1.9 Kb
1.5Kb
Over 3.6 Kb
P
P
P
864 bp cDNA fragment for screening the mutant collection
~4.8 Kb fragment used for rescue experiments
Genomic DNA probe region
B
Wild-type
T8a4-11
Primer pair 1
Primer pair 2
Primer pair 3
C
Wild-type
YH6
Rescued
6R29
6R32
6R34
6R35
6R36
6R37
6R38
1.9Kb
1.5Kb
D
Wild-type
YH6
Rescued
6R29
6R32
6R34
6R35
6R36
6R37
6R38
IFT46
Tubulin

Figure 5.4. **Flagellar assembly is defective in *ift46* mutant cells.** (A) Electron micrographs show that *ift46* flagella are short with normal basal bodies and transition zones. The mutant flagella lack dynein arms, and central pair assembly is defective. a, b, and c: cross sections of wild-type (*WT*) flagella. d: cross section of the flagella of the rescued cell line 6R32 (*R*). e: longitudinal section of the flagella of 6R32. f-k: cross sections of *ift46* flagella (*M*). l-p: longitudinal sections of *ift46* flagella (*M*). The membrane vesicles or bulges frequently present at the tips of the short mutant flagella are also observed in the *ift88* mutant (e.g., see Figure 3 of Pazour et al., 2000). Scale bars: 100 nm. (B) Western blotting shows that *ift46* flagella lack outer dynein arm and inner dynein arm components even though these components exist in the cell cytoplasm. In contrast, the outer dynein arm docking complex is transported into *ift46* flagella. Flagellar samples (Fla) and whole cell lysates (Cell) from *ift46* or wild-type cells were probed with antibodies to IC2 (an outer dynein arm component), IC138 (an inner dynein arm I1 component), or DC2 (a subunit of the outer dynein arm docking complex). Tubulin was probed as a loading control.

Figure 5.4

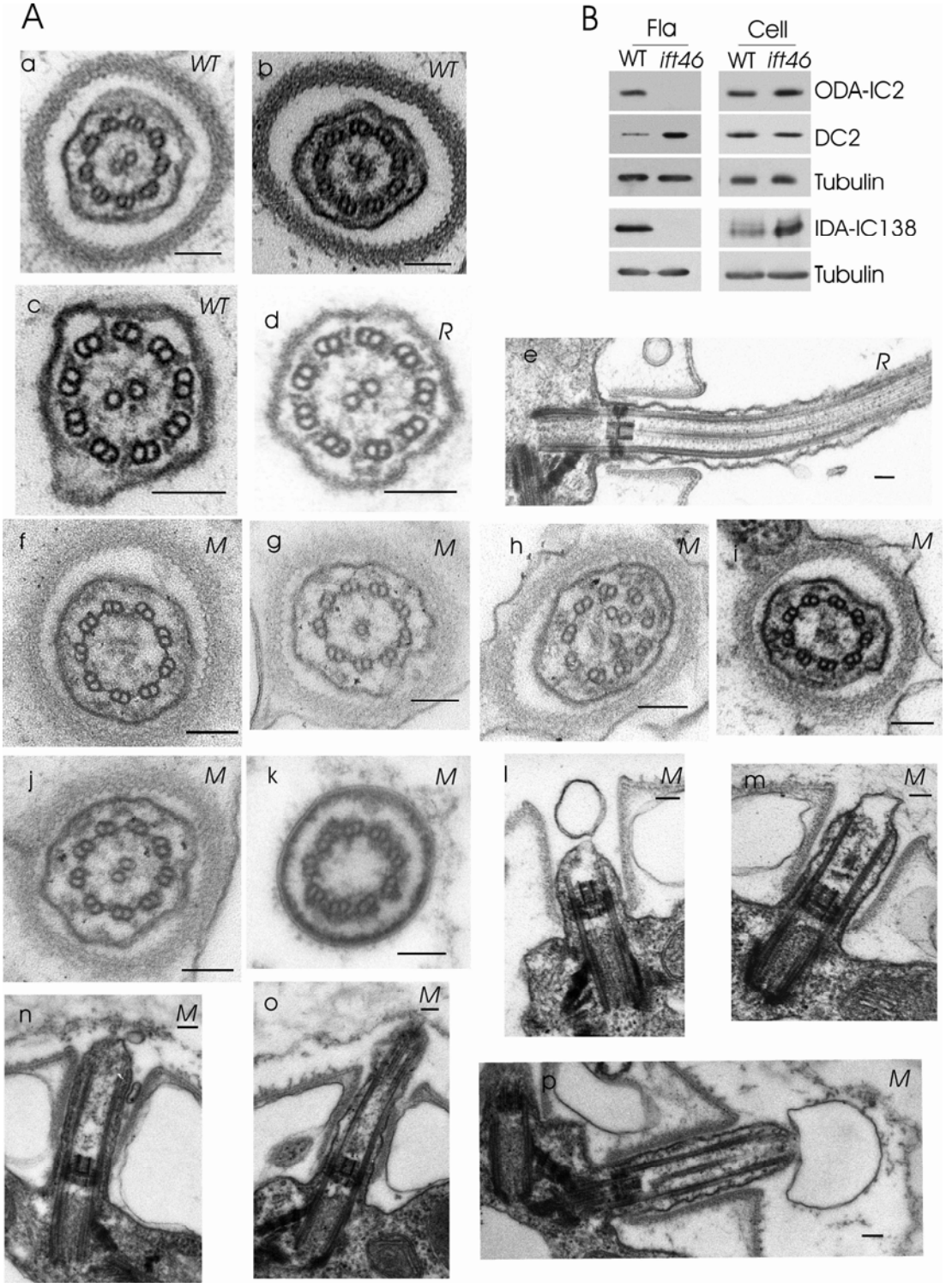
A
a WT
b WT
c WT
d R
e R
f M
g M
h M
i M
j M
k M
l M
m M
n M
o M
p M
B
Fla
Cell
WT ift46
WT ift46
ODA-IC2
DC2
Tubulin
IDA-IC138
Tubulin

Figure 5.5. **IFT complex B is unstable in the *ift46* mutant but stabilized in the partially suppressed strain.** Whole cell lysates from wild-type cells, $Sup_{ift46}1$ cells, and *ift46* cells were analyzed in western blots probed with antibodies to several IFT-particle proteins, IC2, and DC2. Complex A protein levels are increased in *ift46* compared to wild-type cells. With the exception of IFT172, complex B protein levels are dramatically decreased in *ift46* compared to wild-type cells. The levels of these proteins in $Sup_{ift46}1$ cells are between those in *ift46* and wild-type cells. IFT172 is increased in $Sup_{ift46}1$ cells. Tubulin was used to normalize the loading of the samples. Note that both *ift46* cells and $Sup_{ift46}1$ cells have IC2 and DC2.

Figure 5.5

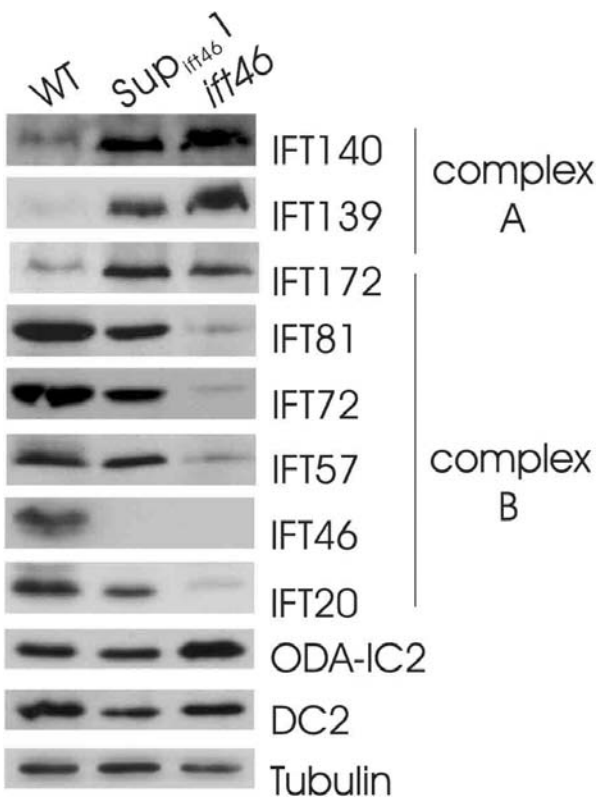
WT
sup ift46-1
ift46
IFT140
IFT139
IFT172
IFT81
IFT72
IFT57
IFT46
IFT20
ODA-IC2
DC2
Tubulin
complex A
complex B

Figure 5.6. **Complex A and complex B proteins differ in cellular distribution, and loss of IFT46 affects the cell body localization of IFT172, but not IFT139.** (A) *ift46* cells were double-labeled either with antibodies to IFT172 (a) and tubulin (b) or with antibodies to IFT139 (e) and tubulin (f). c and g are merged images; d and h are enlargements of the flagella and basal body regions. IFT172 and IFT139 are both present in the short flagella (arrows). In the basal body region, IFT139 localizes more anteriorly than IFT172. (B) Wild-type cells were double-labeled either with antibodies to IFT172 (a) and IFT46 (b) or with antibodies to IFT139 (d) and IFT46 (e). The merged images are shown in c and f; the inserts show enlargements of the basal body regions. IFT172 usually co-localizes with IFT46. However, IFT139 usually only partially co-localizes with IFT46 in the anterior part of the basal body region. (C) In the absence of IFT46, the remaining complex B proteins are still transported into the flagella. *ift46* cells were labeled with an antibody to IFT57, which is located in flagella (arrows) as well as in the basal body region. Scale bars: 5 μm.

Figure 5.6

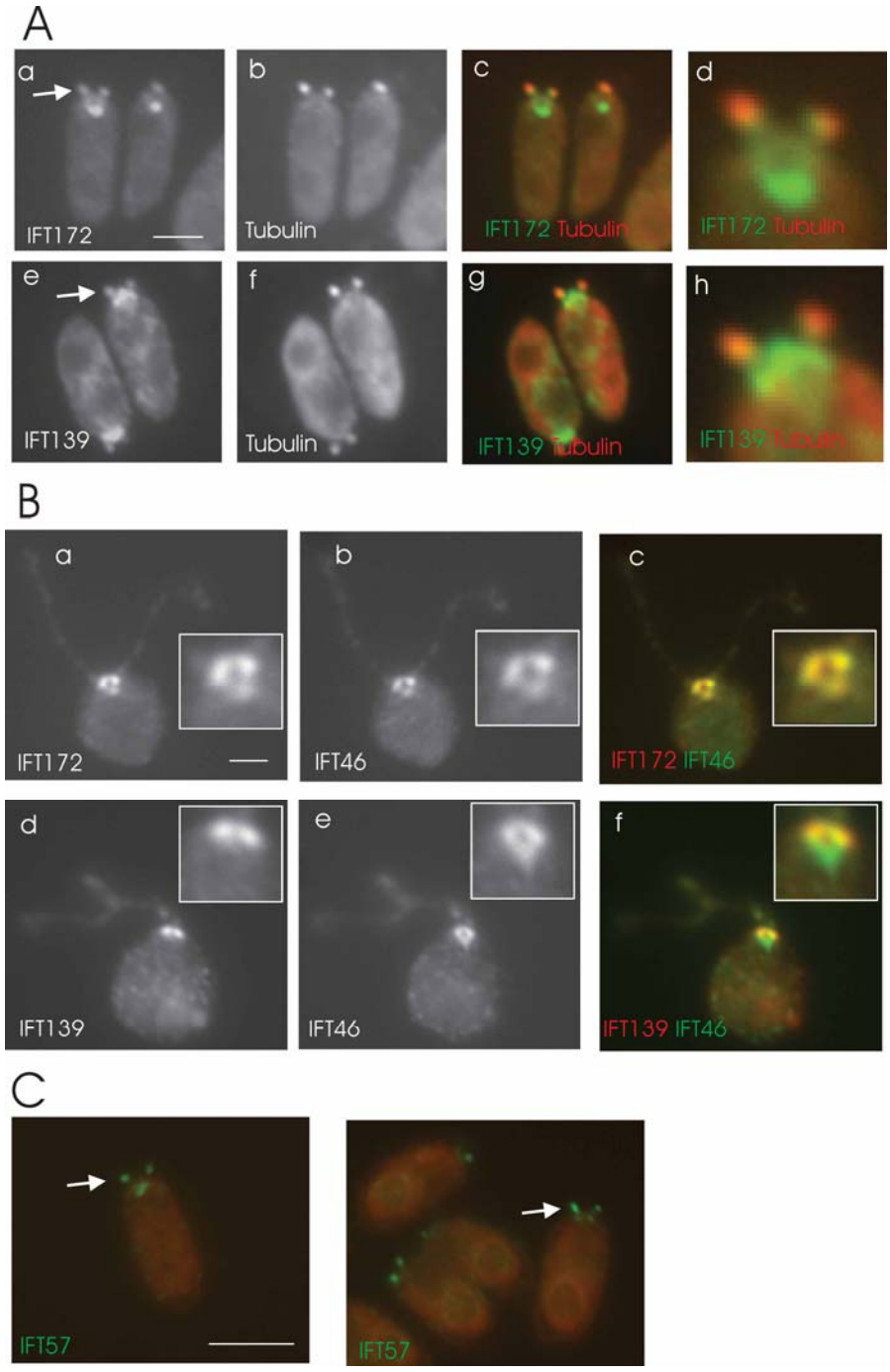
A
a
IFT172
b
Tubulin
c
IFT172 Tubulin
d
IFT172 Tubulin
e
IFT139
f
Tubulin
g
IFT139 Tubulin
h
IFT139 Tubulin
B
a
IFT172
b
IFT46
c
IFT172 IFT46
d
IFT139
e
IFT46
f
IFT139 IFT46
C
IFT57
IFT57

Figure 5.7. **The partial suppressor of *ift46* has defects in assembly of the outer dynein arm, but not inner dynein arm I1.** (A) Cells were double labeled either with antibodies to outer dynein arm heavy chain α (a, d, and g) and tubulin (b, e, and h) or with antibodies to inner dynein arm intermediate chain IC138 (j, m, and p) and tubulin (k, n, and q). The right column shows the merged images. a-f and j-o are $Sup_{ift46}1$ cells; g-i and p-r are wild-type (WT) cells. Note that $Sup_{ift46}1$ cells have variable length flagella. Scale bar: 5 μm. (B) Electron micrographs of wild-type flagella (a) and $Sup_{ift46}1$ flagella (b-d). $Sup_{ift46}1$ flagella lack outer arms but axonemal ultrastructure is otherwise normal. Scale bars: 100 nm.

Figure 5.7

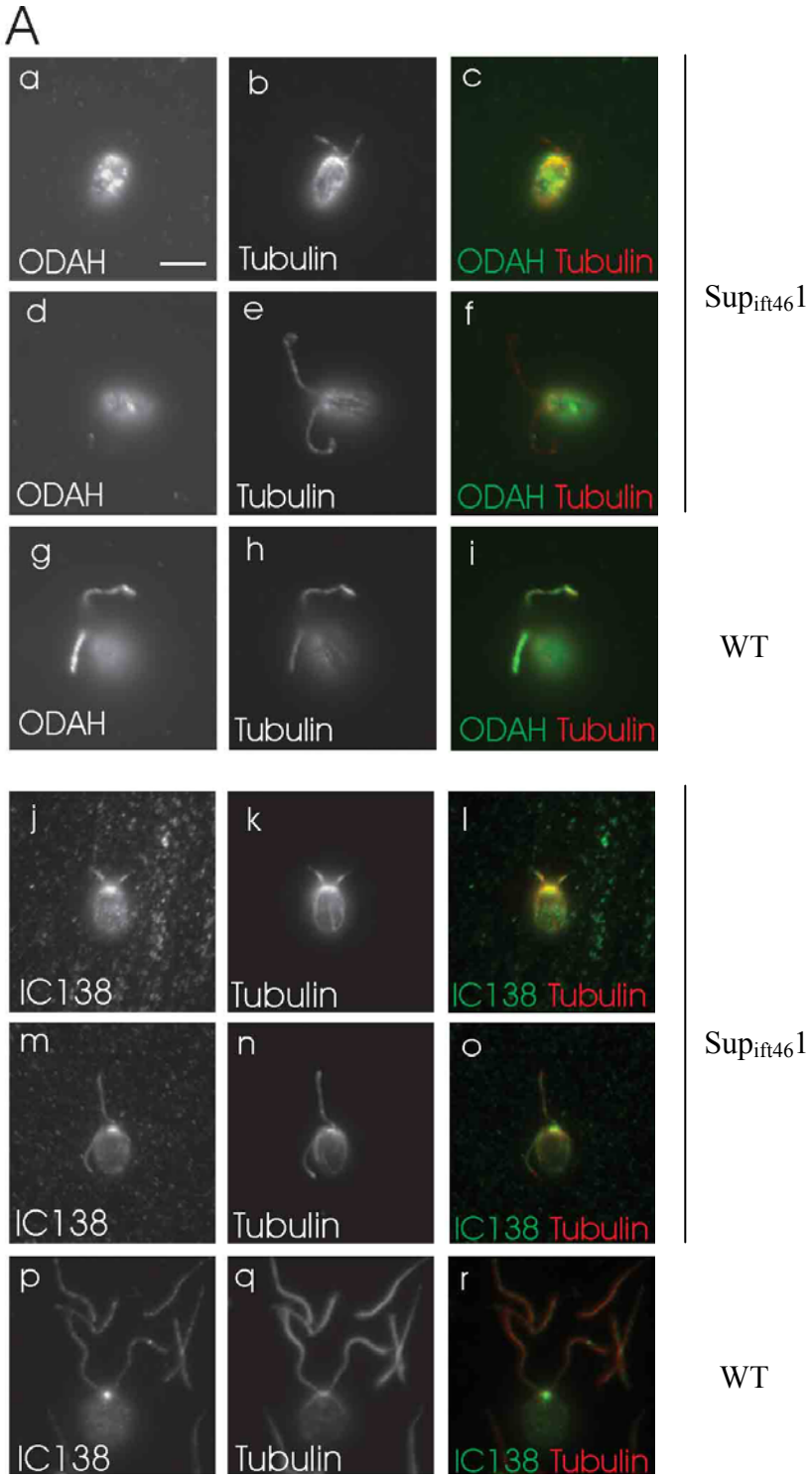
A
a
ODAH
b
Tubulin
c
ODAH Tubulin
d
ODAH
e
Tubulin
f
ODAH Tubulin
Supift461
g
ODAH
h
Tubulin
i
ODAH Tubulin
WT
j
IC138
k
Tubulin
l
IC138 Tubulin
m
IC138
n
Tubulin
o
IC138 Tubulin
Supift461
p
IC138
q
Tubulin
r
IC138 Tubulin
WT

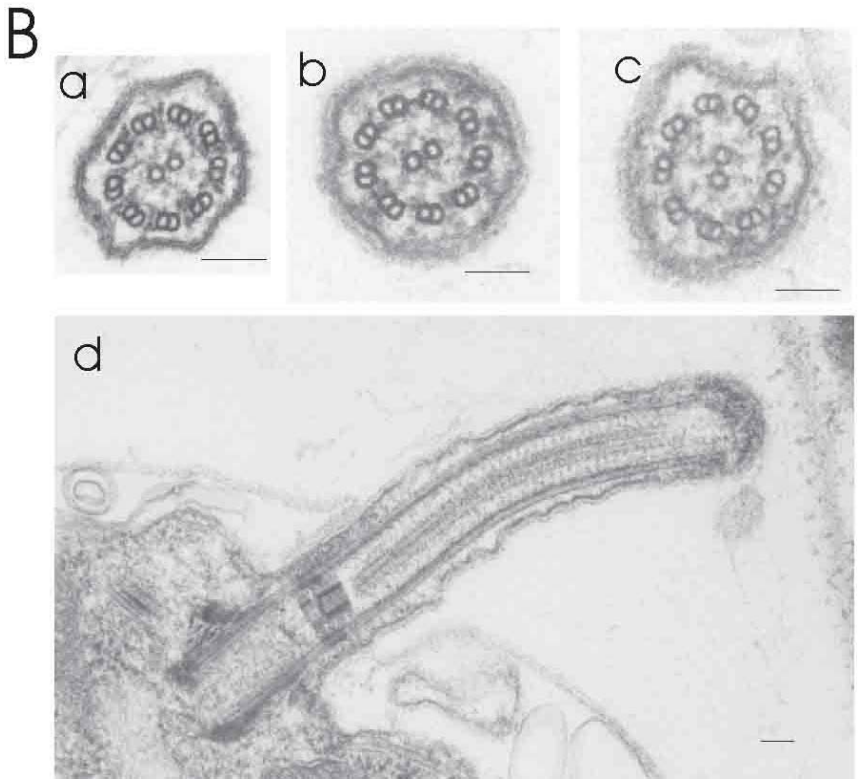
B
a
b
c
d

Figure 5.8. **The 3' end of the *IFT46* gene is expressed in the suppressor but not in the *ift46* mutant.** Reverse transcription PCR was carried out with no added DNA (control, C), or cDNA isolated from wild-type cells (WT), *ift46* cells without aeration (*ift46*s), *ift46* cells with aeration (*ift46*), $Sup_{ift46}1$ cells without aeration (Sups), and $Sup_{ift46}1$ cells with aeration (Sup) using primers designed to amplify transcripts from the 5', middle, and 3' regions of the *IFT46* gene. The products were then electrophoresed in 1.5% agarose gels. The results show that the 5' portion of the *IFT46* gene is transcribed in all the cells. The middle region is not transcribed in either the *ift46* mutant cells or the suppressed cells. The 3' region is not transcribed in the *ift46* mutant cells, but is transcribed in the suppressed cells. The transcription of the 3' region of the *IFT46* gene is not dependent on the growth condition. This result implies that the suppression is due to expression of the 3' region of the *IFT46* gene.

Figure 5.8

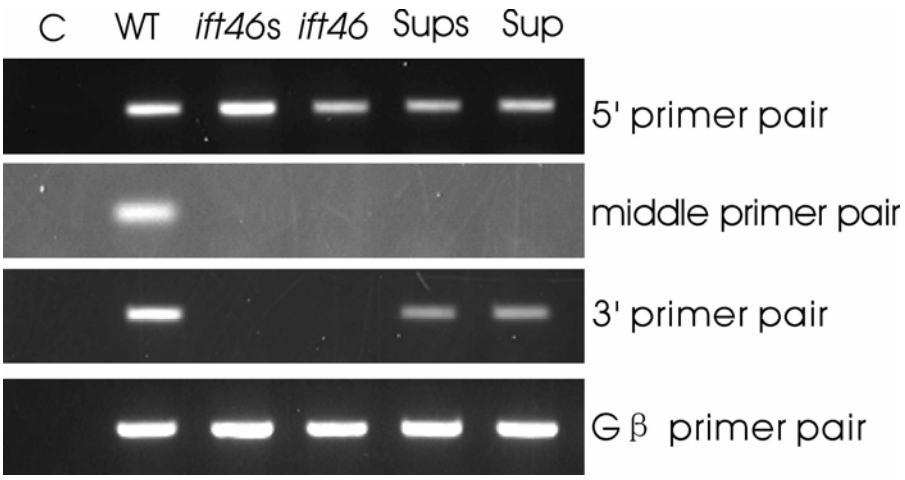
C
WT
ift46s
ift46
Sups
Sup
5' primer pair
middle primer pair
3' primer pair
Gβ primer pair

Figure 5.9. **The majority of IFT46 is phosphorylated *in vivo* and the phosphorylation is not essential for the function of IFT46 in flagellar assembly.** (A) The antibody to IFT46 always detected a doublet in western blots of both whole cell lysates and flagellar samples. WC, whole cell lysate; fla, flagella. (B) The upper band of the doublet is the phosphorylated form of IFT46 and the lower band of the doublet is the non-phosphorylated form of IFT46. Flagellar samples were treated with or without calf intestinal phosphatase (CIP) and then were analyzed by western blotting using the anti-IFT46 antibody. After the CIP treatment, the upper band disappeared and the intensity of the lower band increased. (C and D) The modified *ift46* genes, designed to express products that either mimic the non-phosphorylated form of IFT46 or the phosphorylated form of IFT46, rescued the non-motile phenotype of *ift46* to wild-type motility. (C) Southern blot probed with an *IFT46* genomic probe. The probe hybridized to bands originating from the endogenous *IFT46* gene in wild-type, and to bands originating from the disrupted *ift46* gene in the *ift46* mutant and the rescued strains (YH6MA 2-8 and YH6MD 1-7). In the rescued strains, the probe also hybridized to novel bands, indicating that the modified *ift46* transgenes were incorporated at different sites. When the modifications were introduced into the constructs used for the rescue experiments, a HindIII site was created at the sites of mutation. Genomic DNAs were cut by PstI and HindIII. The arrow indicates the band that is specific for the modified *ift46* transgenes. Western blots (D) probed with the anti-IFT46 antibody showed that the rescued cell lines express the modified IFT46

proteins. Proteins expressed from the A construct and the D construct each migrate as single bands, but with different mobilities. Tubulin was used as a loading control (lower panel).

Figure 5.9

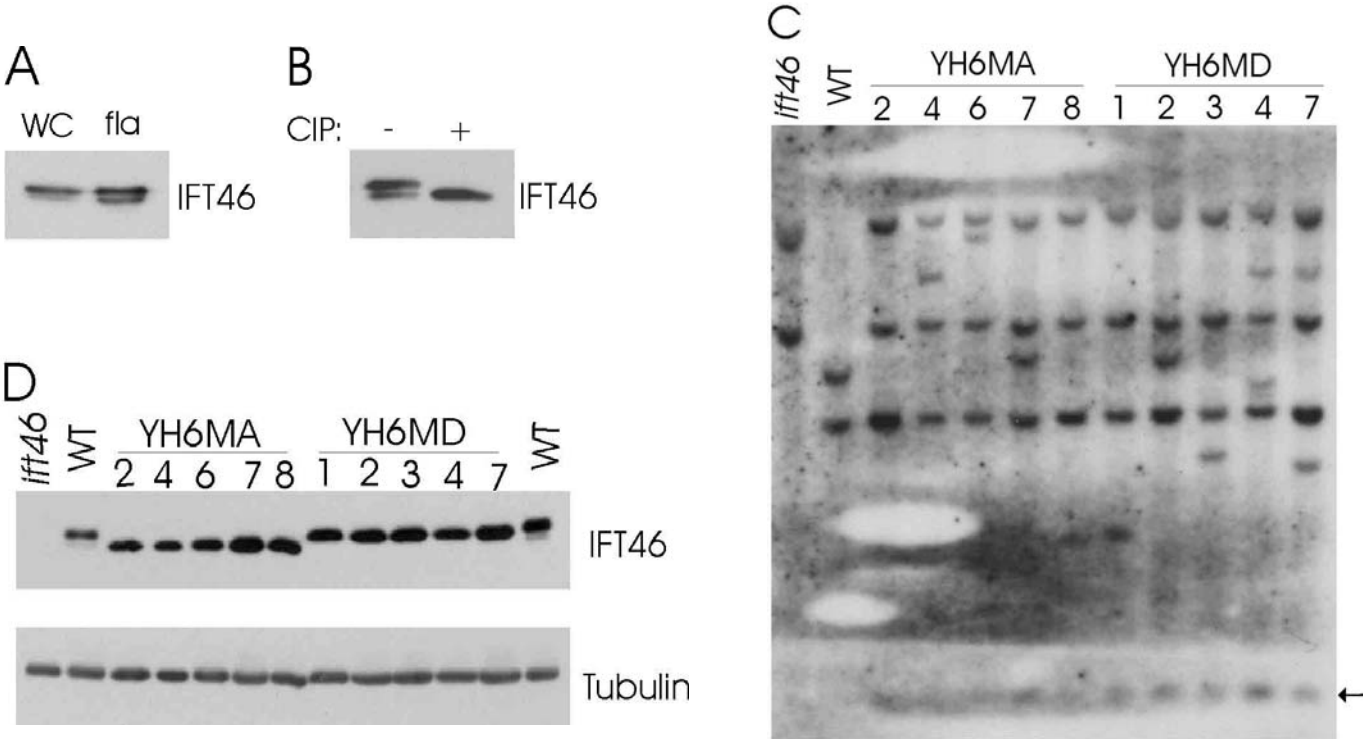
A
WC
fla
IFT46
B
CIP:
-
+
IFT46
C
ift46
WT
YH6MA
2 4 6 7 8
YH6MD
1 2 3 4 7
D
ift46
WT
YH6MA
2 4 6 7 8
YH6MD
1 2 3 4 7
WT
IFT46
Tubulin

CHAPTER VI

DISCUSSION

D1bLIC is a subunit of the retrograde IFT motor

Previously, two genes were identified as being required for retrograde IFT in *Chlamydomonas*. One, *FLA14*, encodes LC8, whereas the other, *DHC1b*, encodes the heavy chain of cytoplasmic dynein 1b. Both *fla14* and *dhc1b* mutants accumulate IFT-particle proteins in their short flagella, indicating that retrograde IFT is defective in these mutants. Here, I show that a *d1blic* mutant also accumulates IFT-particle proteins in its flagella, which is consistent with a defect in retrograde IFT. These results are also consistent with the recent report that XBX-1, the *C. elegans* homologue of D1bLIC, is required for retrograde IFT and the assembly of sensory cilia in the nematode (Schafer et al., 2003).

My findings that the level of DHC1b is decreased in the *d1blic* mutant and vice versa provide strong genetic evidence for an interaction between DHC1b and D1bLIC. Such an interaction is supported by our observations that D1bLIC and DHC1b 1) colocalize in the peri-basal body region and along the flagella, 2) have a similar distribution among different flagella fractions, 3) comigrate with each other when the flagella matrix is fractionated by sucrose density gradient centrifugation, and 4) are coimmunoprecipitated from the flagellar matrix fraction by an anti-D1bLIC antibody. Similar biochemical observations were made in a recent parallel study on D1bLIC

(Perrone et al., 2003). Taken together, these observations conclusively demonstrate that D1bLIC is a subunit of the retrograde IFT motor, cytoplasmic dynein 1b, in the flagella. The results indicate that D1bLIC also is associated with DHC1b in the cell body, where a large pool of cytoplasmic dynein 1b is maintained in the peri-basal body region.

I observed that, after their release from the flagellum by freeze-thaw, DHC1b and D1bLIC comigrated in a sharp peak at ~12S in sucrose density gradients. Sedimentation at 12S implies that the particle is a single-headed dynein containing one heavy chain, as in the case of the 12S particle consisting of the γ-DHC and two light chains (Pfister et al., 1982, Witman et al., 1983) or the 13.1S particle consisting of the α-DHC and one light chain (Pfister and Witman, 1984), both obtained by dissociation of outer arm dynein. In contrast, Perrone et al. (2003) observed that cytoplasmic dynein 1b sedimented in a broad peak at ~19S after its release from demembranated axonemes by treatment with 10 mM MgATP. A particle sedimenting at 19S would likely represent a two-headed dynein containing two DHCs, as in the case of the 18S particle consisting of the α and β DHCs and their associated subunits from the outer arm dynein (Pfister et al., 1982), or the ~21S particle containing inner arm DHCs 1α and 1β plus an intermediate chain (Piperno et al., 1990). It is possible the freeze-thaw step that I used to release cytoplasmic dynein 1b from the flagellum caused it to dissociate into the smaller 12S complex. However, an alternative possibility is that dynein 1b is in a two-headed form when actively transporting IFT particles, but is in a one-headed form when being passively transported to the tip of the flagellum as cargo. The former

would be expected to remain associated with the axoneme by rigor bonds after demembranation and then be released by ATP, whereas the latter would be released with the IFT particles by demembranation or freeze-thaw. If dynein 1b is transported in an anterograde direction as a single-headed species, this would severely limit its ability to interact with the doublet microtubules to produce competing force in the retrograde direction.

Role of D1bLIC in cytoplasmic dynein 1b

The phenotype of the *d1blic* mutant is not as severe as that of the *dhc1b* mutant. The d*hc1b* mutants are nonmotile with short, stumpy flagella (Pazour et al., 1999; Porter et al., 1999). Although most *d1blic* mutant cells are nonmotile with short, stumpy flagella, some have variable length flagella of up to normal length. Moreover, EM showed that some *dhc1b* mutant cells have an apparently normal axoneme and some do not (Pazour et al., 1999), whereas all *d1blic* mutant cells, including those with short stumpy flagella, have an apparently normal axoneme. A likely explanation for the difference between the *d1blic* and *dhc1b* mutants is that D1bLIC serves as an intimate partner for DHC1b to help stabilize the dynein 1b complex, but that DHC1b can function to some extent even in the absence of D1bLIC. A role for D1bLIC in stabilizing dynein 1b is strongly supported by the observation that the level of DHC1b is reduced in the mutant cells lacking D1bLIC. Moreover, even though the cellular level of DHC1b is reduced in the *d1blic* mutant, what remains must be at least partially functional to support sufficient

IFT to assemble flagella of up to normal length and maintain them at that length. It is probable that in the *d1blic* mutant cells, DHC1b, reduced in amount and probably impaired in cargo binding (see below), is unable to transport IFT particles out of the flagellum as effectively as the fully functional anterograde IFT motor can move them into the flagellum, so that the particles gradually accumulate in the flagellum. The variability in the length of the flagella in the *d1blic* mutant probably reflects cell-to-cell differences in the remaining amount of DHC1b. The large accumulation of IFT particles undoubtedly impairs the movement of the flagella, so that even cells with normal length flagella swim in an abnormal manner.

Studies on isoforms of DLIC1, the LIC for cytoplasmic dynein 1/1a, imply that LICs may be involved in cargo binding (Purohit et al., 1999; Tynan et al., 2000) and motor regulation (Niclas et al., 1996; Dell et al., 2000; Bielli et al., 2001). The phenotype of the *d1blic* mutant suggests a similar role for D1bLIC. Indeed, the observation that the distribution of DHC1b in *d1blic* mutant flagella is not noticeably different than that observed in wild-type flagella, whereas IFT-particle proteins accumulate dramatically in *d1blic* mutant flagella, strongly implies that D1bLIC stabilizes the interaction of cytoplasmic dynein 1b with its cargo, or increases the affinity of the motor for its cargo. However, because the stability of DHC1b is dependent on the presence of D1bLIC, it will be necessary to test the cargo binding and motor regulatory functions of D1bLIC by means of site-directed mutations that do not prevent expression of the subunit and its incorporation into the dynein 1b complex. The

d1blic null mutant described here should be very useful as a recipient of such transgenes in future studies.

Role of the conserved P-loop

The P-loop is commonly found in many adenine and guanine nucleotide-binding proteins, where it coordinates the β, γ -phosphate group of the nucleotide and is necessary for nucleotide hydrolysis (Via et al., 2000). Although LICs are not known to bind ATP or GTP, *Chlamydomonas* D1bLIC and mammalian D2LIC have a conserved P-loop motif, suggesting that this P-loop has a function in D1bLIC activity. To test this hypothesis *in vivo*, I transformed the *d1blic* null mutant with constructs designed to express D1bLIC subunits carrying mutations known to disrupt P-loop function in other proteins (Saraste et al., 1990; Silvanovich et al., 2003). The mutated constructs fully rescued the flagella assembly defect of *d1blic* mutant cells, implying that D1bLIC's P-loop is not critical for the protein's function in retrograde IFT. The cells rescued with the mutated constructs also mate normally, implying that the P-loop is not essential for the mating process. This result is consistent with previous results on the P-loops of *C. elegans* and mammalian cytoplasmic dynein 1 LICs (Tynan et al., 2000; Yoder and Han, 2001) and with the fact that the *C. elegans* dynein 2 LIC does not have a P-loop (Schafer et al., 2003).

Other functions of cytoplasmic dynein 1b

My results together with previous studies show that in *Chlamydomonas*, D1bLIC/DHC1b is involved in flagella formation, maintenance and function by acting as the retrograde IFT motor. My observation that the *d1blic* null mutant grows normally indicates that D1bLIC is not important for any essential cell function. However, it might have other functions, in addition to being the retrograde IFT motor, related to flagellar assembly. One possibility is that, as a microtubule minus-end directed motor, cytoplasmic dynein 1b also is involved in transporting flagellar proteins from the cell body to the basal body region. However, because the *dhc1b* null mutant has short, stumpy flagella filled with IFT particles and sometimes containing an apparently normal axoneme (Pazour et al., 1999), these IFT particle-proteins and many axonemal structural proteins apparently are not dependent on DHC1b for their transport from the cell body to the basal body region. Moreover, mastigoneme protein, which normally is an extracellular component of the flagellar membrane, localizes at the apex of *dhc1b* mutant cells (M. Chapman and G. Witman, unpublished results). Therefore, it is unlikely that the transport of this protein from the site of synthesis to the site of incorporation into the cell or flagellar plasma membrane is disrupted by the DHC1b mutation.

A second possibility is that the DHC1b complex is involved in maintaining the Golgi apparatus. DHC2, the mammalian homologue of DHC1b, has been localized to the Golgi apparatus, and microinjection of DHC2 antibodies caused the Golgi complex

to disperse (Vaisberg et al., 1996). Moreover, D2LIC colocalized with DHC2 at the Golgi apparatus throughout the cell cycle, and the two proteins colocalized with Golgi fragments induced by the depolymerization of microtubules with nocodazole (Grissom et al., 2002). After brefeldin A treatment, some D2LIC lost its association with the Golgi and remained localized in the vicinity of the centrosome (Grissom et al., 2002). However, in *Chlamydomonas*, it appears that DHC1b/D1bLIC is not important for Golgi maintenance, because both *d1blic* (this study) and *dhc1b* (Pazour et al., 1999) mutants have normal Golgi.

Although the observations in *Chlamydomonas* do not address the role of DHC2/D2LIC in mammalian cells, it has been reported that antibodies to DHC2, D2LIC, and an IFT-particle protein strongly stained the ependymal layer lining the lateral ventricles (Mikami et al., 2002). Both DHC2 and D2LIC staining also were observed associated with connecting cilia in the retina and within primary cilia of nonneuronal cultured cells, supporting a specific role for dynein 2 in the generation and maintenance of cilia (Mikami et al., 2002). Perrone et al. (2003) also found that DHC2 and D2LIC colocalized in the apical cytoplasm and axonemes of ciliated epithelia cells in the lung, brain, and efferent duct. Therefore, it is very likely that cytoplasmic dynein 2 is involved in cilia formation in mammals. It remains controversial whether it also has a role in Golgi maintenance in mammals.

IFT46 is important for the stability of complex B

In the *Chlamydomonas* mutant lacking IFT46, levels of both complex A and B mRNAs increased relative to their levels in wild-type cells. This strongly suggests that the genes encoding proteins of both complexes are constitutively induced when the cell cannot assemble flagella. The mutant exhibited a corresponding increase in levels of complex A proteins. However, levels of complex B proteins other than IFT172 decreased in the mutant, suggesting that these proteins are broken down in the absence of IFT46. These results indicate that a) in the absence of IFT46, complex B is unstable; b) stability of complex A proteins is not dependent on the presence of complex B; c) the normal 1:1 stoichiometry between complex A and complex B proteins (Cole et al., 1998) is uncoupled in the absence of IFT46; and d) flagella assembly requires complex B, even in the presence of increased amounts of complex A.

Biochemical analysis (Lucker et al., 2005) has shown that complex B is composed of a 500-kD "core" that includes IFT88, IFT81, IFT74/72, IFT52, IFT46, and IFT27, and four "peripheral" subunits including IFT172, IFT80, IFT57, and IFT20. (The term "core" here refers to a group of proteins that are tightly associated with one another, and has no implication with regard to whether the proteins are or are not exposed on the surface of the IFT particles.) My finding that IFT46 is required for the stability of all complex B proteins tested except for IFT172 is consistent with this model. In the absence of IFT46, the complex B core is destabilized, leading to degradation of the core subunits as well as the peripheral subunits other than IFT172.

This is in contrast to the situation when another complex B core protein, IFT88, is disrupted; loss of this protein in an *ift88* mutant had little or no effect on the levels of IFT172 and IFT81, but caused a significant decrease in IFT57 (Pazour et al., 2000). This difference suggests that although IFT46 and IFT88 may both be components of the complex B core, the former is essential for the core's stability whereas the latter is not. IFT46 is required for the stability of both IFT81 and IFT88, but the stability of IFT81 is not dependent on IFT88, in agreement with a model in which IFT81 and IFT88 are in different domains of the core (Lucker et al., 2005), and suggesting that the assembly or stability of both core domains is dependent upon IFT46. Because IFT57 is a peripheral protein, it requires either an intact complex B core or direct interaction with IFT88 for its stability.

The *ift46* mutant can form very short flagella with normal outer doublet microtubules, a phenotype distinct from that of the other published *Chlamydomonas* IFT complex B null mutants, *ift88* and *ift52*, which are bald with no axonemal structures extending beyond the transition zone (Pazour et al., 2000; Brazelton et al., 2001). No information is available on how loss of IFT52 affects the other complex B proteins. However, one possible explanation for the difference between the *ift46* and *ift88* mutants is that the residual complex B proteins in both mutants form incomplete complex B particles, and that those formed in the absence of IFT46 have some functionality, whereas those formed in the absence of IFT88 are completely unable to form a flagellum. This could occur if IFT46 served primarily to transport a non-

essential axonemal protein such as outer arm dynein, but IFT88 was necessary for transport of a protein, such as tubulin, absolutely necessary for axonemal assembly.

It is of interest that the level of IFT172 in the *ift46* mutant did not show the decrease observed for the other complex B proteins. IFT172 also differs from the other complex B proteins in that it readily dissociates from the rest of the complex B particle during sucrose gradient centrifugation (Cole et al., 1998 and see Figure 5.2C), and that it interacts with the *Chlamydomonas* microtubule-end-binding protein CrEB1 in a manner that does not require association with the other complex B proteins (Pedersen et al., 2005). Thus, IFT172 is unique in that its cellular level is regulated independently of other complex B proteins, that it binds relatively weakly to complex B, and that it can interact with other proteins independently of complex B.

IFT46 is required for transport of outer dynein arms into flagella

In addition to being very short, *ift46* flagella have defects in central pair and dynein arm assembly. Aspects of this phenotype are undoubtedly caused by the greatly reduced amount of complex B in the *ift46* mutant. Because there is not enough IFT machinery to transport a full complement of axonemal proteins, the flagella are short and assembly of specific axonemal structures is affected.

However, my discovery of a suppressor mutation that stabilizes complex B in the absence of full-length IFT46 and restores flagellar assembly, including assembly of the central pair and the inner dynein arms, but does not restore outer dynein arm

assembly, even though outer arm proteins are present in the cytoplasm, strongly argues that IFT46 has a specific role in outer dynein arm transport. This is the first direct evidence that the outer dynein arms require IFT for transport into the flagellum, and the first evidence connecting a specific IFT-particle protein with a specific cargo. Because the outer arm components are pre-assembled in the cytoplasm into complexes as large as 1,200 kD (Fowkes and Mitchell, 1998), it is likely that IFT is needed to move them efficiently into the flagellum and out to the flagellar tip, which is the site of axonemal assembly (Witman, 1975; Johnson and Rosenbaum, 1992).

Further work will be necessary to determine if IFT46 is involved directly in outer arm binding, or if loss of IFT46 causes a conformational change in the IFT particle that eliminates an outer arm binding site at some distance from IFT46. However, the fact that the suppressor mutant has a partially stabilized complex B but still fails to transport outer arms into the flagella strongly supports the first possibility. The first possibility is further supported by the recent finding that the human homologue of ODA16, a *Chlamydomonas* flagellar protein that is not a component of dynein but is essential for outer arm transport into the flagellum (Ahmed et al., 2005), interacts with the mouse homologue of IFT46 in a yeast two-hybrid system and thus may be an adaptor coupling IFT46 to the outer arm (Ahmed, N.T., B. Lucker, D. G. Cole and D. R. Mitchell. 2006. 46th Annual Meeting of the American Society for Cell Biology. Abstract No. 1612).

My finding that IFT is involved in transport of outer arm complexes explains a previous observation that antibodies to complex B proteins IFT52 and IFT72 co-immunoprecipitated subunits of the outer dynein arm from a flagellar membrane-plus-matrix fraction (Qin et al., 2004). An earlier study had reported that inner dynein arms but not outer dynein arms required the activity of FLA10, which is one motor subunit of the anterograde IFT motor Kinesin-2, for transport into the flagellum (Piperno, et al., 1996). There are at least two possible explanations for the difference between these results and our own. First, as discussed by Qin et al. (2004), the earlier studies utilized a *fla10* temperature-sensitive mutant and observations 45-75 min after shift to the restrictive temperature, which may not have been adequate for complete cessation of FLA10 activity. Second and more interestingly, it is possible that there is more than one kinesin for anterograde IFT in *Chlamydomonas*, as there is in *C. elegans* (Snow et al., 2004). Phylogenetic analysis on complete kinesin repertoires of a diversity of organisms revealed that some kinesin families are specific for ciliated species (Wickstead and Gull, 2006). The *Chlamydomonas* Kinesin-2 motor subunits FLA10 and FLA8, the central pair kinesin KLP1, as well as several novel kinesins were grouped in these sub-families; two of the latter (C_250150 in the Kinesin-9 family, and C_710026 in the newly proposed Kinesin-17 family) were each identified by multiple hits to a single peptide (shared with FLA8) in the *Chlamydomonas* flagellar proteome (Pazour et al., 2005 and see http://labs.umassmed.edu/chlamyfp/protector_login.php).

It is possible that one of the novel kinesins is an IFT anterograde motor, and that it and Kinesin-2 transport IFT particles linked to different cargos.

I also observed that the outer dynein arm docking complex, as represented by its DC2 subunit, was transported into the *ift46* mutant flagella. The movement of the docking complex but not the outer dynein arm into *ift46* flagella is consistent with previous results that the docking complex is preassembled in the cytoplasm as a distinct complex not associated with the outer arm (Wakabayashi et al., 2001), and is transported into the flagellum independently of the outer arm (Takada and Kamiya, 1994; Wirschell et al., 2004). DC2 was co-immunoprecipated by antibodies to IFT-particle proteins (Qin et al., 2004), indicating that it interacts with the IFT machinery and probably is dependent upon it for transport into the flagellum. My results clearly show that the docking complex does not specifically require IFT46 for entry into the flagellum.

Although both *C. elegans* cilia and mammalian primary cilia lack outer arms, it may be that IFT46 is required for transport of other cargos in these immotile cilia, or simply is needed for complex B assembly, as in *Chlamydomonas*.

Complex A and complex B occur in distinct but overlapping compartments in the basal body region

Complexes A and B are associated with each other in large linear assemblages during transport within the flagellum (Qin et al., 2004), and it has been proposed that turnover

of IFT-particle proteins and motors at the tip of the flagellum involves the dissociation of complex A from complex B, followed by their reassociation prior to retrograde transport (Pedersen et al., 2006). However, virtually nothing has been known about the interactions of the complexes at the base of the flagellum. My immunofluorescence microscopy observations have now revealed different patterns of localization for complex A and complex B proteins in the wild-type cell, with the former localized more apically in the peri-basal body region. In contrast, the complex B proteins IFT172 and IFT46 usually colocalized precisely with each other. These results suggest that complex A and complex B separate from each other upon passage from the flagellum into the cytoplasm, are then sorted into separate albeit overlapping compartments, and subsequently are reassembled prior to their transport into the flagellum, in a reversal of the process proposed to occur at the tip of the flagellum. The region of overlap at the apical end of the peri-basal body region may correspond to the basal body transition fibers, which are proposed to be docking sites where the IFT particles are assembled or disassembled prior to entry into the flagellum or cytoplasm respectively (Deane et al., 2001; Rosenbaum and Witman, 2002). Within the cell body of the *ift46* mutant, the IFT172 in excess over other complex B proteins localizes primarily to the posterior peri-basal body region and has little or no overlap with IFT139 in the anterior peri-basal body region, indicating that IFT172 does not interact directly with complex A in the cell body.

The immunofluorescence microscopy studies also showed that both complex A and residual complex B proteins are transported into the short flagella of the *ift46* mutant, indicating that even in the absence of suppression, transport of the IFT complexes into the flagella does not require *ift46*.

Stability of complex B in $Sup_{ift46}1$ cells may be due to expression of the C-terminus of IFT46

The analysis of the $Sup_{ift46}1$ cells revealed that they differ from *ift46* cells in that the suppressor mutation causes transcription of the 3'-end of the IFT46 gene. This could come about as a result of an intragenic mutation that allows transcription of the 3' end of the IFT46 gene from the *NIT1* promoter present in the vector originally used to generate the *ift46* insertional mutant, or as a result of mutation of some other gene that allows read-through from the *NIT1* gene. Irrespective of the mechanism, the results suggest that the C-terminal portion of IFT46 is expressed, possibly as part of a fusion protein with nitrate reductase (which is encoded by the *NIT1* gene). This fragment may then be incorporated into complex B, stabilizing it.

Expression of the suppressed phenotype was observed only in $Sup_{ift46}1$ cells grown in the absence of aeration. A possible explanation for this is that under stress conditions (probably hypoxia), a chaperone is produced that helps stabilize complex B. *ift46* cells do not form flagella in the absence of aeration, so this hypothetical chaperone does not stabilize complex B in the complete absence of IFT46. It may be

that a stress-induced chaperone can stabilize complex B in the presence of a C-terminal fragment of IFT46, but not in the absence of the fragment.

Flagella are formed in $Sup_{ift46}1$ cells, but the flagella lack the outer dynein arms. Therefore, if complex B is indeed stabilized by a C-terminal fragment of IFT46 in $Sup_{ift46}1$ cells, this would imply that the N-terminal end of IFT46 is essential for transport of outer arms into the flagellum.

Cells can compensate for defects in IFT complex B

My identification of a partial suppressor of the *ift46* phenotype is the second report of suppression of the phenotype resulting from disruption of a complex B protein. Brown et al. (2003) identified a spontaneous partial suppressor of a null mutant of the complex B protein IFT52 in *Tetrahymena*. The *Tetrahymena ift52* null mutant has basal bodies that fail to form flagella or form short flagella that lack the central pair of microtubules, whereas a variable number of cells of the partially suppressed strain had slightly longer flagella, of which about 13% had a central pair of microtubules, depending on growth conditions. As was likely the case with the *Chlamydomonas ift46* suppressor, the suppressed phenotype of the *Tetrahymena* strain was stimulated by pericellular hypoxia; suppression of the *Tetrahymena* strain also was stimulated by growth at abnormally low temperature. This suppression differed from that which I observed in that it arose spontaneously with high frequency, whereas the event in *Chlamydomonas* was rare and observed only once in two years of culturing the cells; however, in both cases the

phenotype was stable. Therefore, the mechanism of suppression may be similar in both *Chlamydomonas* and *Tetrahymena*. In the case of $Sup_{ift46}1$, western blotting showed that the IFT proteins were restored to levels between those of wild-type cells and the *ift46* mutant cells, indicating that restoration of the ability to form flagella was due to stabilization of complex B in the absence of full-length IFT46.

IFT46 is phosphorylated *in vivo*

Chlamydomonas IFT46 is the first IFT-particle protein shown to be phosphorylated *in vivo*; MS indicates that it is phosphorylated at at least three sites. Presently, the physiological significance of these phosphorylations is uncertain, as concerted mutagenesis of the phosphorylated amino acids to residues that should mimic the completely phosphorylated or completely dephosphorylated states had no detectable effects on the kinetics of flagellar growth, on the final length of the flagella, or on their final motility. Moreover, the phosphorylation sites are near the N-terminus, beyond the region conserved in IFT46 orthologues in other organisms, although the N-terminal region of vertebrate IFT46 contains a high concentration of aspartic acids and glutamic acids, which, like the phosphorylations in *Chlamydomonas* IFT46, would increase the negative charge of this end of the protein. It is possible that the phosphorylation of IFT46 in this region only has subtle influence on IFT46's function. Since the data on the suppressor suggest that the N-terminus of IFT46 might be involved in dynein transport into the flagella, future studies might compare the dynamics of the recovery of

cell motility during flagella regeneration in wild-type cells versus mutant cells transformed with S or D constructs to see if the dynein assembly speed is affected.

Prospective research

IFT opens a door to the study of ciliary function, but this approach can be fully utilized only when the mechanism of IFT is completely understood. Further studies of the mechanism of IFT are likely to take two directions. One direction is to identify more IFT components. The current IFT components were identified either by biochemical analysis in *Chlamydomonas* using a kinesin-2 temperature sensitive mutant, or by forward genetic analysis on *C. elegans* mutants defective in cilia functions. Due to the limits on the techniques, it is still possible that some IFT components remain undiscovered. To identify more components, in addition to the retrograde IFT mutants identified in CHAPTER III, the flagellar proteomic database is a resource. The flagella proteomic data revealed three kinesins that might be involved in anterograde IFT (C_250150, C_60057, and C_710026). Two of them (C_250150 and C_710026) were also grouped into the cilia-related kinesin sub-family by Wickstead and Gull (2006). For the retrograde IFT motor, a search of the flagella proteomic data for dynein subunits that have similar distribution among different flagellar fractionations as D1bLIC revealed one candidate (C_20188). It is a novel protein similar to dynein ICs. To identify more potential IFT-particle proteins, I searched the flagella proteomic data to generate a list of proteins (Table 6.1) that meet the following criteria: 1) mainly

localize in the membrane plus matrix fraction; 2) no transmembrane domain; 3) highly conserved between human and *Chlamydomonas*, yet not conserved in non-ciliated organisms, such as *Arabidopsis thaliana*; 4) if it was checked for expression upon deflagellation, it is up-regulated; 5) at least three peptides were identified in the membrane plus matrix fraction. This list includes all the identified IFT-particle proteins, a protein (C_10017) whose homologue was shown to undergo IFT in *C. elegans*, and several other proteins (C_140070, C_6980002, C_320063, and C_1010056). These proteins are potential IFT-particle proteins. Experiments can be designed to test if this is the case.

The other direction for future research on IFT machinery is to focus on the functions of individual IFT components. For D1bLIC, since the remaining DHC1b does not accumulate in the flagella in the absence of D1bLIC while IFT particles do, D1bLIC might be involved in binding the cargos to the retrograde motor. Therefore, it will be of interest to identify D1bLIC interacting proteins. For IFT46, since IFT46 is required for transport of outer dynein arms into flagella and is required for the stability of complex B as a complex B core protein, research also should be carried out to identify the interacting proteins. Potential interacting proteins include outer dynein arm components, ODA16, and other complex B proteins. Once the interacting proteins are identified, it will be possible to identify specific domains of IFT46 that are required for interaction.

By addressing other aspects of IFT, one can probably understand more about the function of IFT as a whole and how cilia are involved in cell cycle regulation. These aspects include: 1) What cargos are carried by IFT in addition to the identified membrane channels, radial spokes and inner and outer dynein arms? Does it carry signaling molecules in addition to the structural proteins? How does the cell body react to these signals? 2) What is the signal to initiate the IFT machinery to make flagella? Is it simply up-regulation of IFT proteins that initiates flagellar assembly, or is there another event (e.g., docking of centriole to plasma membrane, uncapping of plus ends of basal body microtubules, activation of kinesin-2) that initiates flagellar assembly? 3) Like other flagellar proteins, IFT proteins are up-regulated upon deflagellation. How is the expression of IFT proteins regulated? In *C. elegans*, many genes encoding IFT components have a special motif (X-box) in the promoter and are regulated by DAF19. DAF19 is the sole *C. elegans* RFX-type transcription factor (Swoboda et al., 2000). Mouse RFX3 (one of the five RFX family members in the mouse) regulates the expression of D2LIC, but does not affect the expression of Tg737 (Bonnafe et al., 2004). Although there is no *Chlamydomonas* homologue for DAF19 or RFX3, is there a similar transcription regulation system in *Chlamydomonas*? Similarly, in mammals, what transcription factors are responsible for the expression of IFT-particle proteins? 4) *Chlamydomonas* cells resorb their flagella during mating and before they divide. Is IFT actively involved in these processes? If yes, what is the signal that IFT machinery receives to start these processes? Clearly, there is much more to learn about IFT.

Table 6.1 **Proteins that share the same criteria as IFT-particle proteins**

Name	Description from flagellar proteomic database	More information	Number of peptides found			
			M	A	K	T
C_170190	IFT172, Intraflagellar Transport Protein 172		46	0	3	3
C_410035	IFT72/74, Intraflagellar Transport Protein 72 and 74		32	0	2	0
C_10177	IFT81, Intraflagellar Transport Protein 81		26	0	1	0
C_270146	FAP60, Conserved Uncharacterized Flagellar Associated Protein	IFT139	24	0	2	0
C_210077	FAP66, Conserved Uncharacterized Flagellar Associated Protein	IFT144 DYF-2	22	0	3	1
C_640055	IFT140, Intraflagellar Transport Protein 140		17	0	0	1
C_10017	FAP22, Danio Cystic Kidney Disease Gene, qilin		16	0	2	0
C_1190053	FAP80, IFT122A, Intraflagellar Transport Protein 122A		15	0	1	1
C_720060	IFT88, Intraflagellar Transport Protein 88		14	0	0	0
C_140070	FAP116, Flagellar Associated Protein Similar to Microtubule Interacting TNF Receptor-Associated Factor 3 Interacting Protein 1		11	0	0	0
C_1970008	FAP118, Conserved Uncharacterized Flagellar Associated Protein	IFT122B IFTA-1	9	0	2	0
C_6980002	FAP163, Conserved Uncharacterized WD-Repeat Flagellar Associated Protein		8	0	0	0
C_1630013	IFT57, Intraflagellar Transport Protein 57		7	0	1	0
C_2130007	IFT46, FAP32, Conserved Uncharacterized Flagellar Associated Protein		6	0	0	0
C_120075	FAP167, IFT80, Intraflagellar Transport protein 80		6	0	1	0
C_1260018	IFT52, Intraflagellar Transport Protein 52		5	0	1	0
C_1510005	IFT20, Intraflagellar Transport Protein 20		5	0	0	0
C_320063	FAP232, Conserved Uncharacterized Flagellar Associated Protein		5	0	0	0
C_1010056	FAP14, Conserved Uncharacterized Protein		3	0	0	0

M: membrane plus matrix fraction; A: KCl extracted axoneme; K: KCl extracted fraction; T: tergitol extracted fraction.
Previously identified IFT proteins are shown in black and uncharacterized proteins or proteins not identified as IFT proteins are shown in red.

BIBLIOGRAPHY

Adams, G.M.W., B. Huang, and D.J.L. Luck. 1982. Temperature-sensitive, assembly-defective flagella mutants of *Chlamydomonas reinhardtii*. *Genetics*. 100: 579-586.

Ahmed, N.T., and D.R. Mitchell. 2005. ODA16p, a *Chlamydomonas* flagellar protein needed for dynein assembly. *Mol. Biol. Cell*. 16:5004-5012.

Baker, S.A., K. Freeman, K. Luby-Phelps, G.J. Pazour, and J.C. Besharse. 2003. IFT20 links kinesin II with a mammalian intraflagellar transport complex that is conserved in motile flagella and sensory cilia. *J Biol. Chem*. 278:34211-34218.

Bell, L.R., S. Stone, J. Yochem, J.E. Shaw, and R.K. Herman. 2006. The molecular identities of the *Caenorhabditis elegans* intraflagellar transport genes dyf-6, daf-10, and osm-1. *Genetics*. 173:1275-1286.

Bielli, A., P.O. Thornqvist, A.G. Hendrick, R. Finn, K. Fitzgerald, and M.W. McCaffrey. 2001. The small GTPase Rab4A interacts with the central region of cytoplasmic dynein light intermediate chain-1. *Biochem. Biophys. Res. Commun*. 281:1141-1153.

Blacque, O.E., and M.R. Leroux. 2006. Bardet-Biedl syndrome: an emerging pathomechanism of intracellular transport. *Cell Mol. Life Sci*. 63:2145-2161.

Blacque, O.E., C. Li, P.N. Inglis, M.A. Esmail, G. Ou, A.K. Mah, D.L. Baillie, J.M. Scholey, and M.R. Leroux. 2006. The WD Repeat-containing Protein, IFTA-1,

Is Required for Retrograde Intraflagellar Transport. *Mol. Biol. Cell*. 17:5053-5062.

Blacque, O.E., E.A. Perens, K.A. Boroevich, P.N. Inglis, C. Li, A. Warner, J. Khattra, R.A. Holt, G. Ou, A.K. Mah, S.J. McKay, P. Huang, P. Swoboda, S.J. Jones, M.A. Marra, D.L. Baillie, D.G. Moerman, S. Shaham, and M.R. Leroux. 2005. Functional genomics of the cilium, a sensory organelle. *Curr. Biol*. 15:935-941.

Blacque, O.E., M.J. Reardon, C. Li, J. McCarthy, M.R. Mahjoub, S.J. Ansley, J.L. Badano, A.K. Mah, P.L. Beales, W.S. Davidson, R.C. Johnsen, M. Audeh, R.H. Plasterk, D.L. Baillie, N. Katsanis, L.M. Quarmby, S.R. Wicks, and M.R. Leroux. 2004. Loss of *C. elegans* BBS-7 and BBS-8 protein function results in cilia defects and compromised intraflagellar transport. *Genes. Dev*. 18:1630-1642.

Bonnafe, E., M. Touka, A. AitLounis, D. Baas, E. Barras, C. Ucla, A. Moreau, F. Flamant, R. Dubruille, P. Couble, J. Collignon, B. Durand, and W. Reith. 2004. The transcription factor RFX3 directs nodal cilium development and left-right asymmetry specification. *Mol. Cell Biol*. 24:4417-4427.

Brazelton, W.J., C.D. Amundsen, C.D. Silflow, and P.A. Lefebvre. 2001. The bld1 mutation identifies the *Chlamydomonas* osm-6 homolog as a gene required for flagellar assembly. *Curr. Biol*. 11:1591-1594.

Brown, J.M., N.A. Fine, G. Pandiyan, R. Thazhath, and J. Gaertig. 2003. Hypoxia regulates assembly of cilia in suppressors of *Tetrahymena* lacking an intraflagellar transport subunit gene. *Mol. Biol. Cell*. 14:3192-3207.

Carlen, B., and U. Stenram. 2005. Primary ciliary dyskinesia: a review. *Ultrastruct Pathol*. 29:217-220.

Church, G.M., and W. Gilbert. 1984. Genomic sequencing. *Proc. Natl. Acad. Sci. USA*. 81:1991-1995.

Cole, D.G. 2003. The intraflagellar transport machinery of *Chlamydomonas reinhardtii*. *Traffic*. 4:435-442.

Cole, D.G., D.R. Diener, A.L. Himelblau, P.L. Beech, J.C. Fuster, and J.L. Rosenbaum. 1998. *Chlamydomonas* kinesin-II-dependent intraflagellar transport (IFT): IFT particles contain proteins required for ciliary assembly in *Caenorhabditis elegans* sensory neurons. *J. Cell Biol*. 141:993-1008.

Collet, J., C.A. Spike, E.A. Lundquist, J.E. Shaw, and R.K. Herman. 1998. Analysis of osm-6, a gene that affects sensory cilium structure and sensory neuron function in *Caenorhabditis elegans*. *Genetics*. 148:187-200.

Corbit, K.C., P. Aanstad, V. Singla, A.R. Norman, D.Y. Stainier, and J.F. Reiter. 2005. Vertebrate Smoothened functions at the primary cilium. *Nature*. 437:1018-1021.

Davenport, J.R., and B.K. Yoder. 2005. An incredible decade for the primary cilium: a look at a once-forgotten organelle. *Am. J. Physiol. Renal. Physiol*. 289:F1159-1169.

Deane, J.A., D.G. Cole, E.S. Seeley, D.R. Diener, and J.L. Rosenbaum. 2001. Localization of intraflagellar transport protein IFT52 identifies basal body transitional fibers as the docking site for IFT particles. *Curr. Biol*. 11:1586-1590.

Dell, K.R., C.W. Turck, and R.D. Vale. 2000. Mitotic phosphorylation of the dynein light intermediate chain is mediated by cdc2 kinase. *Traffic*. 1:38-44.

DiBella, L.M., and S.M. King. 2001. Dynein motors of the *Chlamydomonas* flagellum. *Int. Rev. Cytol*. 210:227-268.

Efimenko, E., O.E. Blacque, G. Ou, C.J. Haycraft, B.K. Yoder, J.M. Scholey, M.R. Leroux, and P. Swoboda. 2006. *Caenorhabditis elegans* DYF-2, an orthologue of human WDR19, is a component of the intraflagellar transport machinery in sensory cilia. *Mol. Biol. Cell*. 17:4801-4811.

Follit, J.A., R.A. Tuft, K.E. Fogarty, and G.J. Pazour. 2006. The Intraflagellar Transport Protein IFT20 Is Associated with the Golgi Complex and Is Required for Cilia Assembly. *Mol. Biol. Cell*. 17:3781-3792.

Fowkes, M.E., and D.R. Mitchell. 1998. The role of preassembled cytoplasmic complexes in assembly of flagellar dynein subunits. *Mol. Biol. Cell*. 9:2337-2347.

Frolenkov, G.I., I.A. Belyantseva, T.B. Friedman, and A.J. Griffith. 2004. Genetic insights into the morphogenesis of inner ear hair cells. *Nat. Rev. Genet*. 5:489-498.

Fujiwara, M., T. Ishihara, and I. Katsura. 1999. A novel WD40 protein, CHE-2, acts

cell-autonomously in the formation of *C. elegans* sensory cilia. *Development*. 126:4839-4848.

Gervais, F.G., R. Singaraja, S. Xanthoudakis, C.A. Gutekunst, B.R. Leavitt, M. Metzler, A.S. Hackam, J. Tam, J.P. Vaillancourt, V. Houtzager, D.M. Rasper, S. Roy, M.R. Hayden, and D.W. Nicholson. 2002. Recruitment and activation of caspase-8 by the Huntingtin-interacting protein Hip-1 and a novel partner Hippi. *Nat. Cell Biol*. 4:95-105.

Gorman, D.S., and R.P. Levine. 1965. Cytochrome f and plastocyanin: their sequence in the photosynthetic electron transport chain of *Chlamydomonas reinhardi*. *Proc. Natl. Acad. Sci. USA*. 54:1665-1669.

Grissom, P.M., E.A. Vaisberg, and J.R. McIntosh. 2002. Identification of a novel light intermediate chain (D2LIC) for mammalian cytoplasmic dynein 2. *Mol. Biol. Cell*. 13:817-829.

Harris, E.H. 2001. *Chlamydomonas* as a Model Organism. *Annu. Rev. Plant Physiol. Plant Mol. Biol*. 52:363-406.

Haycraft, C.J., J.C. Schafer, Q. Zhang, P.D. Taulman, and B.K. Yoder. 2003. Identification of CHE-13, a novel intraflagellar transport protein required for cilia formation. *Exp. Cell Res*. 284:251-263.

Hendrickson, T.W., C.A. Perrone, P. Griffin, K. Wuichet, J. Mueller, P. Yang, M.E. Porter, and W.S. Sale. 2004. IC138 is a WD-repeat dynein intermediate chain

required for light chain assembly and regulation of flagellar bending. *Mol. Biol. Cell*. 15:5431-5442.

Hoops, H.J., and G.B. Witman. 1983. Outer doublet heterogeneity reveals structural polarity related to beat direction in *Chlamydomonas* flagella. *J. Cell Biol*. 97:902-908.

Hou, Y., H. Qin, J.A. Follit, G.J. Pazour, J.L. Rosenbaum, and G.B. Witman. 2007. Functional analysis of an individual IfT protein: IFT46 is required for transport of outer dynein arms into flagella. *J. Cell Biol*. Accepted.

Hou, Y., G.J. Pazour, and G.B. Witman. 2004. A dynein light intermediate chain, D1bLIC, is required for retrograde intraflagellar transport. *Mol. Biol. Cell*. 15:4382-4394.

Houde, C., R.J. Dickinson, V.M. Houtzager, R. Cullum, R. Montpetit, M. Metzler, E.M. Simpson, S. Roy, M.R. Hayden, P.A. Hoodless, and D.W. Nicholson. 2006. Hippi is essential for node cilia assembly and Sonic hedgehog signaling. *Dev. Biol*. 300:523-533.

Howard, P.W., and R.A. Maurer. 2000. Identification of a conserved protein that interacts with specific LIM homeodomain transcription factors. *J. Biol. Chem*. 275:13336-13342.

Huang, B., M.R. Rifkin, and D.J. Luck. 1977. Temperature-sensitive mutations affecting flagellar assembly and function in *Chlamydomonas reinhardtii*. *J. Cell Biol*. 72:67-85.

Huang, K., D.R. Diener, R. Karki, L.B. Pedersen, S. Geimer, and J.L. Rosenbaum. 2005. The Cilium/flagellum: A Secretory Organelle? ASCB 45th annual meeting. Abstract 1513.

Huangfu, D., A. Liu, A.S. Rakeman, N.S. Murcia, L. Niswander, and K.V. Anderson. 2003. Hedgehog signalling in the mouse requires intraflagellar transport proteins. *Nature*. 426:83-87.

Ibanez-Tallon, I., A. Pagenstecher, M. Fliegauf, H. Olbrich, A. Kispert, U.P. Ketelsen, A. North, N. Heintz, and H. Omran. 2004. Dysfunction of axonemal dynein heavy chain Mdnah5 inhibits ependymal flow and reveals a novel mechanism for hydrocephalus formation. *Hum. Mol. Genet*. 13:2133-2141.

Jenkins, P.M., T.W. Hurd, L. Zhang, D.P. McEwen, R.L. Brown, B. Margolis, K.J. Verhey, and J.R. Martens. 2006. Ciliary targeting of olfactory CNG channels requires the CNGB1b subunit and the kinesin-2 motor protein, KIF17. *Curr. Biol*. 16:1211-1216.

Johnson, K.A., and J.L. Rosenbaum. 1992. Polarity of flagellar assembly in *Chlamydomonas*. *J. Cell Biol*. 119:1605-1611.

Jurczyk, A., A. Gromley, S. Redick, J. San Agustin, G. Witman, G.J. Pazour, D.J. Peters, and S. Doxsey. 2004. Pericentrin forms a complex with intraflagellar transport proteins and polycystin-2 and is required for primary cilia assembly. *J. Cell Biol*. 166:637-643.

Kamiya, R. 2002. Functional diversity of axonemal dyneins as studied in

Chlamydomonas mutants. ***Int. Rev. Cytol***. 219:115-155.

Kessel, R.G., and R.H. Kardon. 1979. TISSUES AND ORGANS: a text-atlas of scanning electron microscopy. W. H. Freeman and Company. San Francisco. 132pp.

Kindle, K.L. 1990. High-frequency nuclear transformation of *Chlamydomonas reinhardtii*. Proc. ***Natl. Acad. Sci. USA***. 87:1228-1232.

King, S.M. 2000. The dynein microtubule motor. ***Biochim. Biophys. Acta***. 1496:60-75.

King, S.M., J.F. Dillman, 3rd, S.E. Benashski, R.J. Lye, R.S. Patel-King, and K.K. Pfister. 1996. The mouse t-complex-encoded protein Tctex-1 is a light chain of brain cytoplasmic dynein. ***J. Biol. Chem***. 271:32281-32287.

King, S.M., T. Otter, and G.B. Witman. 1985. Characterization of monoclonal antibodies against *Chlamydomonas* flagellar dyneins by high-resolution protein blotting. Proc. ***Natl. Acad. Sci. USA***. 82:4717-4721.

King, S.M., T. Otter, and G.B. Witman. 1986. Purification and characterization of *Chlamydomonas* flagellar dyneins. ***Methods Enzymol***. 134:291-306.

Kozminski, K.G., P.L. Beech, and J.L. Rosenbaum. 1995. The *Chlamydomonas* kinesin-like protein FLA10 is involved in motility associated with the flagellar membrane. ***J. Cell Biol***. 131:1517-1527.

Kozminski, K.G., K.A. Johnson, P. Forscher, and J.L. Rosenbaum. 1993. A motility in the eukaryotic flagellum unrelated to flagellar beating. ***Proc. Natl. Acad. Sci. USA***. 90:5519-5523.

Kulaga, H.M., C.C. Leitch, E.R. Eichers, J.L. Badano, A. Lesemann, B.E. Hoskins, J.R. Lupski, P.L. Beales, R.R. Reed, and N. Katsanis. 2004. Loss of BBS proteins causes anosmia in humans and defects in olfactory cilia structure and function in the mouse. *Nat. Genet*. 36:994-998.

Lefebvre, P.A., and J.L. Rosenbaum. 1986. Regulation of the synthesis and assembly of ciliary and flagellar proteins during regeneration. *Annu. Rev. Cell Biol*. 2:517-546.

Liu, A., B. Wang, and L.A. Niswander. 2005. Mouse intraflagellar transport proteins regulate both the activator and repressor functions of Gli transcription factors. *Development*. 132:3103-3111.

Lucker, B.F., R.H. Behal, H. Qin, L.C. Siron, W.D. Taggart, J.L. Rosenbaum, and D.G. Cole. 2005. Characterization of the intraflagellar transport complex B core: direct interaction of the IFT81 and IFT74/72 subunits. *J. Biol. Chem*. 280:27688-27696.

Lumbreras, V., D.R. Stevens, and S. Purton. 1998. Efficient foreign gene expression in *Chlamydomonas reinhardtii* mediated by an endogenous intron. *Plant J*. 14:441-448.

Lupas, A. 1996. Prediction and analysis of coiled-coil structures. *Methods Enzymol*. 266:513-525.

Lupas, A., M. Van Dyke, and J. Stock. 1991. Predicting coiled coils from protein sequences. *Science*. 252:1162-1164.

Mikami, A., S.H. Tynan, T. Hama, K. Luby-Phelps, T. Saito, J.E. Crandall, J.C. Besharse, and R.B. Vallee. 2002. Molecular structure of cytoplasmic dynein 2 and its distribution in neuronal and ciliated cells. *J. Cell Sci*. 115:4801-4808.

Miller, M.S., J.M. Esparza, A.M. Lippa, F.G. Lux, 3rd, D.G. Cole, and S.K. Dutcher. 2005. Mutant kinesin-2 motor subunits increase chromosome loss. *Mol. Biol. Cell*. 16:3810-3820.

Mueller, J., C.A. Perrone, R. Bower, D.G. Cole, and M.E. Porter. 2005. The FLA3 KAP subunit is required for localization of kinesin-2 to the site of flagellar assembly and processive anterograde intraflagellar transport. *Mol. Biol. Cell*. 16:1341-1354.

Murayama, T., Y. Toh, Y. Ohshima, and M. Koga. 2005. The dyf-3 gene encodes a novel protein required for sensory cilium formation in *Caenorhabditis elegans*. *J. Mol. Biol*. 346:677-687.

Nelson, J.A., P.B. Savereide, and P.A. Lefebvre. 1994. The CRY1 gene in *Chlamydomonas reinhardtii*: structure and use as a dominant selectable marker for nuclear transformation. *Mol. Cell Biol*. 14:4011-4019.

Niclas, J., V.J. Allan, and R.D. Vale. 1996. Cell cycle regulation of dynein association with membranes modulates microtubule-based organelle transport. *J. Cell Biol*. 133:585-593.

Nonaka, S., Y. Tanaka, Y. Okada, S. Takeda, A. Harada, Y. Kanai, M. Kido, and N. Hirokawa. 1998. Randomization of left-right asymmetry due to loss of nodal

cilia generating leftward flow of extraembryonic fluid in mice lacking KIF3B motor protein. *Cell*. 95:829-837.

Ou, G., O.E. Blacque, J.J. Snow, M.R. Leroux, and J.M. Scholey. 2005. Functional coordination of intraflagellar transport motors. *Nature*. 436:583-587.

Ou, G., H. Qin, J.L. Rosenbaum, and J.M. Scholey. 2005. The PKD protein qilin undergoes intraflagellar transport. *Curr. Biol*. 15:R410-411.

Pan, J., and W.J. Snell. 2002. Kinesin-II is required for flagellar sensory transduction during fertilization in *Chlamydomonas*. *Mol. Biol. Cell*. 13:1417-1426.

Pazour, G.J., N. Agrin, J. Leszyk, and G.B. Witman. 2005. Proteomic analysis of a eukaryotic cilium. *J. Cell Biol*. 170:103-113.

Pazour, G.J., S.A. Baker, J.A. Deane, D.G. Cole, B.L. Dickert, J.L. Rosenbaum, G.B. Witman, and J.C. Besharse. 2002. The intraflagellar transport protein, IFT88, is essential for vertebrate photoreceptor assembly and maintenance. *J. Cell Biol*. 157:103-113.

Pazour, G.J., B.L. Dickert, Y. Vucica, E.S. Seeley, J.L. Rosenbaum, G.B. Witman, and D.G. Cole. 2000. *Chlamydomonas* IFT88 and its mouse homologue, polycystic kidney disease gene Tg737, are required for assembly of cilia and flagella. *J. Cell Biol*. 151:709-718.

Pazour, G.J., B.L. Dickert, and G.B. Witman. 1999. The DHC1b (DHC2) isoform of cytoplasmic dynein is required for flagellar assembly. *J. Cell Biol*. 144:473-481.

Pazour, G.J., J.T. San Agustin, J.A. Follit, J.L. Rosenbaum, and G.B. Witman. 2002. Polycystin-2 localizes to kidney cilia and the ciliary level is elevated in orpk mice with polycystic kidney disease. *Curr. Biol*. 12:R378-380.

Pazour, G.J., O.A. Sineshchekov, and G.B. Witman. 1995. Mutational analysis of the phototransduction pathway of *Chlamydomonas reinhardtii*. *J. Cell Biol*. 131:427-440.

Pazour, G.J., C.G. Wilkerson, and G.B. Witman. 1998. A dynein light chain is essential for the retrograde particle movement of intraflagellar transport (IFT). *J. Cell Biol*. 141:979-992.

Pazour, G.J., and G.B. Witman. 2003. The vertebrate primary cilium is a sensory organelle. *Curr. Opin. Cell Biol*. 15:105-110.

Pazour, G.J., and G.B. Witman. 2000. Forward and reverse genetic analysis of microtubule motors in *Chlamydomonas*. *Methods*. 22:285-298.

Peden, E.M., and M.M. Barr. 2005. The KLP-6 kinesin is required for male mating behaviors and polycystin localization in *Caenorhabditis elegans*. *Curr. Biol*. 15:394-404.

Pedersen, L.B., S. Geimer, and J.L. Rosenbaum. 2006. Dissecting the molecular mechanisms of intraflagellar transport in *Chlamydomonas*. *Curr. Biol*. 16:450-459.

Pedersen, L.B., M.S. Miller, S. Geimer, J.M. Leitch, J.L. Rosenbaum, and D.G. Cole. 2005. Chlamydomonas IFT172 is encoded by FLA11, interacts with CrEB1, and regulates IFT at the flagellar tip. *Curr. Biol*. 15:262-266.

Perrone, C.A., D. Tritschler, P. Taulman, R. Bower, B.K. Yoder, and M.E. Porter. 2003. A novel dynein light intermediate chain colocalizes with the retrograde motor for intraflagellar transport at sites of axoneme assembly in *Chlamydomonas* and Mammalian cells. *Mol. Biol. Cell*. 14:2041-2056.

Pfister, K.K., R.B. Fay, and G.B. Witman. 1982. Purification and polypeptide composition of dynein ATPases from *Chlamydomonas* flagella. *Cell Motil*. 2:525-547.

Pfister, K.K., and G.B. Witman. 1984. Subfractionation of *Chlamydomonas* 18 S dynein into two unique subunits containing ATPase activity. *J Biol. Chem*. 259:12072-12080.

Piperno, G. 1990. Functional diversity of dyneins. *Cell Motil. Cytoskeleton*. 17:147-149.

Piperno, G., and K. Mead. 1997. Transport of a novel complex in the cytoplasmic matrix of *Chlamydomonas* flagella. Proc. *Natl. Acad. Sci. USA*. 94:4457-4462.

Piperno, G., K. Mead, and S. Henderson. 1996. Inner dynein arms but not outer dynein arms require the activity of kinesin homologue protein KHP1(FLA10) to reach the distal part of flagella in *Chlamydomonas*. *J Cell Biol*. 133:371-379.

Porter, M.E., R. Bower, J.A. Knott, P. Byrd, and W. Dentler. 1999. Cytoplasmic dynein heavy chain 1b is required for flagellar assembly in *Chlamydomonas*. *Mol. Biol. Cell*. 10:693-712.

Praetorius, H.A., and K.R. Spring. 2001. Bending the MDCK cell primary cilium increases intracellular calcium. *J. Membr. Biol*. 184:71-79.

Purohit, A., S.H. Tynan, R. Vallee, and S.J. Doxsey. 1999. Direct interaction of pericentrin with cytoplasmic dynein light intermediate chain contributes to mitotic spindle organization. *J. Cell Biol*. 147:481-492.

Qin, H., D.T. Burnette, Y.K. Bae, P. Forscher, M.M. Barr, and J.L. Rosenbaum. 2005. Intraflagellar transport is required for the vectorial movement of TRPV channels in the ciliary membrane. *Curr. Biol*. 15:1695-1699.

Qin, H., D.R. Diener, S. Geimer, D.G. Cole, and J.L. Rosenbaum. 2004. Intraflagellar transport (IFT) cargo: IFT transports flagellar precursors to the tip and turnover products to the cell body. *J. Cell Biol*. 164:255-266.

Qin, H., J.L. Rosenbaum, and M.M. Barr. 2001. An autosomal recessive polycystic kidney disease gene homolog is involved in intraflagellar transport in *C. elegans* ciliated sensory neurons. *Curr. Biol*. 11:457-461.

Reilein, A.R., S.L. Rogers, M.C. Tuma, and V.I. Gelfand. 2001. Regulation of molecular motor proteins. *Int. Rev. Cytol*. 204:179-238.

Rosenbaum, J.L., and G.B. Witman. 2002. Intraflagellar transport. *Nat. Rev. Mol. Cell Biol*. 3:813-825.

Ross, A.J., H. May-Simera, E.R. Eichers, M. Kai, J. Hill, D.J. Jagger, C.C. Leitch, J.P. Chapple, P.M. Munro, S. Fisher, P.L. Tan, H.M. Phillips, M.R. Leroux, D.J. Henderson, J.N. Murdoch, A.J. Copp, M.M. Eliot, J.R. Lupski, D.T. Kemp, H. Dollfus, M. Tada, N. Katsanis, A. Forge, and P.L. Beales. 2005. Disruption of Bardet-Biedl syndrome ciliary proteins perturbs planar cell polarity in vertebrates. *Nat. Genet*. 37:1135-1140.

Sager, R., and S. Granick. 1953. Nutritional studies with *Chlamydomonas reinhardi*. *Ann. N. Y. Acad. Sci*. 56:831-838.

Sambrook, J., Fritsch, E.F., and Maniatis, T. 1987. Molecular Cloning: A Laboratory Manual. Cold Spring Harbor Laboratory, Cold Spring Harbor, NY. 545 pp.

Saraste, M., P.R. Sibbald, and A. Wittinghofer. 1990. The P-loop--a common motif in ATP- and GTP-binding proteins. *Trends Biochem. Sci*. 15:430-434.

Satir, P., and S.T. Christensen. 2006. Overview of Structure and Function of Mammalian Cilia. *Annu. Rev. Physiol*.

Schafer, J.C., C.J. Haycraft, J.H. Thomas, B.K. Yoder, and P. Swoboda. 2003. XBX-1 encodes a dynein light intermediate chain required for retrograde intraflagellar transport and cilia assembly in *Caenorhabditis elegans*. *Mol. Biol. Cell*. 14:2057-2070.

Schafer, J.C., M.E. Winkelbauer, C.L. Williams, C.J. Haycraft, R.A. Desmond, and B.K. Yoder. 2006. IFTA-2 is a conserved cilia protein involved in pathways

regulating longevity and dauer formation in *Caenorhabditis elegans*. *J. Cell Sci*. 119:4088-4100.

Schloss, J.A. 1990. A *Chlamydomonas* gene encodes a G protein beta subunit-like polypeptide. *Mol. Gen. Genet*. 221:443-452.

Schnell, R.A., and P.A. Lefebvre. 1993. Isolation of the *Chlamydomonas* regulatory gene NIT2 by transposon tagging. *Genetics*. 134:737-747.

Scholey, J.M. 2003. Intraflagellar transport. *Annu. Rev. Cell Dev. Biol*. 19:423-443.

Signor, D., K.P. Wedaman, J.T. Orozco, N.D. Dwyer, C.I. Bargmann, L.S. Rose, and J.M. Scholey. 1999. Role of a class DHC1b dynein in retrograde transport of IFT motors and IFT raft particles along cilia, but not dendrites, in chemosensory neurons of living *Caenorhabditis elegans*. *J. Cell Biol*. 147:519-530.

Silflow, C.D., M. LaVoie, L.W. Tam, S. Tousey, M. Sanders, W. Wu, M. Borodovsky, and P.A. Lefebvre. 2001. The Vfl1 Protein in *Chlamydomonas* localizes in a rotationally asymmetric pattern at the distal ends of the basal bodies. *J. Cell Biol*. 153:63-74.

Silflow, C.D., and J.L. Rosenbaum. 1981. Multiple alpha- and beta-tubulin genes in *Chlamydomonas* and regulation of tubulin mRNA levels after deflagellation. *Cell*. 24:81-88.

Silvanovich, A., M.G. Li, M. Serr, S. Mische, and T.S. Hays. 2003. The third P-loop domain in cytoplasmic dynein heavy chain is essential for dynein motor function and ATP-sensitive microtubule binding. *Mol. Biol. Cell*. 14:1355-1365.

Singla, V., and J.F. Reiter. 2006. The primary cilium as the cell's antenna: signaling at a sensory organelle. *Science*. 313:629-633.

Smith, E.F., and P. Yang. 2004. The radial spokes and central apparatus: mechano-chemical transducers that regulate flagellar motility. *Cell Motil. Cytoskeleton.* 57:8-17.

Snow, J.J., G. Ou, A.L. Gunnarson, M.R. Walker, H.M. Zhou, I. Brust-Mascher, and J.M. Scholey. 2004. Two anterograde intraflagellar transport motors cooperate to build sensory cilia on *C. elegans* neurons. *Nat. Cell Biol*. 6:1109-1113.

Swoboda, P., H.T. Adler, and J.H. Thomas. 2000. The RFX-type transcription factor DAF-19 regulates sensory neuron cilium formation in *C. elegans*. *Mol. Cell*. 5:411-421.

Takada, S., and R. Kamiya. 1994. Functional reconstitution of *Chlamydomonas* outer dynein arms from alpha-beta and gamma subunits: requirement of a third factor. *J. Cell Biol*. 126:737-745.

Takeda, S., Y. Yonekawa, Y. Tanaka, Y. Okada, S. Nonaka, and N. Hirokawa. 1999. Left-right asymmetry and kinesin superfamily protein KIF3A: new insights in determination of laterality and mesoderm induction by *kif3A*$^{-/-}$ mice analysis. *J. Cell Biol*. 145:825-836.

Tynan, S.H., A. Purohit, S.J. Doxsey, and R.B. Vallee. 2000. Light intermediate chain 1 defines a functional subfraction of cytoplasmic dynein which binds to pericentrin. *J. Biol. Chem*. 275:32763-32768.

Vaisberg, E.A., P.M. Grissom, and J.R. McIntosh. 1996. Mammalian cells express three distinct dynein heavy chains that are localized to different cytoplasmic organelles. *J. Cell Biol*. 133:831-842.

Via, A., F. Ferre, B. Brannetti, A. Valencia, and M. Helmer-Citterich. 2000. Three-dimensional view of the surface motif associated with the P-loop structure: cis and trans cases of convergent evolution. *J. Mol Biol*. 303:455-465.

Wakabayashi, K., S. Takada, G.B. Witman, and R. Kamiya. 2001. Transport and arrangement of the outer-dynein-arm docking complex in the flagella of *Chlamydomonas* mutants that lack outer dynein arms. *Cell Motil. Cytoskeleton*. 48:277-286.

Wang, Q., J. Pan, and W.J. Snell. 2006. Intraflagellar transport particles participate directly in cilium-generated signaling in *Chlamydomonas*. *Cell*. 125:549-562.

Wessel, D., and U.I. Flugge. 1984. A method for the quantitative recovery of protein in dilute solution in the presence of detergents and lipids. *Anal. Biochem*. 138:141-143.

Wick, M.J., D.K. Ann, and H.H. Loh. 1995. Molecular cloning of a novel protein regulated by opioid treatment of NG108-15 cells. *Brain Res. Mol. Brain Res*. 32:171-175.

Wicks, S.R., C.J. de Vries, H.G. van Luenen, and R.H. Plasterk. 2000. CHE-3, a cytosolic dynein heavy chain, is required for sensory cilia structure and function in *Caenorhabditis elegans*. *Dev. Biol*. 221:295-307.

Wickstead, B., and K. Gull. 2006. A "holistic" kinesin phylogeny reveals new kinesin families and predicts protein functions. *Mol. Biol. Cell*. 17:1734-1743.

Wilkerson, C.G., S.M. King, A. Koutoulis, G.J. Pazour, and G.B. Witman. 1995. The 78,000 M(r) intermediate chain of *Chlamydomonas* outer arm dynein is a WD-repeat protein required for arm assembly. *J. Cell Biol*. 129:169-178.

Wirschell, M., G. Pazour, A. Yoda, M. Hirono, R. Kamiya, and G.B. Witman. 2004. Oda5p, a novel axonemal protein required for assembly of the outer dynein arm and an associated adenylate kinase. *Mol. Biol. Cell*. 15:2729-2741.

Witman, G.B. 1975. The site of in vivo assembly of flagellar microtubules. *Ann. N. Y. Acad. Sci*. 253:178-191.

Witman, G.B. 1986. Isolation of *Chlamydomonas* flagella and flagellar axonemes. *Methods Enzymol*. 134:280-290.

Witman, G.B., K. Carlson, J. Berliner, and J.L. Rosenbaum. 1972. *Chlamydomonas* flagella. I. Isolation and electrophoretic analysis of microtubules, matrix, membranes, and mastigonemes. *J. Cell Biol*. 54:507-539.

Witman, G.B., K.A. Johnson, K.K. Pfister, J.S. Wall. 1983. Fine structure and molecular weight of the outer arm dyneins of *Chlamydomonas*. *J. Submicrosc. Cytol.* 15: 193-197.

Yamazaki, H., T. Nakata, Y. Okada, and N. Hirokawa. 1996. Cloning and characterization of KAP3: a novel kinesin superfamily-associated protein of KIF3A/3B. *Proc. Natl. Acad. Sci. USA*. 93:8443-8448.

Yang, P., D.R. Diener, C. Yang, T. Kohno, G.J. Pazour, J.M. Dienes, N.S. Agrin, S.M. King, W.S. Sale, R. Kamiya, J.L. Rosenbaum, and G.B. Witman. 2006. Radial spoke proteins of *Chlamydomonas* flagella. *J. Cell Sci*. 119:1165-1174.

Yoder, J.H., and M. Han. 2001. Cytoplasmic dynein light intermediate chain is required for discrete aspects of mitosis in *Caenorhabditis elegans*. *Mol. Biol. Cell*. 12:2921-2933.

Zhang, Y., and W.J. Snell. 1995. Flagellar adenylyl cyclases in *Chlamydomonas*. *Methods Cell Biol*. 47:459-465.

APPENDIX-ABBREVIATIONS

BAC: bacterial artificial chromosome

DHC: dynein heavy chain

DIC: differential interference contrast

EST: expressed sequence tag

HA: influenza hemagglutinin epitope

IFT: intraflagellar transport

LC: light chain

LIC: light intermediate chain

IC: intermediate chain

MS: mass spectrometry

P-loop: phosphate-binding domain

SEM: scanning electron microscopy

TEM: transmission electron microscopy